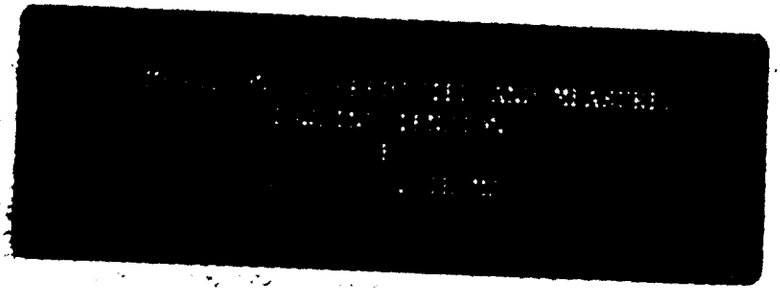

COMPARISON OF PREDICTED AND MEASURED TOWLINE TENSIONS

by

Gregory Robert Thomas

B.S., Mechanical Engineering
United States Naval Academy, 1982

Submitted to the Department of Ocean Engineering and the
Department of Mechanical Engineering
in Partial Fulfillment of the Requirements for the Degrees of

Naval Engineer
and
Master of Science in Mechanical Engineering

at the
Massachusetts Institute of Technology
May 1994

Signature of Author _____

Certified by _____
Jerome H. Milgram, Professor of Ocean Engineering
Thesis Advisor

Certified by _____
Stephen Harry Crandall, Professor of Mechanical Engineering, Emeritus
Thesis Reader

Accepted by _____
Ain Ants Sonin, Professor of Mechanical Engineering
Chairman, Committee on Graduate Students, Department of Mechanical Engineering

Accepted by _____
A. Douglas Carmichael, Professor of Power Systems
Chairman, Committee on Graduate Students, Department of Ocean Engineering

COMPARISON OF PREDICTED AND MEASURED TOWLINE TENSIONS

GREGORY ROBERT THOMAS

Submitted to the Department of Ocean Engineering and the Department of Mechanical Engineering in Partial Fulfillment of the Requirements for the Degrees of Naval Engineer and Master of Science in Mechanical Engineering

ABSTRACT

The extreme towline tension prediction methods used by the U.S. Navy are based on analytical models developed by Milgram, Triantafyllou, Frimm and Anagnostou (1988) . The analysis of the test results for an instrumented offshore tow conducted in 1989 indicated that the analytical model underpredicted extreme tension. The reason for the underprediction of the extreme tension was the analytical model did not account for the second order ship surge motions and resulting low frequency tension fluctuations. Frimm and Milgram (1991) proposed a semi-empirical correction to the extreme tension model based on an analysis of the at sea test results.

This thesis is a continuation of the above efforts to improve the prediction of extreme towline tensions in offshore towing. The goals of this thesis were to:

1. Design and conduct a test program on the tow of a defueled nuclear submarine the ex-USS Ray by the salvage ship USS Bolster to determine the following:
   a The ability to predict the low frequency towline tensions;
   b. The ability of an in-line synthetic spring to reduce dynamic tensions; and,
   c. The accuracy of the semi-empirical correction to the predicted extreme tension.
2. Develop and validate a numerical time simulation of the towing model from which the extreme tension statistics can be determined directly.

The towing test program was successfully performed. The presence and significance of the low frequency tension variations were confirmed and improvements to the semi-empirical correction were developed. A numerical time simulation of the towing model was developed and tension statistics based on the simulated tension time history were calculated and compared with statistics generated from the test results and the existing analysis methods. The ability of an in-line synthetic spring to reduce dynamic tension was demonstrated.

Thesis Advisor: Jerome H. Milgram
Title: Professor of Ocean Engineering

Acknowledgements

I would like to express my sincere appreciation to the following:

This great country and the United States Navy for the opportunity and support provided to me while at MIT and during my naval career.

Professor Jerome Milgram, my thesis advisor, for his patience, concern, and boundless energy. Professor Milgram is what every MIT professor should be.

Professor Stephen Crandall, my thesis reader, for his encouragement and insight.

Dr. Fernando Frimm and the gentlemen in the Marine Instrumentation and Computation Lab, led by D. Noah Eckhouse. Thank you Fernando, John, and Noah for sacrificing your summer in support of this project and the U.S. Navy. Thank you David, Soren, and Hasan for your kind assistance.

Captain Alan Brown and LCDR Jeffery Reed for the leadership, dedication, and enthusiasm they've brought to the 13A program.

The members of the submarine design team- Mark Lusted, Clarke Orzalli, and, on the saxophone, the incomparable David M. Fox, and the other members of the graduating class who have provided three years of solid professional support to all their classmates- George Margelis, Steve Markle, Francis Colberg, and Mark Bracco. A special thanks to Mark Lusted for his friendship and leadership.

The MIT Rugby Football Club, in particular Chevy and Ben Paul, for guidance and leadership far superior to their performance on the field. A special thanks to the extended rugby family, in particular the O'Sullivans, the Caseys, and Jonathon Kutchins. Thank you, Leo for the generosity and friendship you've shown my family.

My mother-in-law, Ann Dickson, for the love and support she's provided my wife and my children.

Captain Jack McNamee for the leadership he's provided throughout my career and for setting standards I can only hope to meet.

My parents and my brothers for many years of encouragement, sacrifice, and support.

Finally, I would like to express my deepest appreciation to my wife Mary for her love, patience, and companionship. I love you.

Dedication

For Sarah, Matthew, and Michael.

Table of Contents

Title Page _____ 1

Abstract _____ 2

Acknowledgement _____ 3

Dedication _____ 4

Table of Contents _____ 5

Chapter 1. Introduction _____ 8

1.1 Motivation _____ 8

1.2 Background _____ 11

1.3 Approach _____ 14

Chapter 2. Theory _____ 16

2.1 Towline Dynamics _____ 17

2.2 Ship Motions and Seakeeping _____ 33

2.3 Statistics _____ 54

2.4 Towline Extreme Tension Prediction _____ 63

Chapter 3. Experimental _____ 69

3.1 Background _____ 69

3.2 Equipment Selection _____ 75

3.3 Project Planning _____ 97

Chapter 4. Results and Analysis _____ 100

4.1 Equipment Performance _____ 100

4.2 Evaluation of Cable Numerical Model _____ 124

4.3 Comparison of Measured Tension with Tension Predicted by the Nonlinear Extreme Tension Prediction Program ____ 126

4.4 Comparison of Measured Tension with Tension Predicted by Time Simulation ____ 133

Chapter 5. Conclusions ____ 140

5.1 Summary ____ 140

5.2 Recommendations for Future Work ____ 143

References ____ 145

Appendix A- Equipment Description ____ 148

Appendix B- Data Acquisition ____ 164

Chapter One

Introduction

1.1 Motivation

Modern seakeeping theory and the principles of extreme statistics can be used to improve the safety and efficiency of towing at sea (Milgram, Triantafyllou, Frimm, and Anagnostou, 1988). The recent loss of two oil barges off the coast of Puerto Rico due to towline failure is an example of the severity of the consequences of towline failure. The ability to accurately predict towline tensions under various environmental conditions influences towline design and the selection of towing speeds and courses (Milgram, 1993).

The United States Navy is presently decommissioning nuclear submarines at a rate of approximately five submarines a year. When a nuclear submarine is taken out of service (decommissioned) she is towed, on the surface, from her homeport to Bremerton, Washington and scrapped. Though her nuclear fuel is removed, the reactor is in place, and a defueled nuclear submarine is still a high value asset.

For many years the only approved method for towing U.S. Navy submarines

has been with an all wire towline attached to an Automatic Towing Machine (ATM). An ATM is mounted on the stern of the towing vessel and is designed to maintain constant tension in the towline. The ATM maintains a preset value of tension in the towline by paying out the towline when the tension exceeds the preset value and retrieving it when the tension is low. The number of United States Navy vessels equipped with ATM's is decreasing at a rapid rate. In 1994 there will not be enough vessels with ATM's to support the number of planned submarine decommissionings.

In order to tow the defueled submarines from the shipyards where their fuel is removed to the location where they will be scrapped the U.S. Navy must have an alternative to all wire towlines and ATM towing.

A typical towline consists of a short length of steel chain in series with a length of wire towline (Figure 1.1).

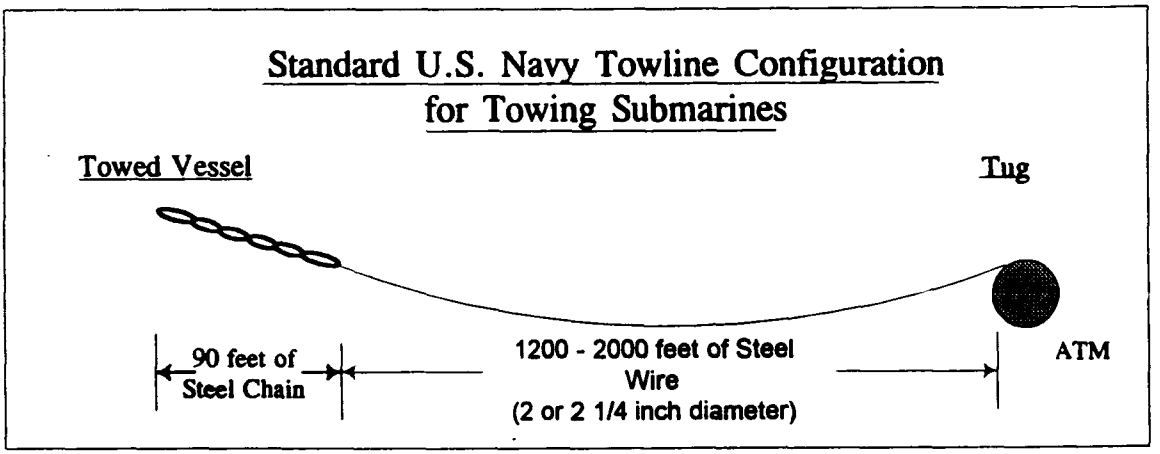

Figure 1.1

A towline's stiffness is a function of both the towline geometry and the towline's material properties. Endpoint dynamic motions introduce towline-water interactions which affect the relative influence of geometry and material properties on the total towline stiffness.

A "stretcher" can be added to the towline as an alternative to the ATM for controlling towline tension. A stretcher is a length of large diameter fiber rope with low stiffness. As its name implies, a stretcher accommodates changes in endpoint motions by stretching. The low stiffness minimizes the change in towline tension for a given change in endpoint separation. A towline with a length of stretcher, wire towline, and anchor chain is called a composite towline. Figure 1.2 shows an example of a typical composite towline.

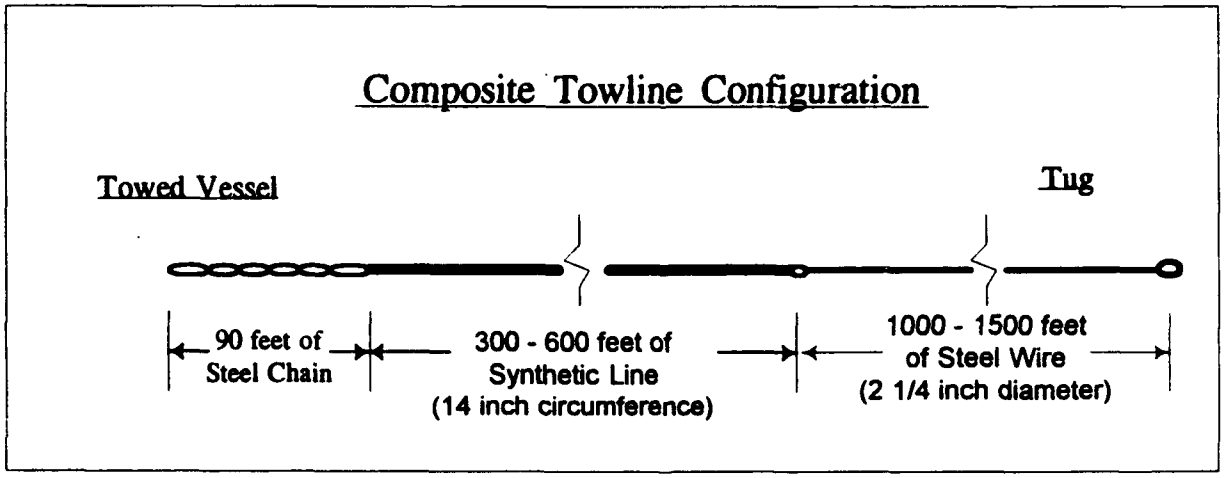

Figure 1.2

ATM's are widely used in the U.S. Navy. Stretchers are common in the commercial towing industry. The purpose of this research is to evaluate the suitability of composite towlines for U.S. Navy use and avoid backfitting of ATM's on the remainder of Navy's fleet of ocean-going tugs. The suitability of composite towlines for U.S. Navy is to be demonstrated by accurately predicting the statistics of their extreme tensions in a range of configurations, applications, and environmental conditions.

1.2 Background

The extreme tension is defined by the U.S. Navy Towing Manual (1988) as the sum of the steady and dynamic tension which has one chance in one thousand of being exceeded in one day of towing. The generation of the statistics of the extreme tensions in composite towlines is a mathematically and physically complicated problem due to the extremely non-linear behavior of the towline and the weakly non-linear hydrodynamic ship motions (Milgram, 1993). The behavior of this coupled non-linear system is driven by deterministic excitations- engine, throttle, and rudder changes) and stochastic excitations- the wind and the waves (Milgram, Triantafyllou, Frimm, and Anagnostou, 1988). The stochastic excitation of primary importance in towing is the excitation due to the wave-ship interactions.

Present towline extreme tension predictions use linear sea-keeping theory to predict ship motions. In linear sea-keeping theory the body's response in each of its degrees of freedom to excitation is expressed as a frequency dependent linear transfer function (Newman, 1977). When a random process is operated upon by a linear system, some aspects of the statistics of the random process are preserved. Wave excitation is typically modelled as a gaussian process, and in linear ship motion theory the ship responses are gaussian.

For most ship-sea interactions, linear sea-keeping theory works well. Non-linear wave-body interactions, specifically, those occurring at the difference frequencies of the incident irregular, random wave field, are important in open ocean towing (Faltinsen, 1990). Unlike motion in the pitch, heave, and roll modes of a freely floating object, surge motion does not experience large hydrostatic restoring forces. Therefore the surge motion of a vessel can be quite large. Normally, this is of little concern. Most sea-keeping prediction programs (MIT Five Degree of Freedom Sea-Keeping Program, 1975, and the David Taylor Model Basin Ship Motion Program, 1981), for example) do not predict surge motions. However, for two vessels coupled through a towline, large surge motions can cause large towline tensions. Accurate prediction of both first and second-order ship responses in irregular, random seas is important for this application and is one focus of current ocean engineering research.

The towing vessel and the towed vessel are free to move in all six of their respective degrees of freedom. The two vessels are coupled through the towline. The geometry of the system is shown in Figure 1.3.

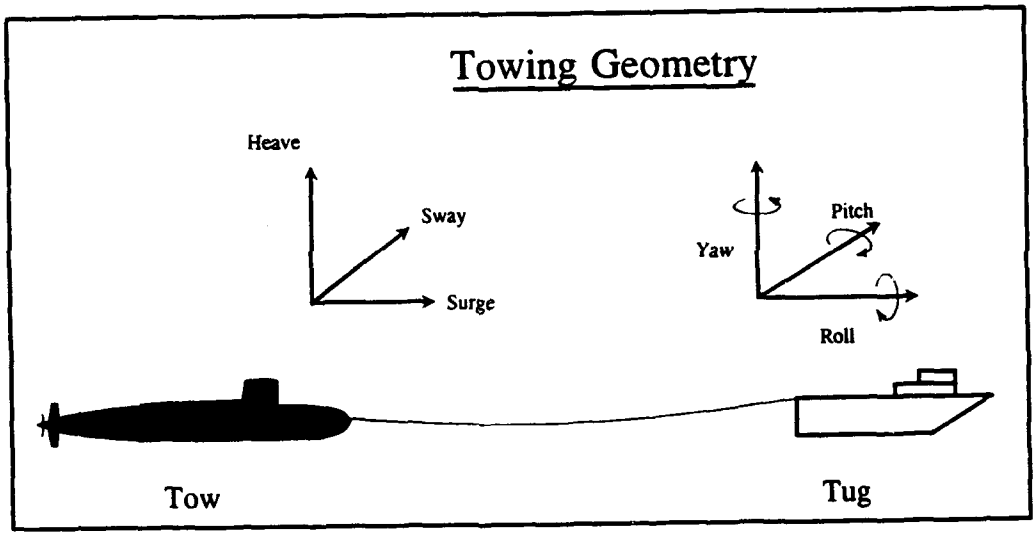

Figure 1.3

The ships' motions are driven by the random wave excitation and time-varying cable tension. The full problem is a twelve-degree-of-freedom system with non-linear feedback (Milgram, et. al., 1988).

The work of Milgram, Triantafyllou, Frimm, and Anagnostou (1988) and Frimm and Milgram (1991) form the basis for current methods for predicting the statistics of the extreme towline tensions in the offshore towing problem defined above. The former introduced the application of modern linear sea-keeping theory to the prediction of ship motions under tow.

Frimm and Milgram (1991) used off-shore towing test data to supplement the previous work. The previous work was found to under-predict the extreme tensions. Frimm and Milgram (1991) used an empirical correction factor based on measured low-frequency tension data to compensate for the under-prediction of the extreme tensions.

1.3 Approach

The purposes of this research are to demonstrate that a composite cable with a stretcher is effective at reducing dynamic tension and to improve the accuracy of prediction of extreme towline tensions.

The effectiveness of composite cables with stretchers in reducing dynamic tension will be demonstrated through the evaluation of test data obtained during a major full-scale open ocean tow measurement program designed and conducted as part of this research. The extreme tension prediction methods of Milgram and Frimm will be compared with the test data.

Extreme tension prediction methods will be improved by accomplishing the following:

(1) Development of a numerical model for solving the cable dynamics equation for a composite towline;

(2) Incorporating recent advancements in the prediction of second-order ship motions in the prediction of extreme tensions;

(3) Performing full time simulations of the tug-tow system and determining extreme tension statistics from these time simulations;

(4) Comparing the tensions predicted by incorporating the above improvements with the existing extreme tension prediction methods and the test data obtained during the open ocean tow; and,

(5) Development and analysis of experimental apparatus for measuring relevant tow system parameters.

Chapter Two

Theory

In this chapter the underlying physical and statistical processes involved in the prediction of the extreme tension in a towline are presented.

Problem Formulation

The prediction of the extreme tension in a towline in open ocean towing requires an accurate characterization or estimation of the following:

a. Sea state (frequency distribution of wave energy);

b. Linear ship motion frequency responses;

c. Second order ship surge frequency response functions;

d. Towline tension changes due to dynamical ship motions; and,

e. Towline extreme tension statistics using item d.

The time varying excitations causing the ship motions are the wave-ship interactions and the ship-towline interactions.

Complications

The numerical prediction of extreme tension is complicated by the following:

a. The towline behavior is highly nonlinear and a solution of the cable dynamics equations can only be done numerically;

b. The underlying physical process, the sea elevation spectrum is a random process;

c. Prediction of second order ship responses is difficult and at the forefront of current research in ship hydrodynamics; and,

d. The prediction of the response of a nonlinear system (the towline) operating on a random process (the sea elevation) is complicated and portions of the work must be performed numerically.

2.1 Towline Dynamics

The cable dynamics equations are (Triantafyllou, 1987):

$$m\frac{\delta^2 q}{\delta t^2} = (\bar{T}+T)\left(\alpha+\frac{\delta^2 q}{\delta s^2}\right) - b\frac{\delta q}{\delta t}\frac{\delta q}{\delta t} - \bar{T}\,\alpha \qquad (1)$$

with the dynamic tension, T, expressed as:

$$T = EA\left[\frac{p_o}{L} - \frac{\alpha}{L}\int_0^L q\,ds + \frac{1}{2L}\int_0^L \left(\frac{\delta q}{\delta s}\right)^2 ds\right] \qquad (2)$$

where:

m = cable mass per unit length

q = normal motions along cable

T = static tension

T = dynamic tension

α = catenary static curvature

s = Lagrangian coordinate along the cable

b = sectional drag factor

E = Young's modulus

A = cross-sectional area

p_o = tangential displacement due to mean static tension

L = unstretched cable length

These equations can not be solved analytically for the dynamic tension so they are solved numerically. The numerical solution is used to generate cable tension representations for use in determining the effect of the cable tension on the vessels in the tow system and for generating the extreme tension statistics. The two tension representations are a third-order polynomial representation and an equivalently linearized representation.

Polynomial Representation of Dynamic Tension

For statistical calculations and for fast numerical towing simulations, it is convenient to represent the towline tension as a polynomial in terms of the towline extension and its time-derivative. Milgram, et. al. (1988) used a third-order polynomial. This representation is expressed as:

$$T(\xi, \dot{\xi}) = \sum_{m=0}^{3} \sum_{n=0}^{3} a_{mn} \xi^m(t) \dot{\xi}^n(t) \tag{3}$$

with:

$$m+n \leq 3 \tag{4}$$

and:

$$(m, n) \neq (0, 0) \tag{5}$$

$\xi(t)$ is the towline extension.

The coefficients for the polynomial are found by minimizing the least square error between tensions calculated by the polynomial representation and tensions determined by numerically integrating the cable dynamics equations for a large set of cable extension time simulations (Milgram, et. al, 1988). The numerical integration scheme is a finite difference scheme with forward Euler time integration.

Figure 2.1 compares the results of the polynomial approximation with a measured towline tension. The measured towline extension, and its calculated time derivative, were used as inputs to the polynomial approximation.

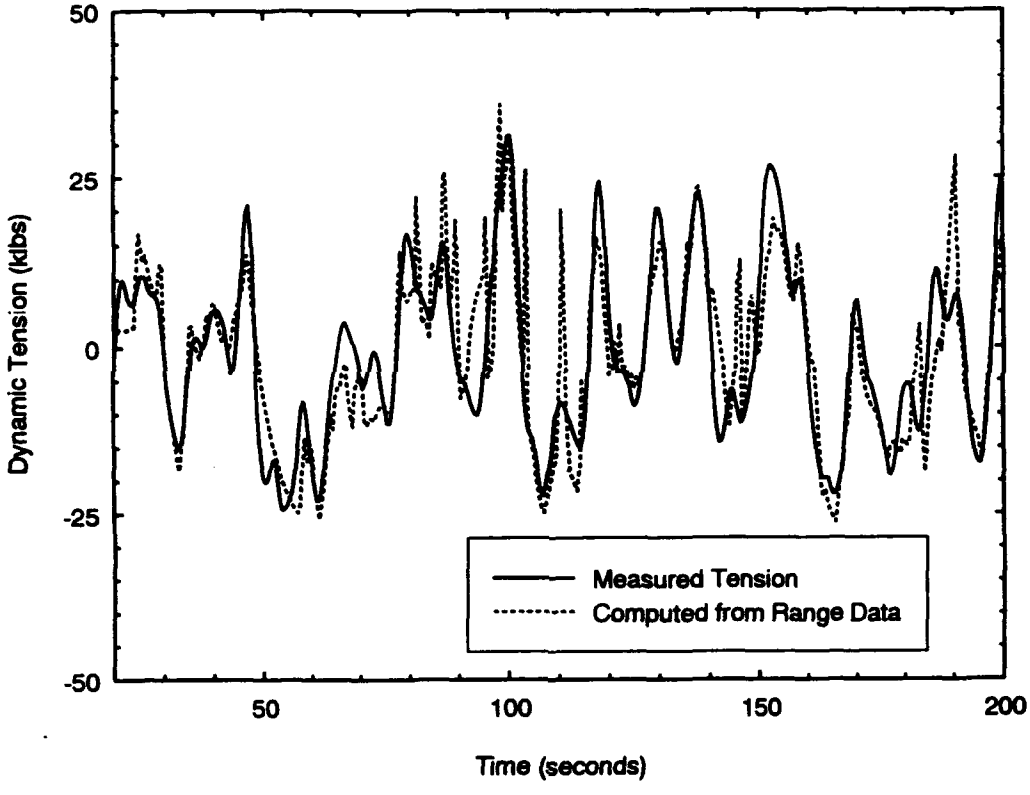

Figure 2.1

The polynomial approximation compares favorably with the measured tension data. The polynomial approximation generally over-predicts the peak tension. Thus, the polynomial's use in predicting extreme tensions is conservative on the side of safety.

In the experiment, the extension data was obtained by the use of a laser range finder. ıg-tow separation distance was measured during the data collection run and the difference between the measured separation and the mean separation distance during the run was recorded as the towline extension.

The towline extension data used as input for the above analysis was numerically corrected to overcome measurement discontinuities which are described in detail in subsequent chapters. The recorded towline extension data is evenly spaced in time with a sampling rate for the laser range finder system of 2Hz. The laser range finder was hand-held on the towing vessel during a data collection run and focused on a reflective target on the submarine. During significant sea states the operator occasionally was unable to maintain the laser range finder "on target" for 1-2 second intervals. These "dropouts" complicated the data analysis. The data collection runs lasted 45 minutes. During a data collection run the operator would average 3 to 4 dropouts per second. The gaps in the data were filled in by a linear function between the endpoints of the dropout. These gaps affect the analysis since the elongation and its time derivative are used in the polynomial approximation.

Equivalently Linearized Cable Model

Milgram et. al. (1988) used the method of equivalent linearization to develop a linear towline model for determining the influence of towline forces on the tug and tow motions. The method of equivalent linearization requires that the cross correlation function for the nonlinear system ($R_{NL}(t)$) equal the cross correlation function for the equivalent linear system ($R_L(t)$). That is:

$$E[T_{NL}(t)\,\xi(t+\tau)] = E[T_L(t)\,\xi(t+\tau)] \qquad (6)$$

where:

T_{NL} is the nonlinear towline tension model in the form of the third-order polynomial

T_L is the equivalent linear towline tension model

The equivalent linear towline tension model is to be expressed in the form:

$$T_L = k_{eq}\xi(t) + b_{eq}\dot{\xi}(t) \qquad (7)$$

Milgram et. al. (1988) assume that the towline extension is a gaussian random process and show that:

$$k_{eq} = a_{10} + 3a_{30}m_{0\xi} + a_{12}m_{2\xi} \qquad (8)$$

and

$$b_{eq} = a_{01} + 3a_{03}m_{2\xi} + a_{21}m_{0\xi} \quad (9)$$

where

a_{ij} are the polynomial coefficients

$m_{0\xi}$, $m_{2\xi}$ are the order zero and order two moments of the extension spectrum

In this project, the equivalent linear towline model is used to characterize the relationship between towline forces and the vessels' pitch and heave ship responses. This is permissible because the towline has only a minor influence on heave and pitch. The polynomial towline model is used in characterizing the effect of the towline force on the surge motions.

Quasi-Static Representation of the Dynamic Tension

Although the dynamic tension is most accurately determined by numerical integration of the cable equations or by use of the resulting polynomial approximation and the equivalently linearized model, a rough estimate and some understanding of the nature and importance of the cable dynamics can be obtained by using the cable's static tension curve and measured extension time history. A plot of cable static tension as a function of extension can be generated from the solution of the equations of static equilibrium for a cable supported between two endpoints. Figure 2.2 shows a differential element of a cable and the forces acting on the element.

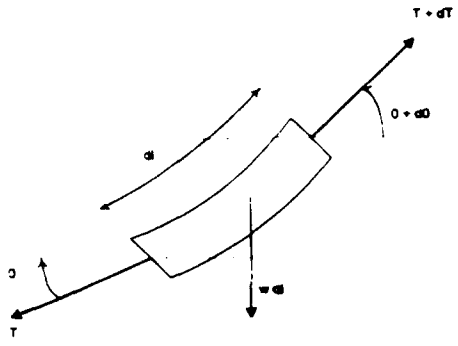

Figure 2.2

The equations of static equilibrium (Triantafyllou, 1990) are:

$$-T - w\sin\theta dl + (T + dT)\cos d\theta = 0 \qquad (10)$$

and

$$-w\cos\theta dl + (T + dT)\sin d\theta = 0 \qquad (11)$$

with

$$dx^2 + dz^2 = dl^2 \qquad (12)$$

and

$$e = \frac{T}{EA} \qquad (14)$$

The strain can be defined as:

$$e = \frac{dl - ds}{ds} \qquad (13)$$

For small angles, the above relations can be grouped to give the shallow sag cable equations (Triantafyllou, 1990):

$$\frac{dT}{ds} = w\sin\theta \tag{15}$$

and

$$\frac{dz}{ds} = (1 + e)\sin\theta \tag{16}$$

and

$$T\frac{d\theta}{ds} = w\cos\theta \tag{17}$$

and

$$\frac{dx}{ds} = (1 + e)\cos\theta \tag{18}$$

The cable equations can be combined and integrated (Triantafyllou, 1990) to yield:

$$T = \frac{H}{\cos\theta} \tag{19}$$

and

$$\tan\theta = \frac{V}{H} - \frac{w}{H}(L - s) \tag{20}$$

Figure 2.3 is a plot of the static tension-extension curves for a typical towline.

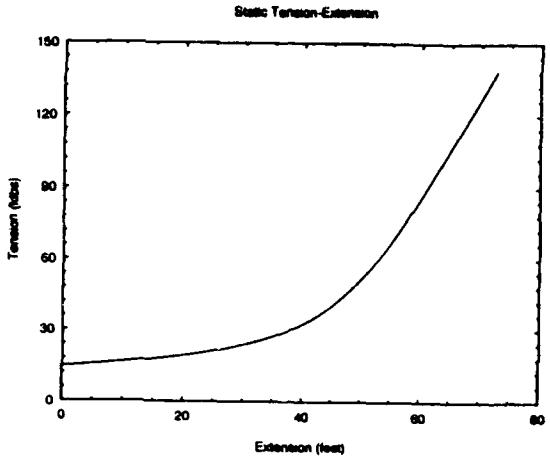

Figure 2.3

This curve and the measured towline extension from a data run were used to generate the quasi-static tension versus time curve shown Figure 2.4. This quasi-static curve, when compared to the measured towline tension time history for the same extension time history, shows considerable estimation error. This demonstrates the importance of the cable dynamics in estimating towline tensions.

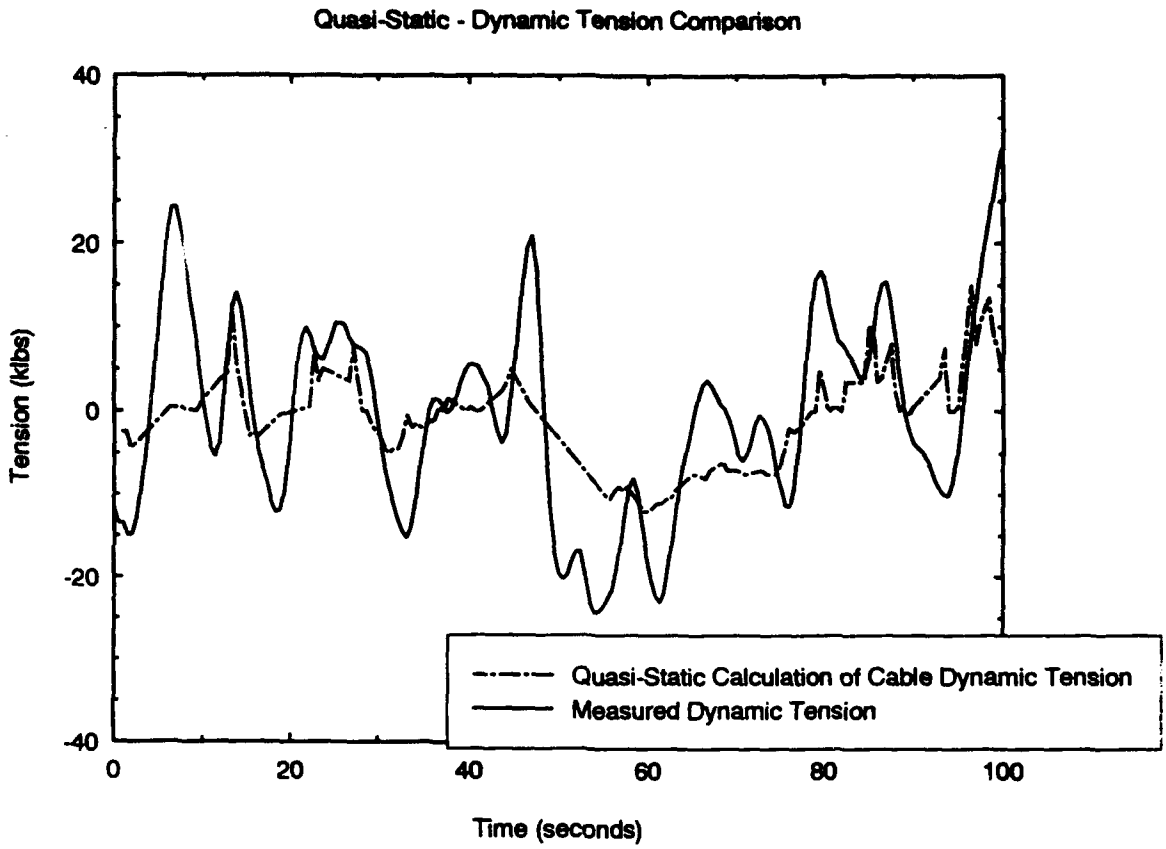

Figure 2.4

Towline Mechanical Properties

Towlines used in U.S. Navy open ocean tows use wire, chain, and synthetic line in various combinations depending on the type of vessel to be towed. A summary of the important mechanical properties of each of these towline components are provided below.

Wire Rope

Current U.S. Navy towing hawsers are usually 6 x 37 class, pre-formed, right-lay Improved Plow Steel (IPS), drawn galvanized wire rope of three types (U.S. Navy Towing Manual, 1988):

a. 2-inch diameter, fiber core

b. 2 1/4-inch diameter, fiber core

c. 2 1/4-inch diameter, Independent Wire Rope Core (IWRC)

Table 2-1 (U.S. Navy Towing Manual) summarizes the material properties of these wire ropes.

Table 2-1. Wire Rope Characteristics

Wire Type	Diameter (inches)	Weight in Air* (lbs/ft)	Breaking Strength (lbs)
Fiber Core	2	6.72	288,000
Fiber Core	2 1/4	8.51	360,000
IWRC	2 1/4	9.36	387,000**

* To get weight in water multiply by 0.87

** Breaking strength for extra improved plow steel is 444,600 lbs

Fiber Rope

Synthetic fiber rope acts as a spring in a composite towline. It responds to changes in dynamic loading by stretching with a relatively small change in tension. The U.S. Navy has used synthetic fiber rope in towlines for many years with mixed results. The synthetic fiber ropes originally used in the U.S. Navy for towing were made of nylon. Based on a large number of failures of nylon ropes, the U.S. Navy placed restrictions on their use (U.S. Navy Towing Manual, 1988) and initiated a program to evaluate the suitability of polyester towing hawsers. While nylon exhibits superior mechanical properties when dry, its properties when wet are significantly degraded. Table 2-2 (U.S. Navy Towing Manual, 1988) summarizes the relative characteristics of synthetic fiber ropes.

Table 2-2. Synthetic Fiber Ropes						
Fiber Type	Strength (1)	Cyclic Fatigue (2)	Bending Fatigue (2)	Abrasion Resis.	Heat Resis.	Creep
Nylon (Dry)	VG	VG	G	E	G	G
Nylon (Wet)	G	F	F	F	-	G
Polyester (Dry)	VG	VG	VG	VG	G	VG
Polyester (Wet)	VG	VG	G	G	-	VG
Polypropy-lene (Dry)	F	F	P	P	P	F
Polypropy-lene (Wet)	F	F	P	F	-	F

E = Excellent VG = Very Good G = Good F = Fair P = Poor

Table 2-3 summarizes the material properties of a sampling of the synthetic fiber towlines currently used by the U.S. Navy (U.S. Navy Towing Manual, 1988).

Table 2-3. Synthetic Fiber Rope Material Characteristics			
Fiber Type	Weight in Air (lbs/ft)	Circumference (inches)	Tensile Strength (lbs)
Polypropylene Three-Strand MIL-R-24049A	2.33	10	115,000
Dry Nylon Double-Braid MIL-R-24050C	5.24	14	508,000*
Polyester Double-Braid MIL-R-24677	6.46	14	527,000

*Wet nylon strength is 15% less than dry strength.

Chain Pendant

The chain pendant is used to connect the towline to the attachment point on the tow and serves one or more of the following functions (U.S. Navy Towing Manual, 1988):

a. A chafing-resistant strong terminal connection to the towed vessel;

and,

b. A means of absorbing dynamic loads in the towline, by virtue of its weight, which increases the depth of the catenary in the towline.

Table 2-4 is a summary of the chain mechanical properties.

Table 2-4. Anchor Chain Mechanical Properties

Weight per Foot (in air)*	39.2 lbs/ft
Typical Length	90 feet (one shot)
Cross Sectional Area of Links	6.28 in^2
Young's Modulus	30 x 10^6 lbs/in^2
Proof Test	322,000 lbs

* Weights in air must be multiplied by 0.87 to obtain weight in sea water

2.2 Ship Motions and Seakeeping

Sway, Heave, Roll, Pitch, and Yaw

The equations of motion for a single ship subject to wave and towline forces (Milgram et. al., 1988) are:

$$\left|-\omega_e^2 [M + A(\omega_e)] + i\omega_e B(\omega_e) + C\right| X e^{i\omega_e t} = F(\omega_e) e^{i\omega_e t} + F_H(\omega_e) e^{i\omega_e t} \quad (1)$$

where:

ω_e is the encounter frequency

M is the mass matrix

A is the added mass matrix

B is the damping coefficient matrix

C is the hydrostatic restoring force matrix

X is the displacement vector

F is the wave excitation force vector

F_H is the towline force vector

In this project no change to the method for predicting the sway, heave, roll, pitch, and yaw wave-ship interactions or the towline influence on these five degrees of motion was made relative to the work of Milgram et. al. (1988). The wave-ship

interactions in these five degrees of freedom are determined by the MIT 5-D Seakeeping Program (1975). The MIT 5-D Seakeeping Program is based on the ship motion theory of Salvesen, Tuck, and Faltinsen (1970). This ship motion theory is a linear theory based on the following assumptions:

a. The responses of a ship to irregular waves are a summation of the responses to regular waves of the contributing frequencies.

b. Strip theory[1] accurately predicts ship responses to wave excitation.

c. Viscous forces are negligible relative to inertial forces.

d. Wave slopes are much less than one.

Surge

The equation of motion for a ship being towed or one towing another ship in the presence of waves can be written in the form of Newton's second law:

$$(m + m_a(\omega))\frac{dV}{dt} = -\frac{1}{2}\rho S C_D(\omega) V(t)^2 + \frac{P}{V(t)} + T(t) + F_W(t) \quad (2)$$

[1]Strip theory assumes that the variation in flow in a ship's cross-sectional plane is much greater than the variation in flow in the longitudinal direction (Faltinsen, 1990). the ship is divided into a manageable number of sections and the hydrodynamic coefficients (added mass and damping) are calculated for each section and combined to determine the total ship added mass and damping coefficients.

where

m = mass of the ship

m_a = added mass; the added mass in surge is small in comparison to the mass, typically 3 - 7% of m, and relatively insensitive to frequency of oscillation.

V = velocity

ρ = density of water

S = wetted surface area

C_D = drag coefficient

P = propulsive power

T = towline force

F_W = force due to incident waves

-The first term on the right hand side of

equation (1) is the fluid drag force.

-P/V(t) is the thrust due to the propeller.

We multiply (1) by V(t):

$$V(t)\,(m + m_a)\,\frac{dV}{dt} = -\frac{1}{2}\rho S C_D V(t)^3 + P + V(t)T(t) + V(t)F_W(t) \quad (3)$$

Then the surge is expressed as a small perturbation about a steady mean velocity:

$$V(t) = V_o + \epsilon(t) \tag{4}$$

We then rewrite (3) as:

$$(V_o + \epsilon(t))\,(m + m_a)\,\frac{d(V_o + \epsilon(t))}{dt} = -\frac{1}{2}\rho S C_D (V_o + \epsilon(t))^3 + P + (V_o + \epsilon(t))T(t) + (V_o + \epsilon(t))F_w(t) \tag{5}$$

Expanding (5), dividing through by V_o, and keeping terms up to first order in ϵ gives:

$$\frac{d\epsilon(t)}{dt}(m + m_a) = -\frac{1}{2}\rho S C_D (V_o^2 + 3\epsilon(t)V_0) + \frac{P}{V_o} + T(t) + \frac{\epsilon(t)T(t)}{V_o} + \frac{(V_o + \epsilon(t))}{V_o}F_w(t) \tag{6}$$

Note that $\epsilon(t)/V << 1$ and $(V_o + \epsilon(t))/V_o \approx 1$. Therefore we can rewrite (6) as:

$$\frac{d\epsilon(t)}{dt}(m + m_a) = -\frac{1}{2}\rho S C_D (V_o^2 + 3\epsilon(t)V_o) + \frac{P}{V_o} + T(t) + F_w(t) \tag{7}$$

P/V_o is the steady thrust from the propeller. $1/2\rho S C_D V_o^2$ is the steady drag. For $V(t) = V_o + \epsilon(t)$ these terms are constants of equal magnitude. Under this assumption, the surge equation becomes

$$\frac{d\epsilon(t)}{dt}(m + m_a) = T(t) + F_w(t) - \frac{1}{2}\rho S C_D 3\epsilon(t) V_o \qquad (8)$$

Wave Excitation

The wave excitation, $F_w(t)$, consists of non-linear and linear wave-ship interactions.

Linear Wave Forces

The linear, or first order, surge exciting force is estimated by the Froude-Krylov force. The Froude-Krylov force is the force corresponding to the unsteady pressure induced by the undisturbed incident waves. The Froude-Krylov force ignores the effect of the ship on the incident waves.

The Froude-Krylov force is calculated by integrating the wave pressure on the ship's hull surface. The wave pressure is obtained by rearranging the linearized unsteady Bernoulli equation into the form:

$$p = -\frac{1}{\rho}\frac{\delta\phi}{\delta t} \qquad (9)$$

where

p = pressure

ρ = fluid density

ϕ = wave potential

The numerical integration of (9) is performed using the method of Milgram, Triantafyllou, Frimm, and Anagnostou (1988). This method uses the Gauss theorem to transform the surface integral of the wave pressure over the hull surface to a volume integral of the wave pressure gradient over the ship's immersed volume:

$$F_{FK} = \iint_S (\bar{I}p) \cdot \bar{n} ds = \iiint_V \frac{\delta p}{\delta x} dV \qquad (10)$$

The Froude-Krylov force oscillates at the frequency of the incident waves.

Second Order Wave Forces

The non-linear wave exciting forces are evaluated to second-order. The solution of the second order problem results in force with a non-zero mean and forces at the difference and sum of the incident wave frequencies (Faltinsen, 1990).

In linear wave theory, the quadratic velocity term in Bernoulli's equation is neglected. This term is retained in the derivation of the second order wave forces in irregular waves. The pressure due to incident waves can be expressed as:

$$p = -\rho \left(\frac{\delta \phi}{\delta t}\right) + \frac{1}{2} (\nabla \phi) \bullet (\nabla \phi) \qquad (11)$$

where:

p = incident wave pressure

ρ = fluid density

ϕ = velocity potential

For purposes of developing the form of the second order forces, the incident wave velocity potential will be expressed as the sum of two potentials of slightly different frequencies:

$$\phi = \frac{gA_1}{\omega_1} e^{k_1 z} \sin(k_1 x - \omega_1 t) + \frac{gA_2}{\omega_2} e^{k_2 z} \sin(k_2 x - \omega_2 t) \qquad (12)$$

where

g = gravitational constant

A = wave amplitude

ω = wave frequency

k = wave number = ω^2/g

The wave velocity potential consists of three separate potentials- the incident potential, the diffraction potential, and the radiated potential. For the purpose of illustrating the origin and nature of the second order forces, the velocity will be expressed as the gradient of a single potential:

$$V = \nabla\phi = \omega_1 A_1 e^{k_1 z}\cos(\omega_1 t + \delta_1) + \omega_2 A_2 e^{k_2 z}\cos(\omega_2 t + \delta_2) \quad (13)$$

where

δ_i = phase angle in x.

Substituting the square of (13) into (11) results in the following expression for the pressure:

$$p = \rho \frac{\delta \phi}{\delta t} + \frac{\rho}{2} [\omega_1^2 \frac{A_1^2}{2} + \omega_2^2 \frac{A_2^2}{2} + \omega_1^2 A_1^2 \cos(2\omega_1 t + 2\delta_1) + \omega_2^2 A_2^2 \cos(2\omega_2 t + 2\delta_2) + \omega_1 \omega_2 A_1 A_2 \cos[(\omega_1 - \omega_2)t + (\delta_1 - \delta_2)] + \omega_1 \omega_2 A_1 A_2 \cos[(\omega_1 + \omega_2)t + (\delta_1 + \delta_2)]] \quad (14)$$

This second order expression contains terms not found in the linear theory:

a. Steady interactions, proportional to the $\omega_i^2 A_i^2/2$ terms.

b. Unsteady interactions, oscillating at:

   1. Twice the wave frequencies
   2. The sum of two wave frequencies
   3. The difference of two wave frequencies

The interactions at the difference frequencies are important to towing. These interactions, for waves with slightly different frequencies, produce slowly varying ("drift") forces and moments which may cause resonance in surge (Faltinsen, 1990). If the natural frequency in surge is close to a difference frequency, large amplitude surge motion will occur, generating large towline tension.

The second-order wave-ship interactions at the difference frequencies are called the slow-drift forces and moments. Various methods have been formulated for estimating the slowly varying wave-drift interactions. The method chosen for this project is outlined below.

Second Order Force Estimation

The first step in determining the slowly varying surge force is to calculate the second order operators, $R(\omega_e)$, for the range of ship-wave encounter frequencies of interest. $R(\omega_e)$ is the ratio of second order force to wave amplitude squared.

The encounter frequency, ω_e , is defined (Newman, 1977) as:

$$\omega_e = \omega_o - \frac{\omega_o^2 U}{g}\cos\beta \qquad (15)$$

where:

ω_o = wave frequency

U = ship speed

g = gravitational constant

β = angle between wave and ship headings

The second order operators used for determining the slowly varying surge forces were generated from the seakeeping program NIREUS (Sclavounous, 1991).

NIREUS determines the second order operators (added resistance operators) by using strip theory and calculating, for each two dimensional section of a hull, the second order pressure due to the incident, diffracted, and radiated velocity potentials.

The second order wave forces are significantly affected by the relative vertical motion between the ship and the incident wave surface (Gerritsma and Beukelman, 1972). NIREUS takes the relative vertical motion into account in its calculation of the second order operators. A large number of closely spaced (in frequency) second order operators are generated by curve fitting through the operators calculated by NIREUS.

Figure 2.5 is a typical wave elevation spectrum (Newman, 1977). The lowest frequency in a standard wave elevation spectrum is typically 0.2 - 0.6 hz and is a function of sea state. The second order forces of practical importance are below this frequency. At frequencies above this cutoff, the second order forces, occurring at the difference frequencies are small compared to the forces occurring at the wave frequencies.

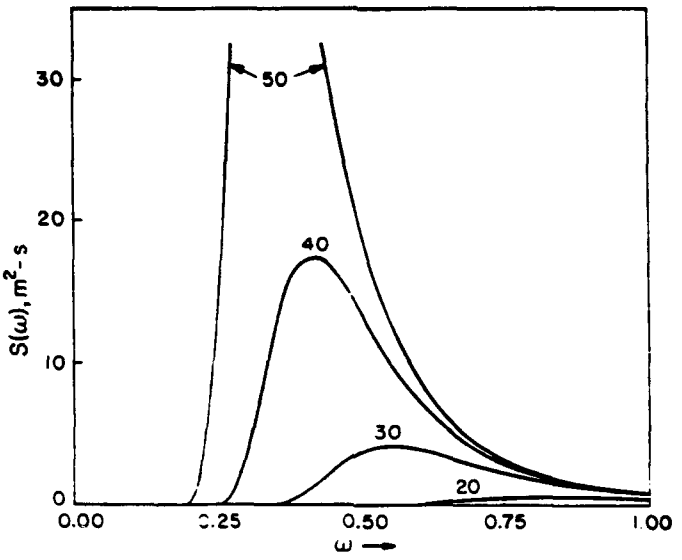

Figure 2.5

There is a second order operator and a wave elevation spectral density associated with each discrete frequency. The second order wave force time history is expressed as the following:

$$F_{SV}(t) = \sum_{j=1}^{N} \sum_{k=1}^{M} R\left(\frac{\omega_j + \omega_k}{2}\right) e^{i(\omega_j - \omega_k)t} \qquad (16)$$

where:

F_{SV} is the second order force

$R\left(\frac{\omega_j + \omega_k}{2}\right)$ is the average of the second order operators

for the two frequencies

If $\omega_j - \omega_k$ is small, the second order force oscillates with a frequency below the wave frequencies shown in Figure 2.5. If $\omega_j - \omega_k$ is large, the force oscillates at a frequency in the wave frequency range. The magnitude of the second order forces in the wave frequency range is small relative to the first order forces, on the order of 10 - 100 times smaller (Faltinsen, 1990).

Figure 2.6 shows two waves of equal amplitude and slightly different frequencies.

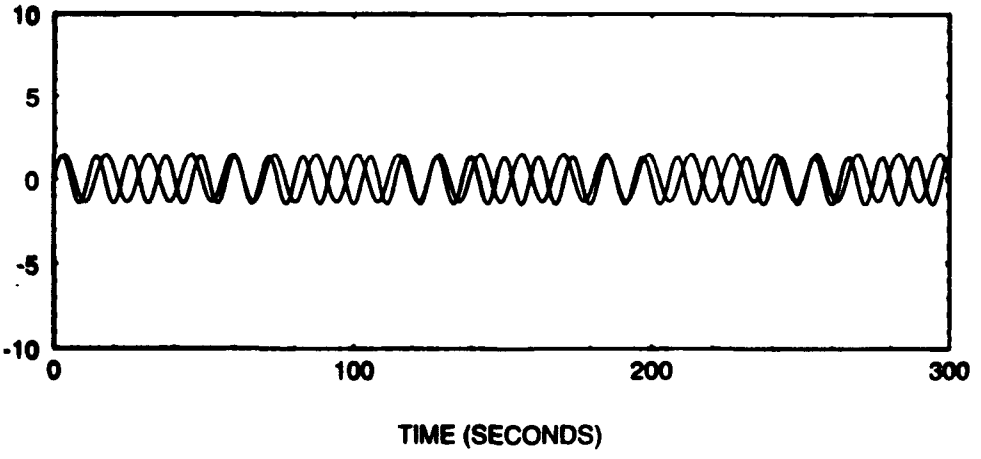

Figure 2.6

Associated with each of the two waves is a second order operator ($R(\omega_e)$). Figure 2.7 shows the wave which results from the interaction of the waves shown in Figure 2.6.

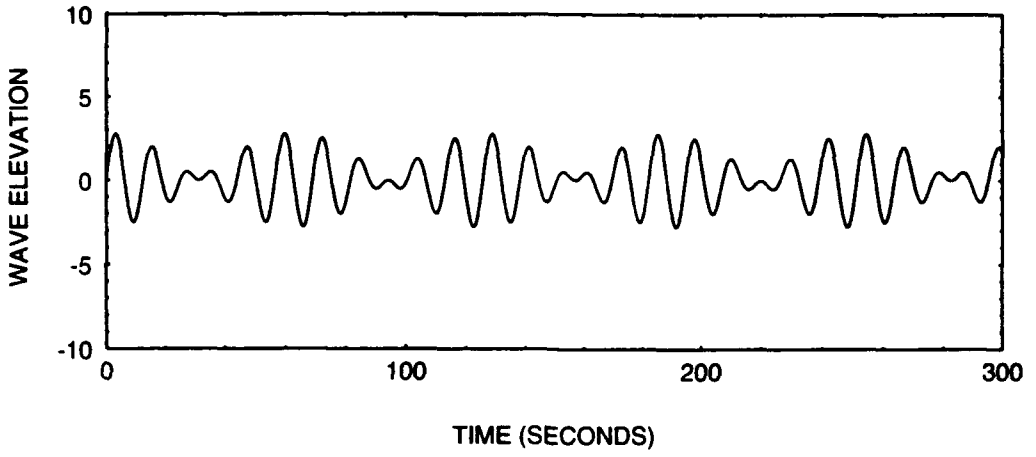

Figure 2.7

The envelope enclosing the wave in figure 2.7 varies with a frequency which corresponds to the difference frequency of the two waves. The amplitude of the slowly varying envelope amplitude is equal to the amplitude of the original waves.

The slowly varying force, F_{sv}, is obtained by applying the average of the second order operators for the two waves to the amplitude of the slowly varying wave.

Comparison of Wave Force and Towline Force Magnitudes

Although it is important to include the towline force in calculating ship motions, since it is the only spring-like surge restoring force, it is helpful to understand that the general magnitude of the time-dependent part of the towline force is small in comparison to wave force magnitudes.

Figure 2.8 is a plot of surge acceleration versus time for a typical data run .

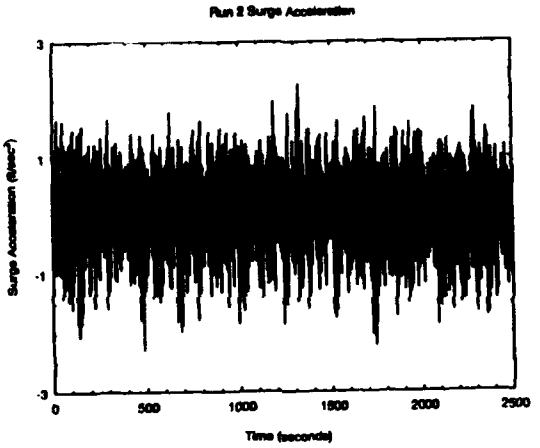

Figure 2.8

The maximum surge acceleration of the towing vessel (tug) for the above run is 2.50 ft/sec^2. The mass of the tug is 133,000 lbm. The total force on the tug is approximately 333,000 lbf. The maximum total towline tension on this data run was 64,000 lbf and the maximum dynamic tension was 30,000 lbf. The maximum wave force is about five times larger than the maximum towline force or about ten times larger than the maximum dynamic towline force.

A similar conclusion regarding the relative magnitude of the wave and towline forces was reached by Hara and Yamakawa (1994) by evaluating the distribution of the peak ship motions. In linear ship motion theory the peak ship motions follow a Rayleigh distribution. If the magnitude of the towline forces is small, the peak motions should follow a Rayleigh distribution despite their presence. Hara and Yamakawa produced experimental results which demonstrate the minimal effect of towline forces on ship motions. However, low frequency surge resonance must be considered as an exception.

System Natural Frequencies

The tow-tug system can be pictured as the spring-mass-dashpot system shown in Figure 2.9.

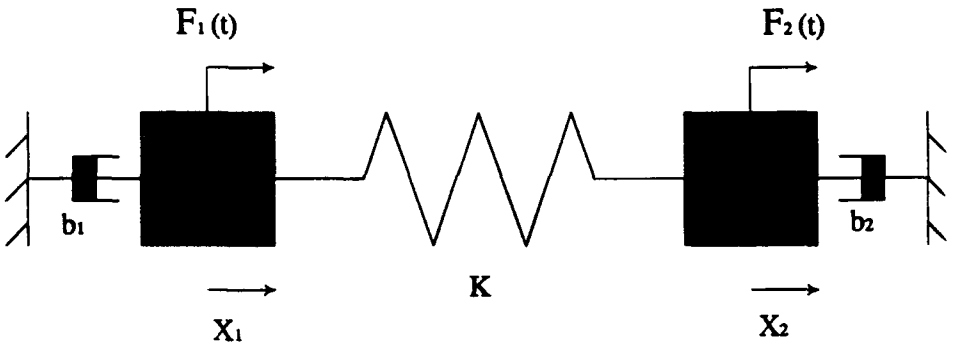

Figure 2.9

This system can be expressed as in matrix form as:

$$\begin{vmatrix} M_1 & 0 \\ 0 & M_2 \end{vmatrix} \begin{vmatrix} \ddot{X}_1 \\ \ddot{X}_2 \end{vmatrix} + \begin{vmatrix} b_1 & 0 \\ 0 & b_2 \end{vmatrix} \begin{vmatrix} \dot{X}_1 \\ \dot{X}_2 \end{vmatrix} + \begin{vmatrix} K & -K \\ -K & K \end{vmatrix} \begin{vmatrix} X_1 \\ X_2 \end{vmatrix} = \begin{vmatrix} F_1(t) \\ F_2(t) \end{vmatrix} \qquad (18)$$

with:

M_i = vessel mass

b_i = vessel damping

K_i = towline stiffness

$F_i(t)$ = external forcing

The system natural frequency is:

$$\omega_N^2 = \frac{K M_1 + K M_2}{M_1 M_2} \qquad (19)$$

System Damping

System damping is due to skin friction, wave radiation, eddy-making, and wave-drift damping (Faltinsen, 1990).

The system damping at wave frequencies (b_i) is determined by the slope of the speed-resistance curve,

$$b_i = \frac{d(\text{resistance})}{d(\text{velocity})} \qquad (20)$$

and, in the case of the tug, by the slope of the speed-resistance curve plus the propeller damping. Figures 2.10 and 2.11 are the speed- resistance curves for the tug and tow respectively.

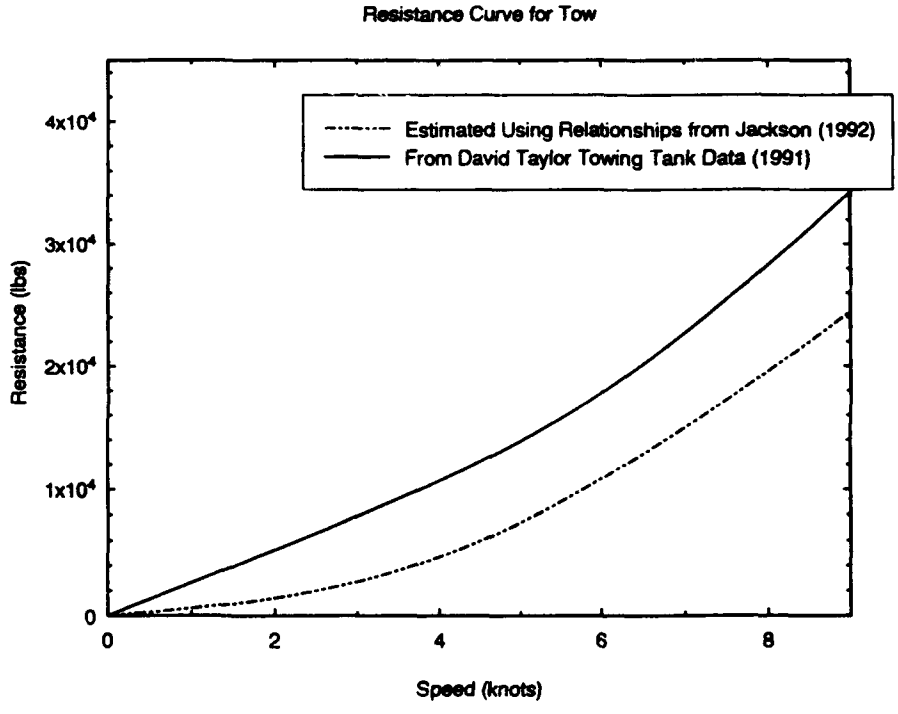

Figure 2.10

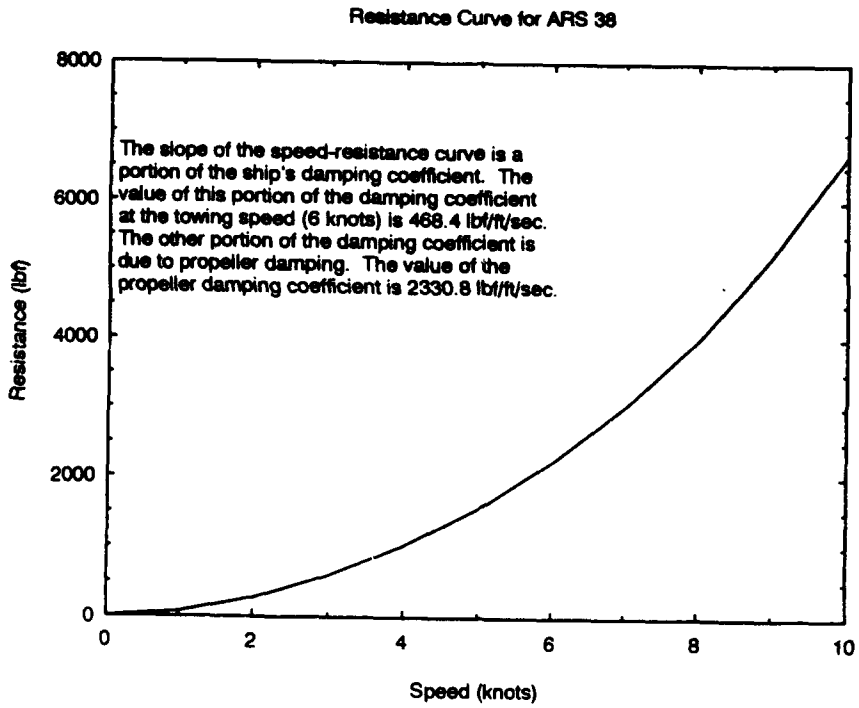

Figure 2.11

The propeller damping is more difficult to calculate. The towing vessels used by the U.S. Navy are powered by diesel engines. For a given throttle setting , a diesel engine is a constant torque machine. As the vessel surges, the propeller inflow velocity changes, changing the effective thrust of the propeller. The propeller damping coefficient as a result of this motion is expressed as (Frimm ,1987):

$$\frac{\delta T}{\delta V} = 2\rho D^2 (1-\omega)^2 \frac{V}{J} \left[\frac{\frac{dK_t}{dJ} K_q - \frac{dK_q}{dJ} K_t}{2K_q - J\frac{dK_q}{dJ}} \right] \qquad (21)$$

with:

T = thrust

V = velocity

ρ = water density

D = propeller diameter

ω = wake fraction

J = advance coefficient

K_t = thrust coefficient

K_q = torque coefficient

For low frequency ship motions, the wave radiation damping can be neglected and, for low frequency motions in higher sea states, the wave-drift damping is the dominant damping component (Faltinsen, 1990).

Stiffness

The spring constants for a towline are found by solving the cable static equations, equations 2.1-19 through 2.1- 20 for the change in tension due to a change in end point separation. These equations were solved numerically for the composite cable. Figure 2.12 shows the tension-extension relationship for the composite cables evaluated during the submarine towing project.

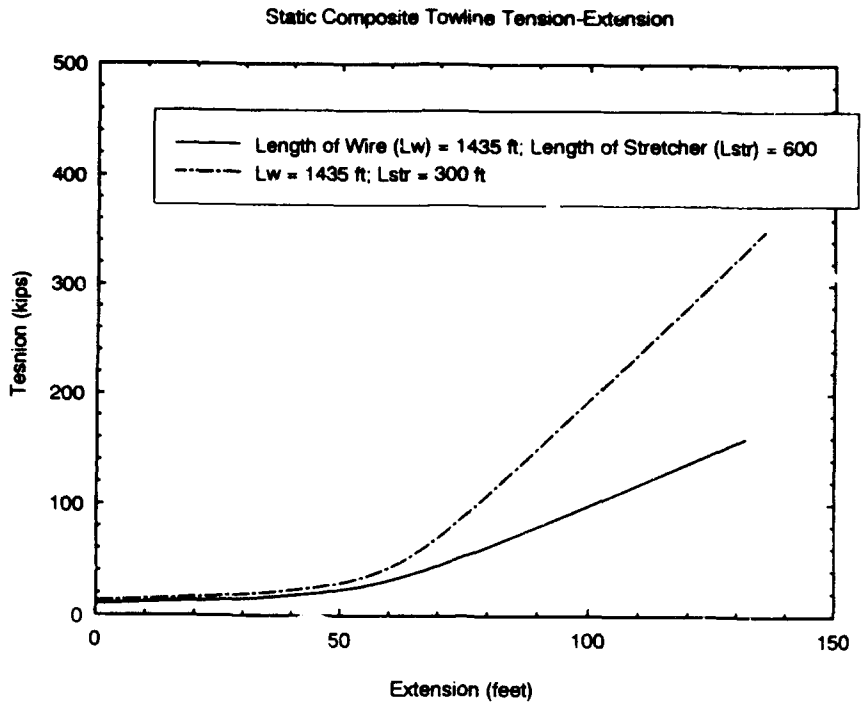

Figure 2.12

Figure 2.13 below is a plot of the spring constant as function of the towline extension for a typical towline.

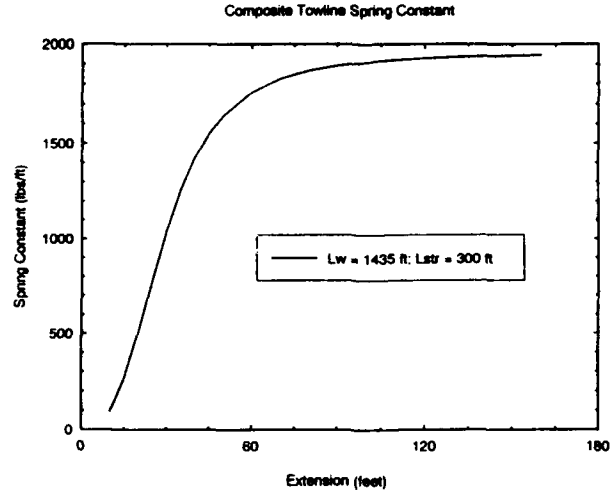

Figure 2.13

2.3 Statistics

Extreme Tension

Theory

The statistic of concern for U.S. Navy open ocean towing is the towline tension that has a 0.1% (α) chance of being exceeded in 24 hours (Δt) of towing (U.S. Navy Towing Manual, 1988). This tension is called the extreme tension. We denote this tension as:

$$T_{\alpha,\Delta t} \tag{1}$$

For a given time period the total tension consists of a steady component and a dynamic component. The steady component is governed by deterministic factors (towing speed, length of towline, tug and tow drag characteristics) while the dynamic component is a randomly distributed value. The statistical analysis required is the determination of the extremal statistics of the dynamic tension.

For a given dynamic tension time history, the probability that a selected tension at time t+dt will be exceeded is a function of the tension and the rate of change of tension at time t (Newland, 1984). Figure 2.14, from Newland, shows this graphically.

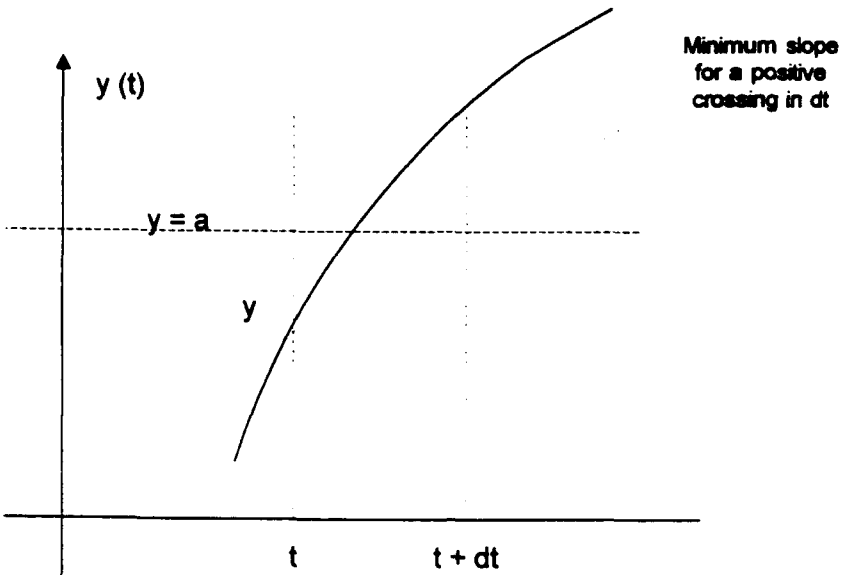

Figure 2.14.

The above concept is applied to the frequency with which the dynamic tension exceeds the extreme value. From the above it is clear that the joint probability density function (pdf) of the tension and its time derivative, $p_{T,\dot{T}} = f(T,\dot{T})$, is required to determine the frequency with which a tension level exceeds the extreme tension value. If the joint pdf is known, the rate of tension level crossings can be found by (Newland, 1984; Milgram et. al. , 1988):

$$N(T_o) = \int_0^{\infty} \dot{T} p_{T,\dot{T}} d(T, \dot{T}) \qquad (2)$$

If the peaks are distributed such that there is one extreme peak for each dynamic tension cycle (each zero level up-crossing), then the probability that the tension level will not be exceeded by any one tension peak is:

$$P_T(T_{ext}) = 1 - \frac{N(T_{ext})}{N(0)} \qquad (3)$$

Milgram et. al. (1988) relate (3) and (1) by the following:

a. The time interval, Δt, is equal to the product of the number of cycles, n, and the period of oscillation. The probability that the extreme tension will be exceeded during Δt is equal to :

$$[P_T(T_o)]^n \qquad (4)$$

where $P_T(T_o)$ is the probability that T_o will be exceeded for a single cycle.

b. $T_{\alpha,\Delta t}$ is defined as the tension level which has a probability of α of being exceed during Δt. Substituting, (1) into (4) gives:

$$[P_T(T_{\alpha,\Delta t})]^n = 1 - \alpha \qquad (5)$$

c. (5) and (3) are combined to yield the following:

$$T_{\alpha,\Delta t} = P_T^{-1}\left[(1 - \alpha)^{\frac{1}{N(0)\Delta t}}\right] \qquad (6)$$

The validity of the above method for estimating $T_{\alpha,\Delta t}$ is a function of the accuracy of the following assumptions:

a.. The extreme tension peaks are statistically independent; and,

b. There is only one peak tension for each zero up-crossing.

The accuracy of these assumptions is determined by:

a. The bandwidth of the underlying random process (Newland, 1984);

b. The sample time, Δt,; and,

c. The magnitude of the extreme peak.

The accuracy of these assumptions can be verified by an analysis of the experimental and simulated tension time histories.

Numerical Implementation

The extreme tension statistics will be estimated two ways. The first way will be to use directly the probability computations of Milgram ,et. al. (1988) with an

empirical correction for the slowly varying ship motion and tension (Frimm and Milgram, 1991). The second way will be to perform a 1000 day time simulation of an open ocean tow and determine the extreme tension by histograms of the generated tension time history. The extreme tensions predicted by both methods- for the same vessels, towline, and environmental conditions, will be compared.

Probability Computations

This project is an extension of the work started by Milgram et. al. (1988) and continued by Christensen (1989) and Frimm and Milgram (1991). The procedure for predicting extreme tensions is taken from this earlier work with the improvements in solving the cable dynamics equations for composite cables and improved low frequency tension predictions developed in this project incorporated into the procedure. A full explanation of the numerical method for predicting the extreme tension is provided by Milgram et. al. (1988). The significant aspects of the method are:

a. The rate of tension level crossings (2) is expressed as an expectation in terms of the pdf of the towline extension and its first and second time derivatives. This expression relies on the approximation of the tension as a third order polynomial in terms of the extension and its time-derivative (equation 2.1-3).

b. The towline extension is approximated as a gaussian random process

with zero mean whose joint pdf, $p_\xi(\xi,\xi,\xi)$, is expressed in terms of its spectral moments using, from (Parzen, 1960),:

$$f_{x_1,\ldots,x_n}(x_1,\ldots,x_n) = \frac{1}{(2\pi)^{n/2}} \frac{1}{|K|^{1/2}} \exp\left[-\frac{1}{2}\sum_{j,k=1}^{n} (x_j)\, K^{jk}\, (x_k)\right] \quad (7)$$

where:

K is the covariance matrix. The matrix elements are determined by the solution, in the frequency domain, of the twelve degree of freedom model of the tug-tow system.

The accuracy of (a) is driven by the accuracy of the polynomial expression for the tension.

The validity of (b) is determined by the extent to which the extension is a gaussian random process, which, in turn, is determined by the extent to which the ship motions can be considered a linear time invariant process operating on a gaussian sea state.

Milgram, et. al. (1988) use strictly linear ship motion theory, justifying the use of (b). Second order surge motions, not included in the earlier theory have been deemed to be important (Frimm and Milgram, 1991). Since these second order motions lead to a non-gaussian process, including them requires an altered theory

(Longuet-Higgins, 1963). Frimm and Milgram (1991) concluded that a conservative estimate of the increase in total extreme tension due to the second order motions is twice the RMS value of the low frequency tension.

Frimm and Milgram (1991) estimated the low frequency tension contribution by determining the low frequency tension component of a measured tension time history as a function of sea state. The measured data were extrapolated to higher sea states. Figure 2.15 is a plot of the estimated low frequency contribution to towline tension.

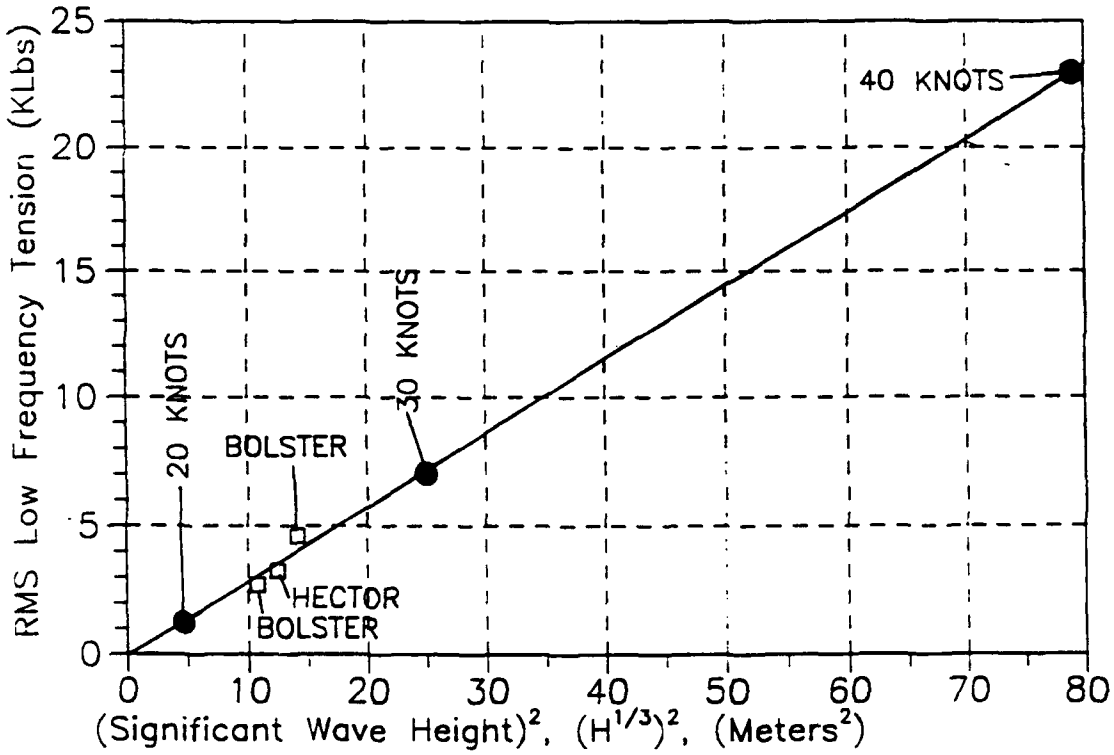

Figure 2.15

Time Simulations

The concept behind generating statistics from time simulations is straightforward. The twelve degree of freedom tug-tow system is modelled completely, solved in the time domain for the time period of interest, and the generated towline tension time history is scanned to determine the extreme tension for the time period.

Like the method above, accuracy of the time simulations depends on an accurate representation of the wave-ship interactions, an accurate representation of the waves, and an accurate towline model. However, the accuracy of the time simulations relative to the method outlined above should improve due to the elimination of the probabilistic approximations.

In the time simulations the vessels' relative position, velocity, and acceleration are determined at time t_o by solving the vessel equations of motion with the excitation provided by the waves and the towline. The wave spectrum used in the simulations is either a measured sea spectrum from a data run or a Pierson-Moskowitz spectrum. The towline tension model used the equivalent linear model for linear ship heave and pitch motions and the polynomial tension expression for the surge simulation and extreme tension prediction. The vessel displacements are calculated form the original

position are calculated and used to update the polynomial and equivalent linear towline models.

2.4 Towline Extreme Tension Prediction

Problem Solution

Two methods for predicting extreme towline tensions in offshore towline presently exist:

a. Nonlinear extreme tension prediction program.

b. Time domain simulation of the complete towing problem.

Figure 2.16 shows the basic flow path for the nonlinear extreme tension prediction program (Milgram, et. al, 1988). Figure 2.17 shows the flow path for the time simulation.

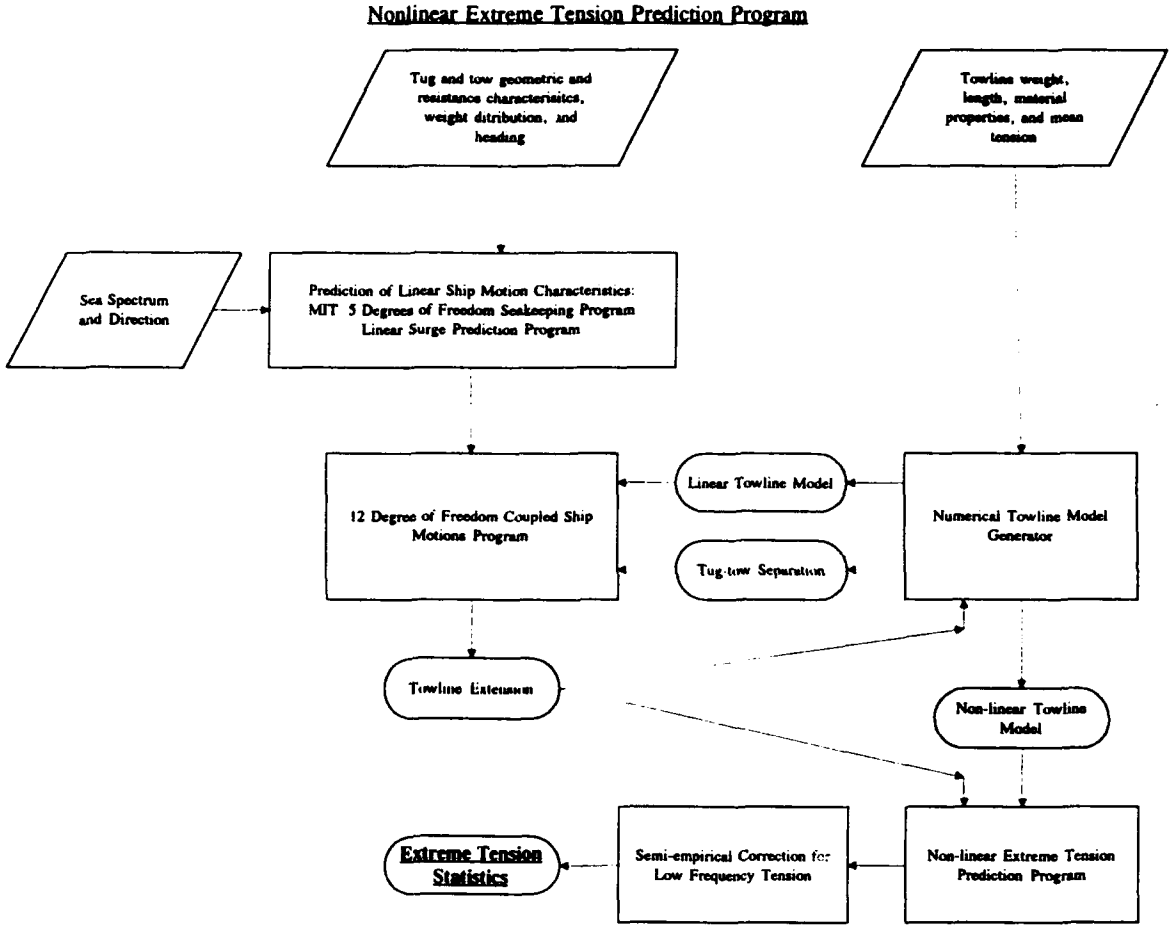
Nonlinear Extreme Tension Prediction Program
Tug and tow geometric and resistance characteristics, weight distribution, and heading
Towline weight, length, material properties, and mean tension
Sea Spectrum and Direction
Prediction of Linear Ship Motion Characteristics: MIT 5 Degrees of Freedom Seakeeping Program Linear Surge Prediction Program
12 Degree of Freedom Coupled Ship Motions Program
Linear Towline Model
Tug-tow Separation
Numerical Towline Model Generator
Towline Extension
Non-linear Towline Model
Extreme Tension Statistics
Semi-empirical Correction for Low Frequency Tension
Non-linear Extreme Tension Prediction Program

Figure 2.16

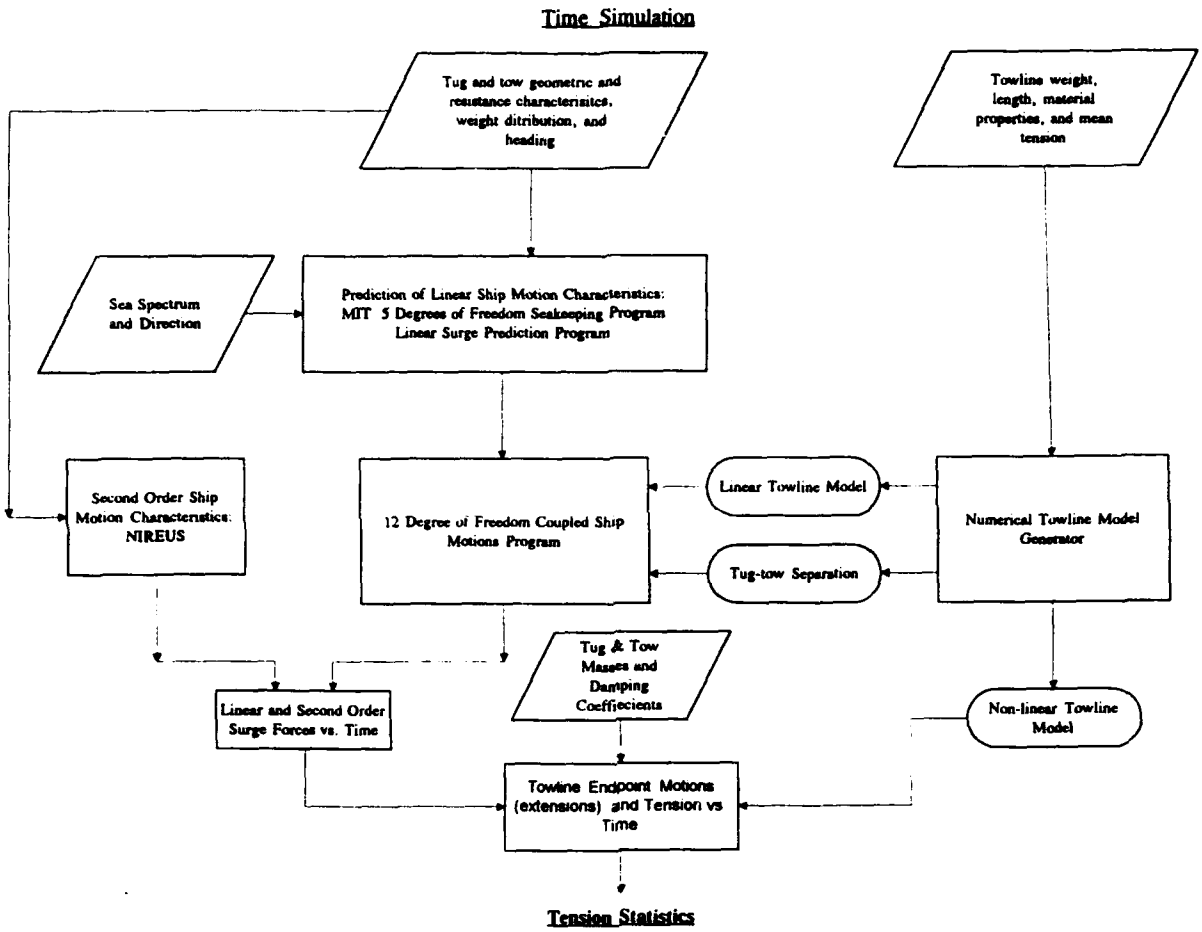
Time Simulation
Tug and tow geometric and resistance characteristics, weight ditribution, and heading
Towline weight, length, material properties, and mean tension
Sea Spectrum and Direction
Prediction of Linear Ship Motion Characteristics: MIT 5 Degrees of Freedom Seakeeping Program Linear Surge Prediction Program
Second Order Ship Motion Characteristics: NIREUS
12 Degree of Freedom Coupled Ship Motions Program
Linear Towline Model
Tug-tow Separation
Numerical Towline Model Generator
Tug & Tow Masses and Damping Coeffiecients
Linear and Second Order Surge Forces vs. Time
Non-linear Towline Model
Towline Endpoint Motions (extensions) and Tension vs Time
Tension Statistics

Figure 2.17

The computer programs required to complete the process charted in Figure 2.16 are:

a. MIT 5D Seakeeping Program. MIT 5D requires as input:

   1. Tug underwater hull geometry, naval architectural characteristics, and propeller characteristics.
   2. Tow underwater hull characteristics, naval architectural characteristics, and propeller characteristics.
   3. Towing speed and relative ship-wave heading.
   4. Frequencies for calculating ship motion responses.

b. NEWSRG1, a linear surge response program. NEWSRG1 requires similar input to that required for executing the MIT 5D program.

c. CABNEXP, a program for determining the coefficients for the polynomial representation of the towline tension. CABNEXP requires as input:

   1. Towline segments' material and geometric properties.
   2. Anticipated mean tension.

d. PMSPEC, a program for generating a Pierson-Moscowitz wave elevation spectrum[1]. The required input for PMSPEC is wind speed.

d. 12DNEW, a program which solves the coupled 12 degree of freedom problem defined earlier, using output from each of the above programs.

e. NLEXTR5, a program for predicting extreme towline tension. NLEXTR5 requires as input:

1. Towline extension spectral moments, m_0, m_2, and m_4 (Output from 12DNEW).
2. Mean tension, towline length, tow speed, relative ship-wave heading, and wind speed.
3. Coefficients for the polynomial representation of the towline tension.

The semi-empirical correction to the towline tension due to low frequency motions identified earlier is added to the extreme tension predicted by NLEXTR5.

The programs required to complete the process indentified in Figure 2.17 are:

a. MIT 5D Seakeeping Program.

b. NEWSRG1.

[1]Any sea spectrum can be used as this portion of the input. A measured sea spectrum is preferred for some applications.

c. CABNEXP.

d. PMSPEC.

d. 12DNEW.

e. RWAVETOW, a program for determining the first and second order forces acting on the tug and tow vessels. RWAVETOW requires the following as input:

1. Output from NEWSRG1 and 12DNEW. These outputs are the ship motion transfer functions.
2. Second order surge added resistance operators (transfer functions).

f. SURGESIM, a program for calculating the towline tension time history using the first and second order forces calculated by RWAVETOW. In addition to the output from RWAVETOW, SURGESIM requires as input:

1. Tug and tow masses and added masses.
2. Tug and tow damping coefficients.
3. The coefficients for the polynomial representation of the towline tension.

SURGESIM is run for 2500 days and the highest tension peak is read directly from the time record.

Chapter Three

Experimental Preparation

3.1 Background

Introduction

The data for this project were acquired during a "Tow of Opportunity". This was the Navy tow of the SSN 637 class submarine ex-USS Ray (SSN 653), first by the ARS 50 class salvage ship USS Grapple (ARS 53), and then by the ARS 38 class rescue ship USS Bolster (ARS 38). The tow of the ex-USS Ray occurred during the summer of 1993. Figure 3.1 is the track of the tow of the ex-USS Ray. It left Charleston, South Carolina on July 18, and arrived in Bremerton, Washington on September 5.

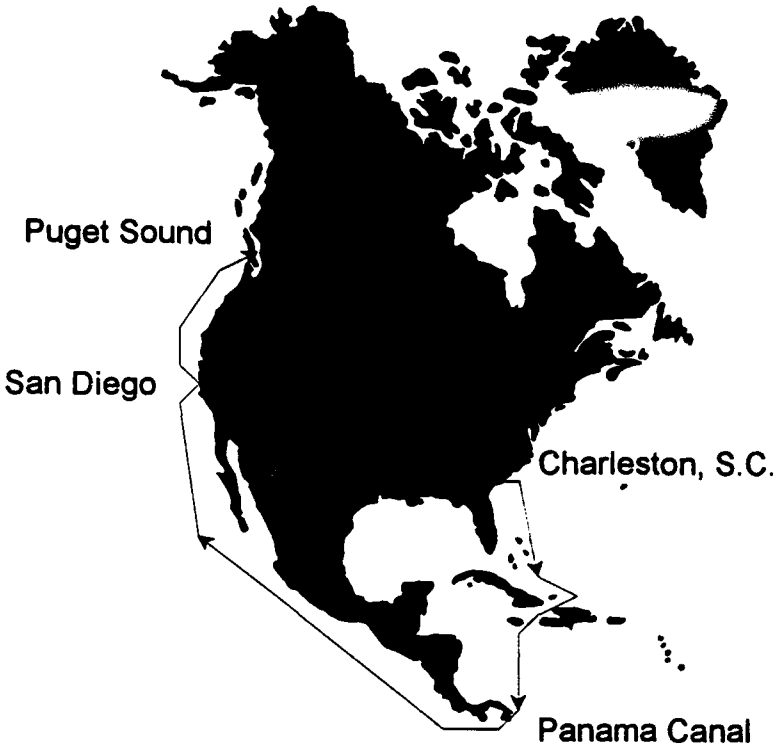

Figure 3.1

The tow consisted of three distinct legs- from Charleston, South Carolina to Panama, from Panama to San Diego, California, and from San Diego, California to Bremerton, Washington. In anticipation of weak seas and anticipated equipment

debugging while in the Atlantic Ocean, the first leg was to be used as a calibration run.

Since the tow was a scheduled Navy event the data acquisition had to be planned to have little or no impact on the progress of the tow. Additionally, personnel are prohibited from boarding nuclear submarines being towed. That is, once underway, the equipment onboard the submarine can not be adjusted or repaired until the tow is pierside. The above two factors significantly affected the data acquisition plan and the data acquisition equipment selection.

Data Requirements

A considerable amount of equipment is required to obtain the data necessary to fully quantify the twelve-degree of freedom problem outlined in the previous chapter. Data must be acquired in four areas. These areas are:

1. Tug motions.
2. Tow motions.
3. Towline tension and elongation.
4. Environmental (Wind and Waves).

Identification of Critical Parameters

Prior to selecting the equipment required to support data acquisition in the four areas listed above, the parameters essential to the prediction of towline extreme tension statistics and to the validation of the analytical and numerical models must be identified. Based on a review of similar towing projects (Frimm and Milgram, 1991; Christensen, 1989), the following parameters were considered to be critical to the success of the project:

1. Towline tension.
2. Towline elongation.
3. Wave spectra.

Towline Tension

The importance of accurately measuring towline tension is obvious.

Towline Elongation

Towline elongation is vital for two fundamentally important reasons.

First, an accurate time history of towline elongation can be used to validate the

composite towline numerical model directly. This can be done in two ways. The first is to use the measured elongation as "input" to the cable differential equations and make a comparison between the tension time history predicted by the numerical solution and the measured tension time history. Alternatively, the towline elongation and its calculated time derivative can be used as the end point motion input to the numerical composite towline model and the predicted towline tension time history can be compared with the measured towline tension time history.

The towline elongation can provide an estimate of the tow system's behavior. For this project, the tow's displacement and drag were significantly larger than that of the tug. The magnitude of the tug's wave frequency surge motions was estimated to be significantly larger than that of the tow. Therefore, most of the towline elongation at wave frequencies was expected to be due to tug surge motion. The towline elongation provides a reliable measure of the relative surge motions between the two vessels.

Wave Measurements

Two principal options are available for measuring waves, ship-mounted sensors and wave measurement buoys. Ship-mounted wave sensors use a microwave radar system that bounces radar waves off the wave surface and measures the doppler shift of the returned signal (Christensen, 1989). The doppler shift is proportional to

the surface relative velocity. A fundamental problem with ship mounted wave measurement devices is that the ship and ship motions influence the surrounding wave field (Sellars, 1967). Additionally, the ship's pitching and heaving motions must be known and the doppler shift corrected for these motions to get the actual sea motion.

The wave motions in the proximity of a moving ship are the sum of the incident waves, the waves diffracted by the ship, and the radiated waves due to the ship's motions. Ship mounted wave measuring devices are typically bow-mounted on extension arms to maximize the distance between the ship and the measuring device and thus minimize the ship's influence on the measured waves. The wave measurement device is calibrated, and ship influence corrected for, by comparing the device's output with the wave spectrum measured by a wave measurement buoy.

Previous towline measurement projects suffered from the use of poorly constructed ship mounted wave measuring devices (Frimm and Milgram, 1991). The output of the ship mounted wave measurement device used by Frimm and Milgram was compared to the wave spectra measured by National Oceanic and Atmospheric (NOAA) buoys. Based on this comparison they determined that the spectra measured by the ship-mounted devices was unusable.

Based on the experience of Frimm and Milgram wave buoys were used for wave measurement.

3.2 Equipment Selection

A general description of the equipment required to obtain data in the four areas identified earlier follows. The selection of the equipment was strongly influenced by the work of Christensen, "Plans and Specifications For A Full Scale Towing Model Validation Experiment" (1989). A detailed description of the experimental apparatus is provided in Appendix A.

Tug Motions

The motions of the tug in its six degrees of freedom were measured using a "Six Degree of Freedom Stable Platform" leased from the National Research Council of Canada's Institute for Marine Dynamics (IMD). The Six Degree of Freedom Stable Platform provides analog output proportional to the following:

1. Roll
2. Pitch
3. Yaw
4. Heave
5. Surge
6. Sway
7. Roll Rate

8. Pitch Rate

9. Yaw Rate

The above motions are defined in Figure 3.2.

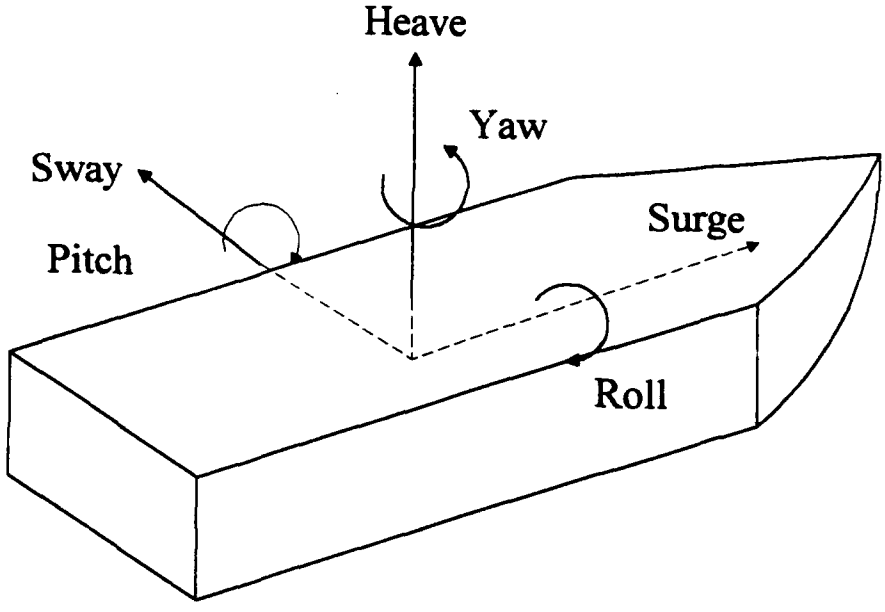

Figure 3.2

It is desirable to locate the motion sensors near the center of gravity (CG) of the vessel. Installed shipboard equipment prevented locating the Six Degree of Freedom sensor at the vessels' CG's. The acquired motion data were corrected for the separation between the sensor's installed location and the ship's CG.

The tug's speed over ground was measured using a Global Positioning System (GPS) receiver. The GPS receiver provides a continuous record of the ship's latitude and longitude. The accuracy of the receiver is +/- 30 meters.

The tug's heading partly defines the tow geometry. The tug's heading was measured using an electronic fluxgate compass.

Tow Motions

A Six Degree of Freedom Stable Platform, a GPS receiver, and a fluxgate compass were used to acquire the motion, speed, and heading of the submarine. Acquisition of the tow data was made difficult by the fact that the tow could not be boarded after leaving port. Therefore, the tow had to be provided with an electrical power system and a system for transmitting data to the tug for analysis.

The relative position of the tug and the tow, as measured by the two GPS

receivers, was to be compared with the tug heading to determine the time history of the "shearing" of the tow. When a tow deviates form a position directly abaft the tug it is said to be "shearing". The acquired GPS data were not accurate enough for this purpose.

Electrical Power

Table 3-1 summarizes the power requirements for the equipment onboard the tow.

Table 3-1. Tow Vessel Power Requirements

Item	Current (Amps)	Voltage (Volts)	Power (Watts)
Stable Platform	2.5	28.0 DC	70.0
Compass	0.080	12.0 DC	0.1
GPS Receiver	0.2	12.0 DC	2.4
FM Telemetry Modem	4.0	12.5 DC	25.0
Load Cell Signal Conditioner	0.001	12.0 DC	0.01

Data Acquisition Computer	2.7	120.0 AC	324.0
Computer Monitor*	0.7	120.0 AC	84.0
Total	9.98	-	505.5

* Turned off during towing.

Six marine gel cell batteries were used as the primary energy source for the equipment listed in Table 3-1. The cells provide 12 volt DC power and have a 450 amp-hour rating.

The batteries did not have sufficient stored energy for continuous operation of the data acquisition system and transmitter over the course of any of the three legs of the tow. Therefore, an automatic timer was installed to turn on the system only during the data acquisition runs. Data acquisition was limited to two 45 minute periods each day.

The batteries were charged during towing by two solar powered and two wind powered electrical generators. The two solar powered generators were each rated for 48 Watts @ 14 volts. The two solar powered generators were capable of producing a total of 36 Amp-hours per day. The two wind powered generators were each rated for 6 Amps at a wind speed of 19 knots.

The wiring diagram for the electrical system is shown as Figure 3.3.

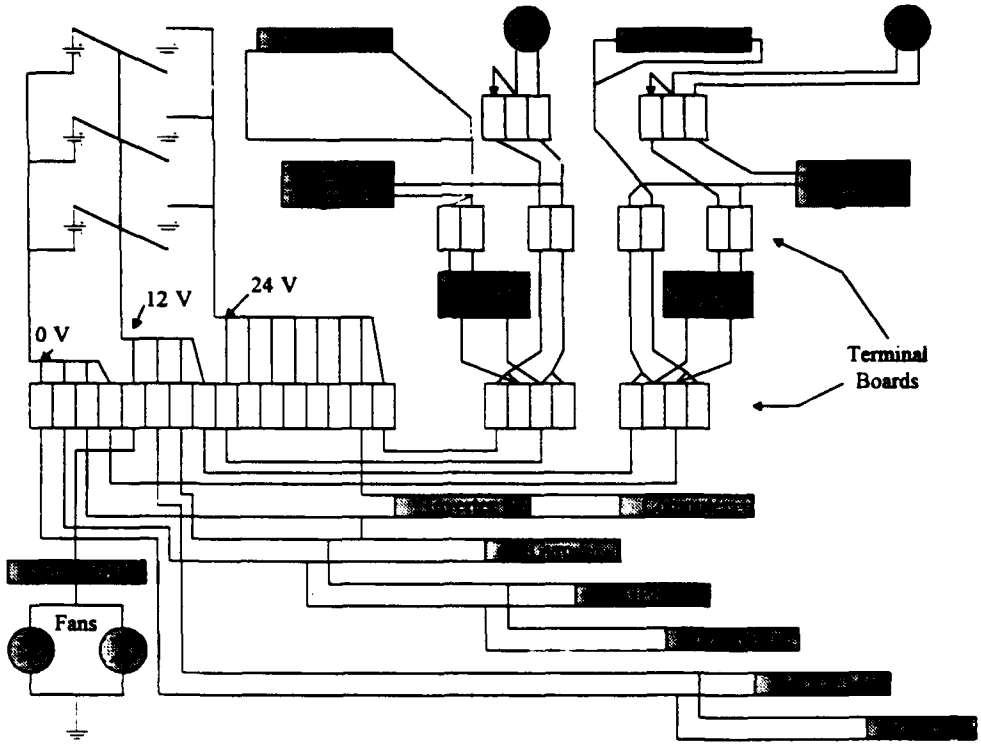

Figure 3.3

Telemetry

The digitized data acquired on the tow was transmitted to the tug via a Radio Frequency (RF) modem. The analog outputs from the data acquisition equipment were linked to the RF modem through a computer with an analog-to-digital converter

housed on the tow.

The advantages and disadvantages of analog FM telemetry and digital data transmission via an RF modem are discussed fully in previous works (Christensen, 1989; DeBord, Purl, Mlady, Wisch, & Zahn, 1987) and are summarized in Table 3-2 below.

Table 3-2. Telemetry System Relative Merits

System	Advantages	Disadvantages
FM	Transmits raw data- analysis not limited by frequency constraints	Frequency sensitive
Digital	Tolerate frequency changes	Bandwidth constraints
	Allows multiplexing	

The data acquired on the tow were also stored on a computer on the tow.

Towline Tension and Extension

Tension

The towline tension was measured by load cells installed at each end of the towline. The load cells are large links instrumented with strain gages for measuring towline tension. The specifications for the load cells are provided in Table 3-3.

Table 3-3. Load Cell Specifications

Item	Specification
Capacity	200,000 lbs
Sensing Element	Dual Bridge 350 OHM Strain Gages
Output	2mV per volt excitation at rated capacity
Excitation	10 volts DC
Calibration Error	Less than 0.25% of full capacity
Material	Stainless Steel

The installed configuration of the load cell at the tow end is shown in Figure 3.4.

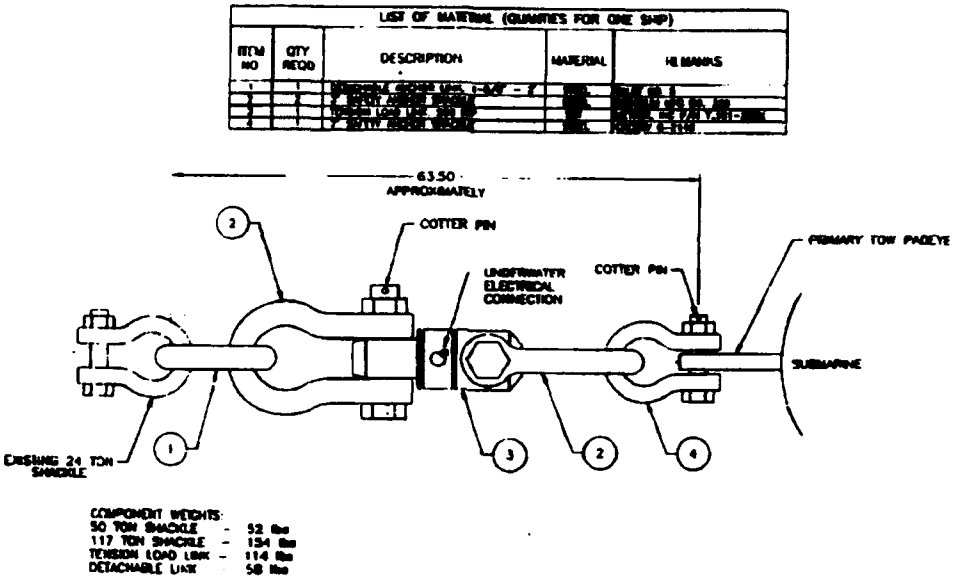

Figure 3.4

The installation of the load cell at the tug end is more complicated. Normally the towline is at the tug end is attached to an automatic towing machine (ATM). The ATM controls the tension in the towline by paying out or retrieving towline as

necessary to maintain a constant towline tension. During the data acquisition period the towline is connected to the load cell using a carpenter stopper. Figure 3.5 shows a carpenter stopper (U.S. Navy Towing Manual).

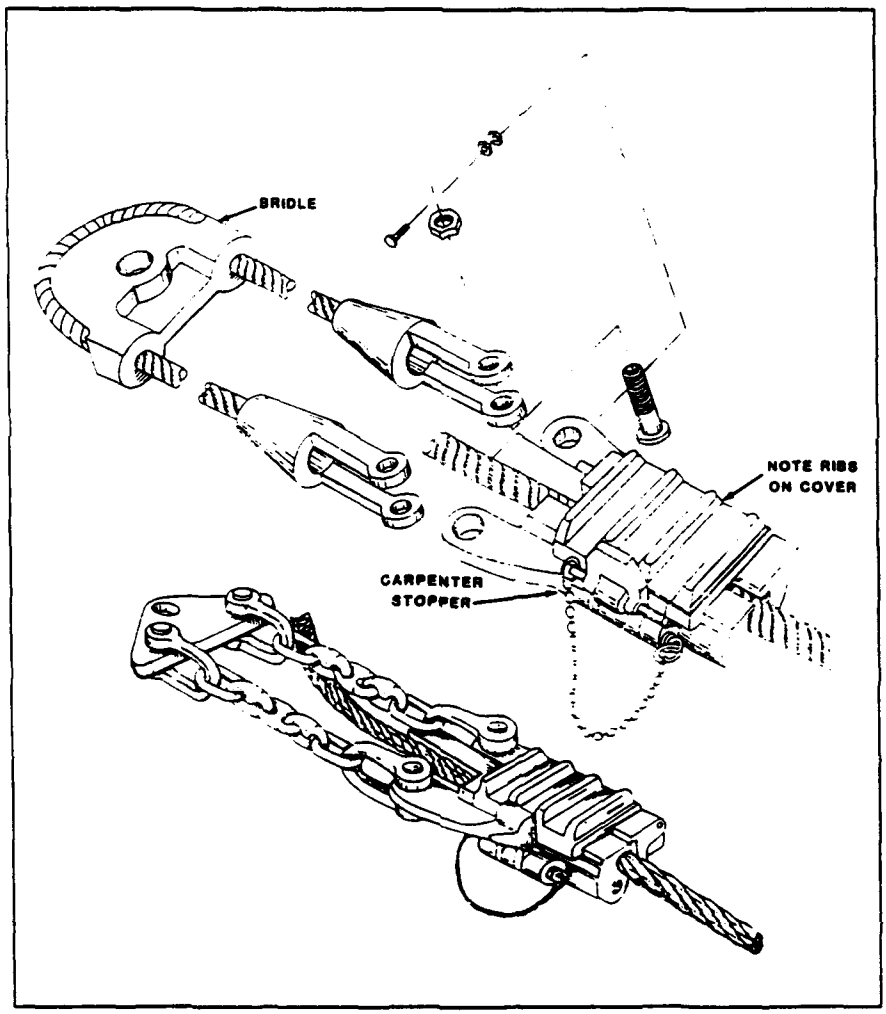

Figure 3.5

Figure 3.6 shows the installed configuration of the carpenter stopper and load cell.

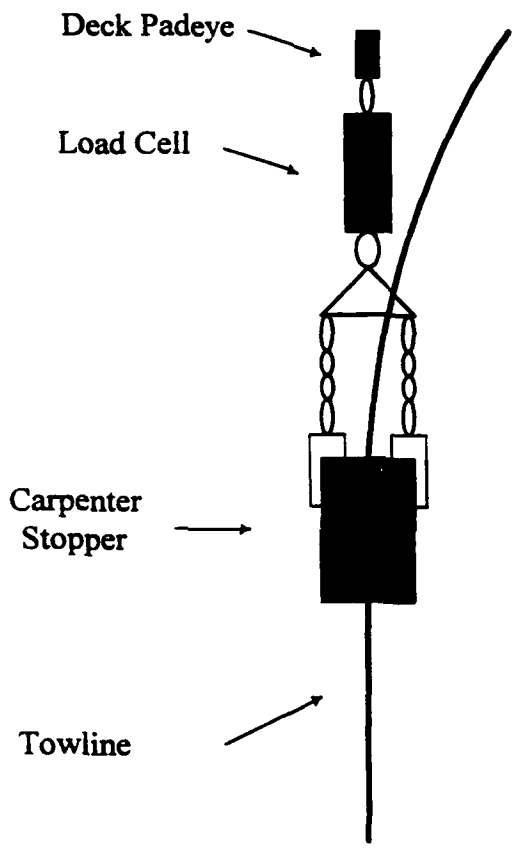

Figure 3.6

A load cell was installed at each end of the towline for two reasons. Towline

tension is one of the three critical parameters for a successful test program and a second load cell provides redundancy. Additionally, concern was expressed by others over the possible existence of a delay between when a tension increase at one end of the towline is felt at the opposite end.

Extension

The importance of accurately measuring towline extension can not be overstated. The most accurate and reliable method for determining towline extension is to measure the tug and tow separation distance. The tug and tow separation distance provides the towline end point displacement time history. The end point displacement is then used in the cable equations of motion to determine cable extension.

An infrared laser range finder was selected for measuring tug and tow separation. The advantage of the laser range finder over radar range finders is that the relatively short measurement intervals of the laser range finder are superior for unstable and moving platforms (Christensen, 1989).

The laser range finder was hand-held. Laser-light reflective targets were placed on the submarine's sail. The output of the laser range finder was fed directly to a data acquisition computer.

Continuous tug-tow range information was difficult to obtain in heavy seas. The operator often had difficulty "hitting" the target on the submarine (drop-out). When dropouts occur the data was smoothed to compensate. Figure 3.7 shows representative laser range finder output after corrective steps were taken to compensate for dropouts.

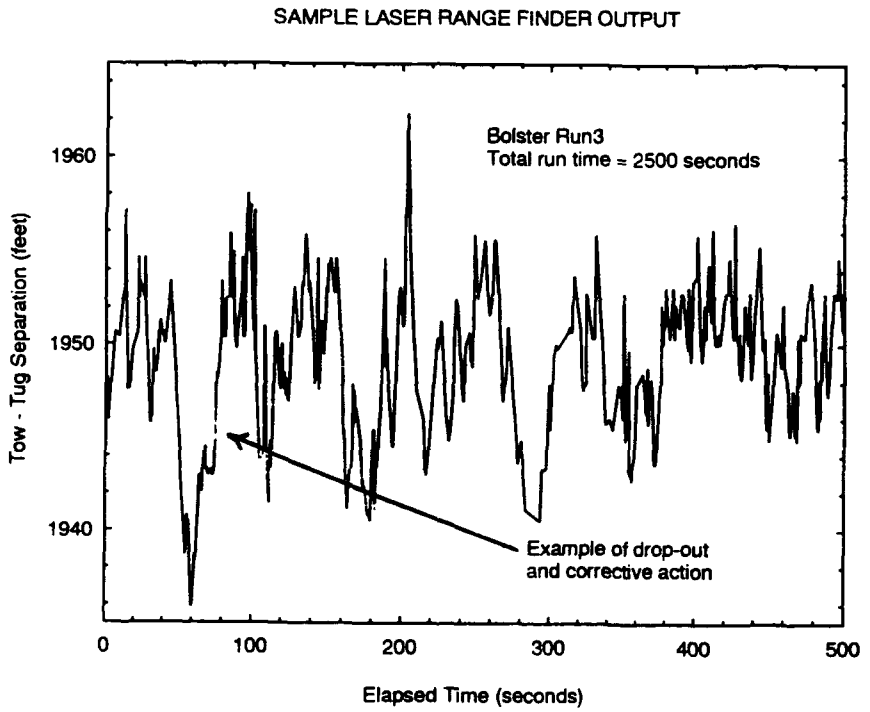

Figure 3.7

Wave Measurement Buoys

Background

The problems encountered on previous projects with ship-mounted wave measurement devices and the operational constraints imposed by a "tow of opportunity" drove the selection of the wave measurement devices. Semi-disposable wave measurement buoys were designed, developed, and used for measuring the wave spectra.

Theory

An object floating on waves much longer than the object is subject to the dynamic conditions of the water it displaces (Principles of Naval Architecture, 1967). Froude ("On the Rolling of Ships", Institute of Naval Architecture Transactions, 1861) confirmed experimentally that the sum of the forces acting on a particle on a wave's surface is perpendicular to the wave's surface by showing experimentally that a plumb bob suspended from a mast on a wave float would remain above the center of buoyancy of the float as the float rides the free surface (Figure 3.8).

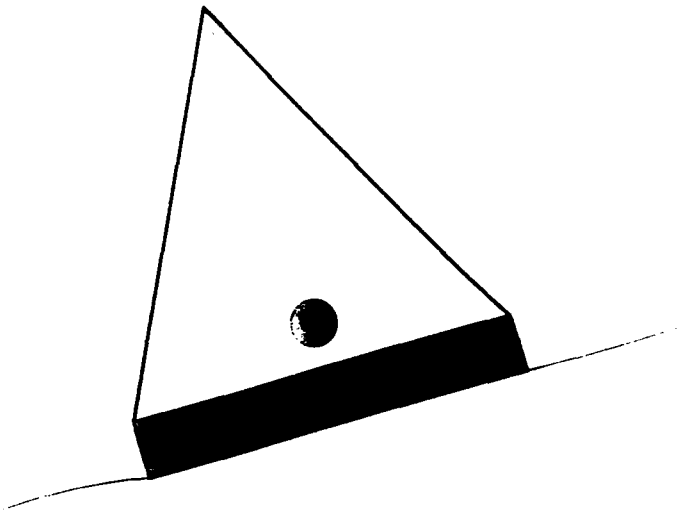

Figure 3.8

Figure 3.9 is a free body diagram of the wave buoy.

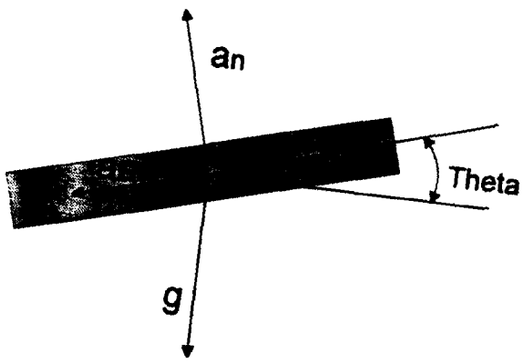

Figure 3.9

The wave buoy was constructed using a single accelerometer, mounted such that the axis of the accelerometer is vertical when the buoy is horizontal. The accelerometer can only sense accelerations along its longitudinal axis. In order to

determine that the measured acceleration time history can be used to generate an accurate wave amplitude spectrum, it is important to demonstrate that measuring accelerations along this axis alone is an adequate measure of the wave acceleration time history.

As the buoy follows the changes in the wave surface, the acceleration it senses is:

$$a_{a_n} = -a_x \sin\theta + a_z \cos\theta + g(1 - \cos\theta) \qquad (1)$$

where

a_{an} is the acceleration along the axis of the accelerometer

a_x is the horizontal acceleration

a_z is the vertical acceleration

θ is the wave slope

If we expand $\cos\theta$ and $\sin\theta$ in Taylor series, i.e.,

$$\sin\theta = \theta - \frac{\theta^3}{3!} + \ldots \qquad (2)$$

and

$$\cos\theta = 1 + \frac{\theta^2}{2!} + \ldots \qquad (3)$$

The acceleration along the accelerometer axis becomes:

$$a_{a_n} = -a_x\theta + a_z + g\frac{\theta^2}{2} + O(A^3) \tag{4}$$

For a wave potential of the form:

$$\phi = \frac{gA}{\omega} e^{kz}\sin(kx - \omega t) \tag{5}$$

The acceleration of a particle on the free surface is:

$$a_z(\xi, \zeta, t) = -A\omega^2\cos\omega t + O(A^3) \tag{6}$$

and

$$a_x(\xi, \zeta, t) = -A\omega^2\sin\omega t + O(A^2) \tag{7}$$

The wave slope, θ, is:

$$\theta(\xi, t) = Ak\sin\omega t + O(A^2) \tag{8}$$

Substituting (6) through (8) into (4) yields:

$$a_{a_n} = -A^2\omega^2 k\sin^2\omega t - A\omega^2\cos\omega t + gA^2k^2\sin^2\omega t + O(A^3) \tag{9}$$

The dispersion relation for a wave in water of infinite depth is:

$$\omega^2 = kg \tag{10}$$

Substituting this into (10) gives:

$$a_{a_n} = -gA^2k^2\sin^2\omega t - A\omega^2\cos\omega t + gA^2k^2\sin^2\omega t + O(A^3) \tag{11}$$

Which reduces to:

$$a_{a_n} = -A\omega^2\cos\omega t + O(A^3) \tag{12}$$

Therefore, if the wave buoy is made small enough to follow the motion that a particle on the free surface would follow, the buoy measures the vertical acceleration at a fixed point of linearized waves with no error of orders 1 and 2. The fractional error is order $(kA)^2$, since:

$$\frac{\text{error}}{\text{measurement}} = \frac{O((kA)^3)}{O((kA))} = O((kA)^2) \tag{13}$$

The measured acceleration is an accurate measurement of the linearized wave surface since the surface elevation is:

$$\eta = A\cos(kx - \omega t) \tag{14}$$

Though unimportant for this wave buoy, the tangential acceleration at the surface was also examined to determine if, in future applications, meaningful information can be obtained by measuring acceleration in the tangential direction.

The tangential acceleration, a_t, is equal to:

$$a_t = a_x\cos\theta + a_z\sin\theta + g\sin\theta \tag{15}$$

If we expand $\cos\theta$ and $\sin\theta$ in Taylor series and keep terms up to first order, a_t can be rewritten as:

$$a_t = a_x + a_z\theta + g\theta \tag{16}$$

For non-breaking waves, $\theta \approx \eta_x$. Equation (15) can be rewritten as:

$$a_t = A\omega^2 \sin(kx - \omega t) + A^2 \frac{\omega^4}{g} \sin(kx - \omega t)\cos(kx - \omega t) + g\theta \tag{17}$$

For non-breaking deep water waves the maximum ratio of wave amplitude to wavelength is 1/7 (Triantafyllou, 1980). The ratio of the RMS value of the first term on the right hand side of (17) to the RMS value of the second term is $\lambda/(A\pi)$. The minimum for this ratio is approximately 2, and is generally much greater than 2, particularly for the wave heights encountered during this project.

Therefore the tangential acceleration on the buoy due to wave motions can be approximated by:

$$a_t = gAk\sin(kx - \omega t) + g\sin\theta \tag{18}$$

The wave slope, η_x, is equal to:

$$\eta_x = -kA\sin(kx - \omega t) \tag{19}$$

For linear waves, $\eta_x \approx \sin\theta$, therefore:

$$a_t = kA\sin(kx - \omega t) - kA\sin(kx - \omega t) = 0 \tag{20}$$

Therefore, there is no benefit, to first order, of attempting to measure tangential accelerations.

Since the wave buoys can not distinguish the directionality of the waves, wave direction was estimated by visual observation for each data run.

Construction

The wave measurement buoy system consisted of an accelerometer and transmitter package mounted to a thin float. The float was sized to freely ride the wave surface. The accelerometer was mounted to the float in a waterproof container such that the accelerometer's axis was perpendicular to the horizontal plane of the wave float. The output of the accelerometer was used to modulate a business band radio transmitter mounted to the wave buoy. The transmitted radio signal was received on board a vessel located far enough away from the buoy to prevent the vessel from affecting the measured wave field. The received signal was recorded on cassette tape and demodulated to provide a record of wave surface acceleration versus time. The wave acceleration spectrum was obtained from the Fourier transform of the windowed auto-correlation function using wave records approximately 30 minutes long.

The wave elevation spectrum, $S_{\eta}(\omega)$, can be obtained from the acceleration

spectrum, $S_a(\omega)$, using the relation:

$$S_a(\omega) = \omega^4 S_\eta(\omega) \qquad (21)$$

Figure 3.10 is representative wave measurement system output.

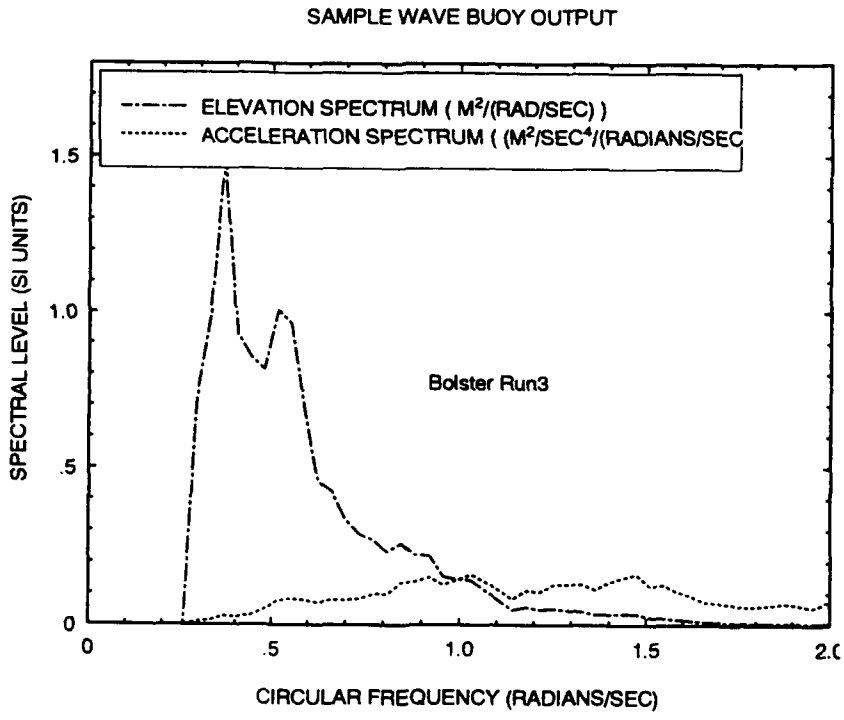

Figure 3.10

Environmental statutes (The Federal Water Pollution Control Act (FWPCA), Chapter 33, Article 1311) prohibit disposal of plastics and other waste at sea. Therefore, the wave buoys had to be made durable enough to be deployed and retrieved from the escort ship, a height of roughly 20 feet.

A detailed description of the wave buoy components is provided in Appendix A.

3.3 Project Planning

Many organizations were involved in the execution of this project. Table 3-4 summarizes the major participants and their responsibilities for the project.

Table 3-4. Tow Project Organization		
Activity	Responsibilities	POC
Naval Sea Systems Command (NAVSEA OOC)	Project Sponsor; Salvage Fleet Liaison	LCDR Rich Hooper; Mr. Will Healy 703-607-2758
Naval Sea Systems Command (PMS 396)	Shipyard Liaison; Funding Source; Submarine Force Liaison	Mr. Bob Horm 703-602-3800
Global Phillips Cartner	Construction and Materiel Support	Mr. Jeff Cane 804-887-7402
M.I.T.	Technical Direction; Test Coordination and Organization	Dr. J.M. Milgram; Mr. Noah Eckhouse 617-253-5900

A detailed test plan was provided to all participants. This test plan provided a complete description of the data acquisition plan. A copy of the test plan is provided as Appendix B.

MIT test support personnel were required for the installation of the data

acquisition equipment onboard the submarine, installation and operation of the data acquisition equipment onboard the tug, and operation of the wave measurement buoys. A minimum of two pe[illegible]e required to operate the test data acquisition equipment onboard the tug.

The support personnel were provided by the Marine Instrumentation and Computation Laboratory.

Nine months of preparation were required to develop the data acquisition plan, design, purchase, and construct the data acquisition equipment, coordinate the shipyard and operational fleet support, and install the data acquisition equipment onboard the tow and the tug.

Chapter Four

Results and Analysis

4.1 Equipment Performance

Tow Summary

The tow consisted of three separate legs. Time was available between the legs of the tow to evaluate and correct equipment problems and to perform an initial assessment of the acquired data's consistency and accuracy.

First Leg (Charleston, South Carolina to the Panama Canal)

The first leg of the towing project was intended to be used for:

1. Evaluating equipment performance;
2. Setting and validating calibration constants;
3. Ensuring computer software interface programs were functioning properly; and,
4. Obtaining as much useful data as possible for a wire towline.

During the first leg of the tow the towline consisted of 1435 feet of wire and 90 feet of chain.

Most of the items to be accomplished during the first leg were not successfully accomplished for the following reasons:

1. Low sea state;
2. Massive electrical failure of all the instruments on the submarine except for the load cell and the GPS receiver;
3. Laser range finder mechanical failure; and,
4. Main engine difficulties on another vessel transiting with the tug and tow limited the group's tow speed to 4 knots or less.

The low sea state and low tow speed combined to maintain the mean towline tension unusually low. The typical mean tension during this leg was 13,000 lbs. The towline catenary for this mean tension and length of towline is deep. A deep catenary prevents high dynamic tensions unless the towline endpoint motions are large or the endpoint motions are fast. The towline endpoint motions are determined by the dynamic ship motions which in turn, are driven by the sea. Due to the low sea state, the ship motions were neither large nor rapid.

All the instruments and data acquisition equipment on the submarine with the

exception of the GPS receiver and the load cell were destroyed by a significant electrical event during the first leg. The destroyed equipments' internal electrical circuits showed signs of being overheated and burned. The significant electrical event which caused the failure was either:

1. Lightening striking the equipment box; or,
2. A short circuit in the ship motion sensing equipment which resulted in application of its 400Hz, 110 Volt gyroscope driving power to the signal lines.

The most likely cause was the former. Though lightening arrestors were installed in line with the antennae, electrical paths into the equipment box existed through the antenna cables on the equipment box side of the arrestors and through the power wires from the solar cells and wind generators.

Replacement motion sensing equipment could not be obtained in time to support the remainder of the project. The computer and data acquisition and transmission equipment were replaced and set-up to record and transmit the load cell and GPS data during the last two legs of the project.

The failure of the laser range finder benefited the long term data collection effort. The accuracy of the laser range finder data obtained prior to the range finder

failure was found to be insufficient for use as input into the governing equations for computing time-varying towline tension. A laser range finder with higher accuracy and higher data sampling rate was obtained as a result of the failure and shipped to Panama for use on the final legs of the project.

Second Leg (Panama Canal to San Diego, California)

During the second leg, the towline was to consist of 1435 feet of wire, 300 feet of stretcher, and 90 feet of chain.

The stretcher was destroyed by the propeller of the Bolster at the start of the second leg due to poor shiphandling and deck seamanship on the part of the Panama Canal Commission tugs. The remnants of the stretcher were removed and the towline configuration from the first leg (1435 feet of wire and 90 feet of chain) was used for the second leg. The signal cable from the submarine tension load cell to the submarine instrument box was irreparably damaged in this incident or shortly thereafter.

Due to the destruction of the stretcher, data was not taken on the second leg of the tow.

Third Leg (San Diego, California to Bremerton, Washington)

A replacement signal cable for the load cell could not be made available to support the tow's anticipated departure time from San Diego. Therefore, the load cell was removed and the attachment of the towline to the submarine was returned to a normal configuration. Tension measurement at the tug end continued.

Data was obtained during the third leg of the tow. Table 4-1 provides the dates and times for the data acquisition runs for the this leg.

Table 4-1. Data Acquisition Run Summary

Run	Date	Start Time	Stop Time
1	24 August 1993	15:02:53	15:36:46
2	25 August 1993	08:56:06	09:41:01
3	26 August 1993	08:57:06	09:39:50
4	26 August 1993	14:52:00	15:28:46

Runs 2, 3, and 4 provided data for useful analysis. The sea state for run 1 was too low to provide useful data.

A towline chain shackle parted on the evening of 26 August 1993. The wire towline was attached to the secondary tow pendant. The towline configuration was all

wire for the rest of the tow. The seas were too rough to take the towline off the ATM for data acquisition. with no stretcher in the towline.

The data obtained on the three good runs are the basis for the data analysis. The sea state and dynamic tensions for these three runs were large enough to facilitate useful analysis.

Equipment Performance

Tension Load Cells

The data from the tension load cell on the tug were consistently good. The data acquisition system provided continuous tension time-history during the data acquisition runs. Figures 4.1 through 4.4 show the dynamic tension time-history for the four runs on the third leg.

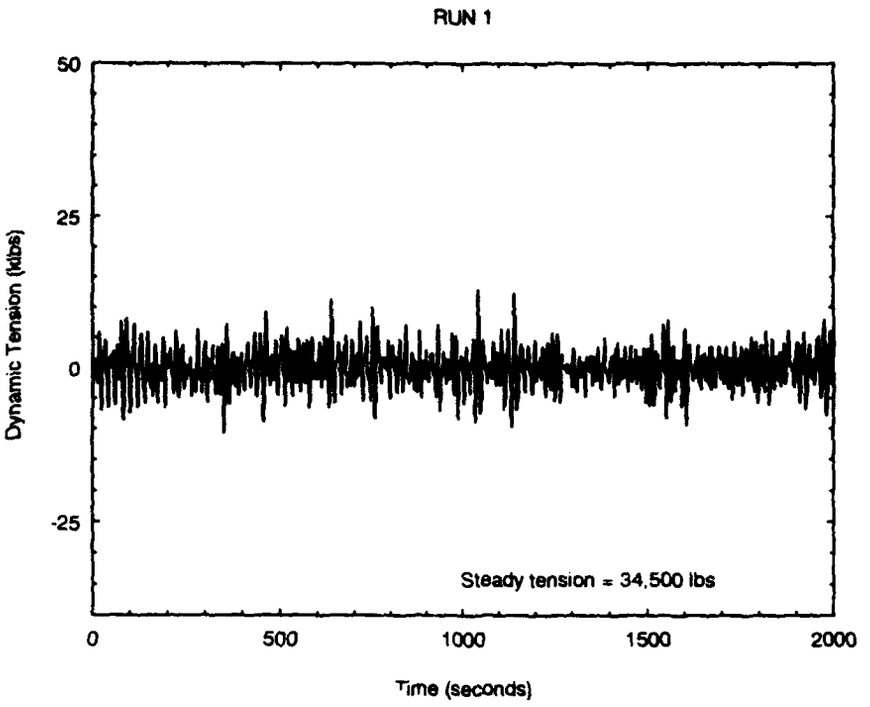

Figure 4.1

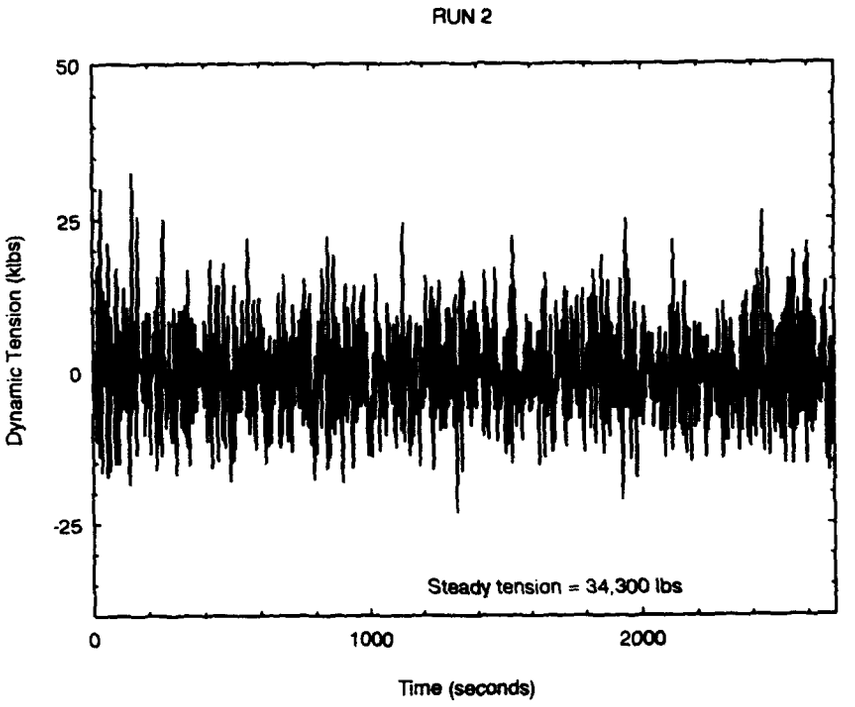

Figure 4.2

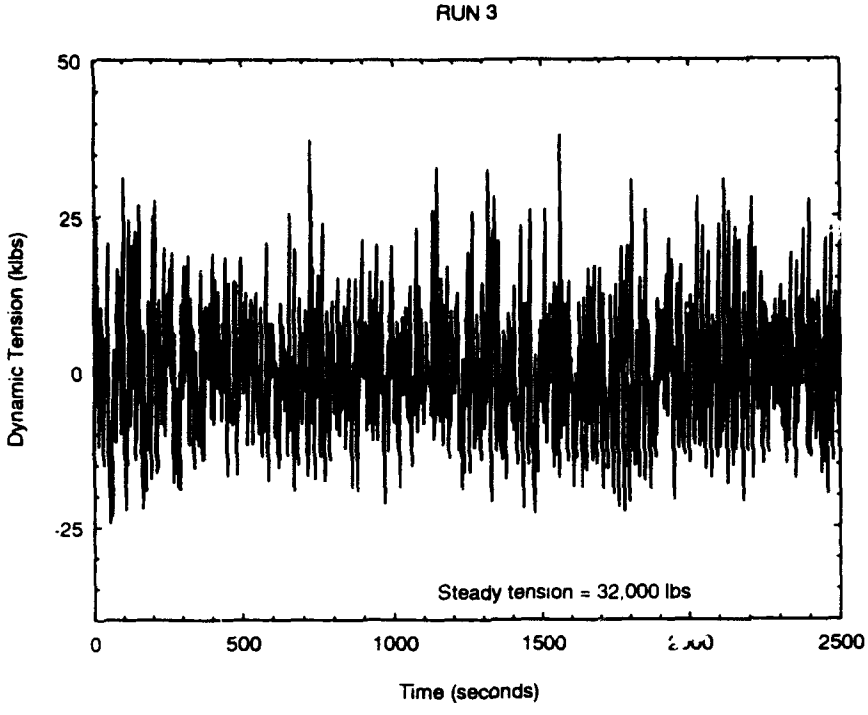

Figure 4.3

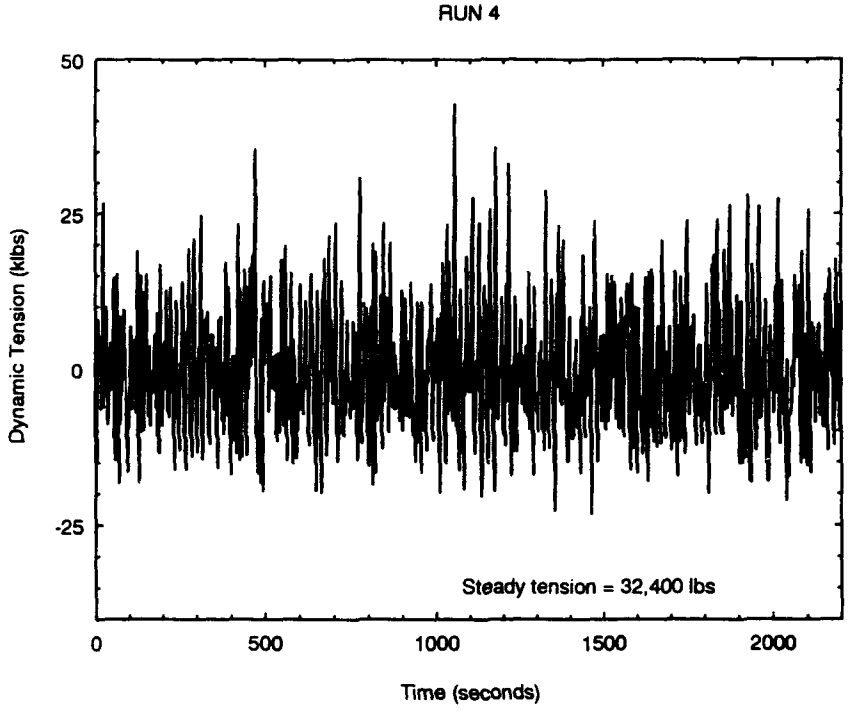

Figure 4.4

Concern was expressed by the tug crew that the dynamic tension at opposite ends of the towline might be significantly different. Theory and previous experiments show that the dynamic tensions at the two ends of the towline are nearly the same. Figure 4.5 shows the dynamic tension time-history measured at the two ends of the towline during the tow of the ex-USS HECTOR by the USS SALVOR (Frimm and Milgram, 1991). The maximum difference between the measured dynamic tension at the two ends is 500 lbs. The differences are within the measurement accuracy of the tension data acquisition system.

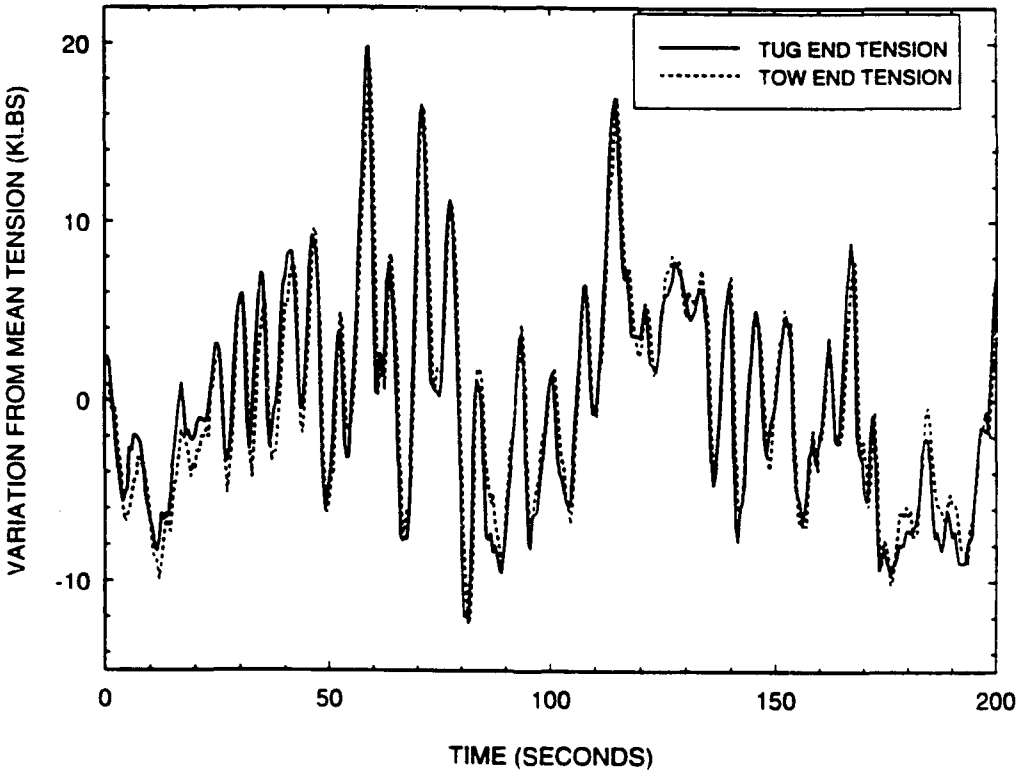

Figure 4.5

The dynamic tension controlling performance of the ATM was evaluated by "observation" during periods when data were not being collected. The ATM was set to limit tension to 60,000 lbs. When large and rapid dynamic tension increases occurred, the ATM's tension meter was noted to rise to its maximum of 103,000 lbs. Actual tensions were larger. Based on these observations, it was concluded that the ATM is ineffective at limiting tension during rapid tension increases. When the tension varies slowly, the ATM performs well. In contrast, the effectiveness of a stretcher in limiting tension is independent of the rate of tension increase.

The measured tension data differ from the tension data at the measured tow point by a small amount due to the friction of the towline on its tug supports.

Laser Range Finder

The laser range finder was used to estimate the time varying extension of the towline. The time varying extension for each run was used as input to the cable dynamics equations. The cable dynamics equations were solved numerically and estimated tension time-histories were generated for each run for comparison with the measured tension time-histories. This process was necessary to evaluate the accuracy of the composite towline numerical models.

The laser range finder was hand-held on the tug. There were two targets on the submarine, each 3 feet by 3 feet. The typical distance to the submarine was 1900 to 2000 feet. The range finder operator occasionally missed the target and either received a return from a reflecting surface elsewhere on the submarine or missed the submarine entirely. The laser range finder data transmission rate was 0.5 Hz. The generated range data were reviewed and missing and unreasonably varying points were filled in or modified by interpolating between valid data points. Figures 4.6 through 4.8 are the measured range data of importance.

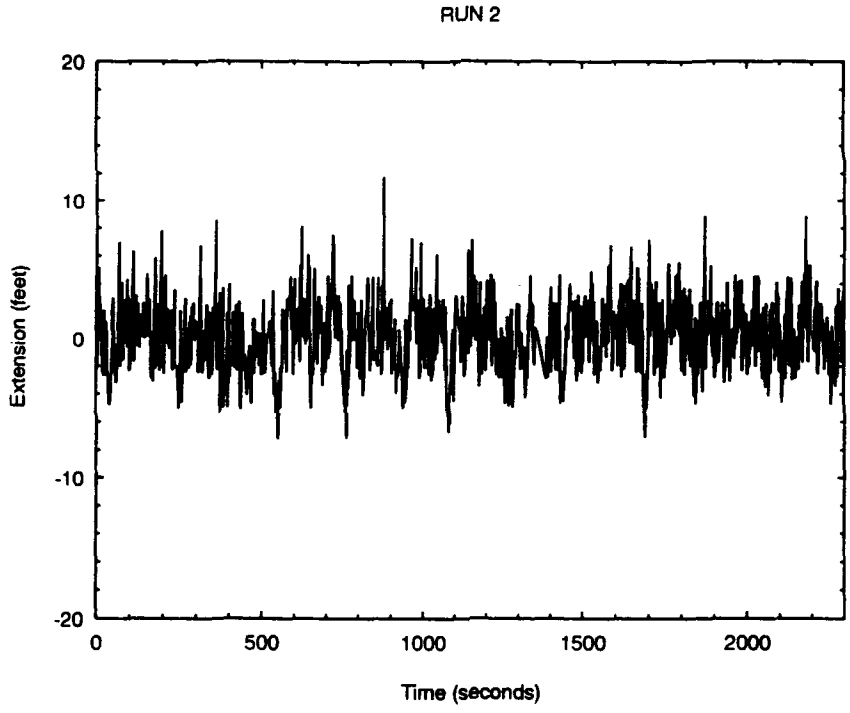

Figure 4.6

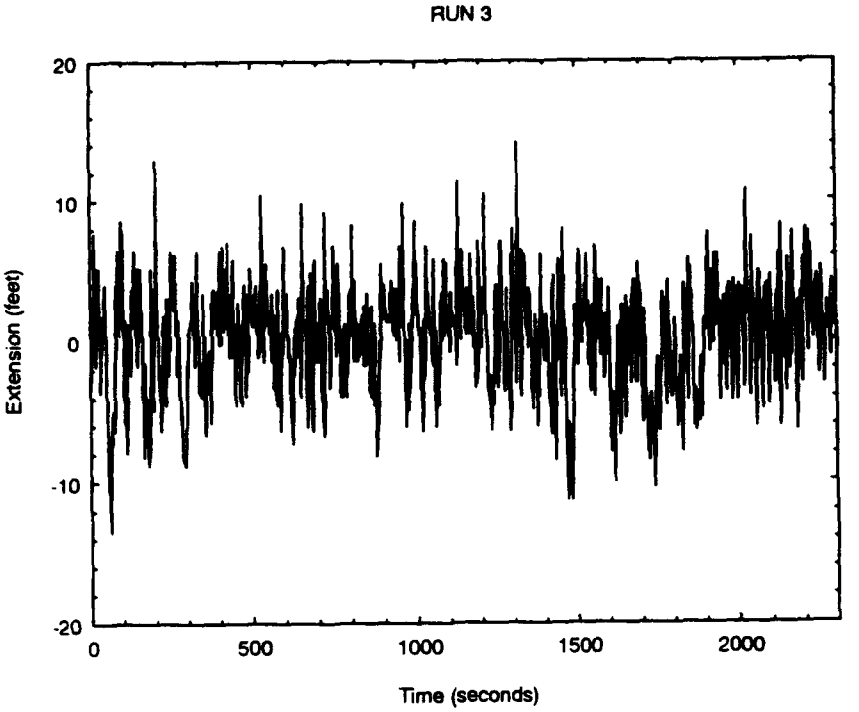

Figure 4.7

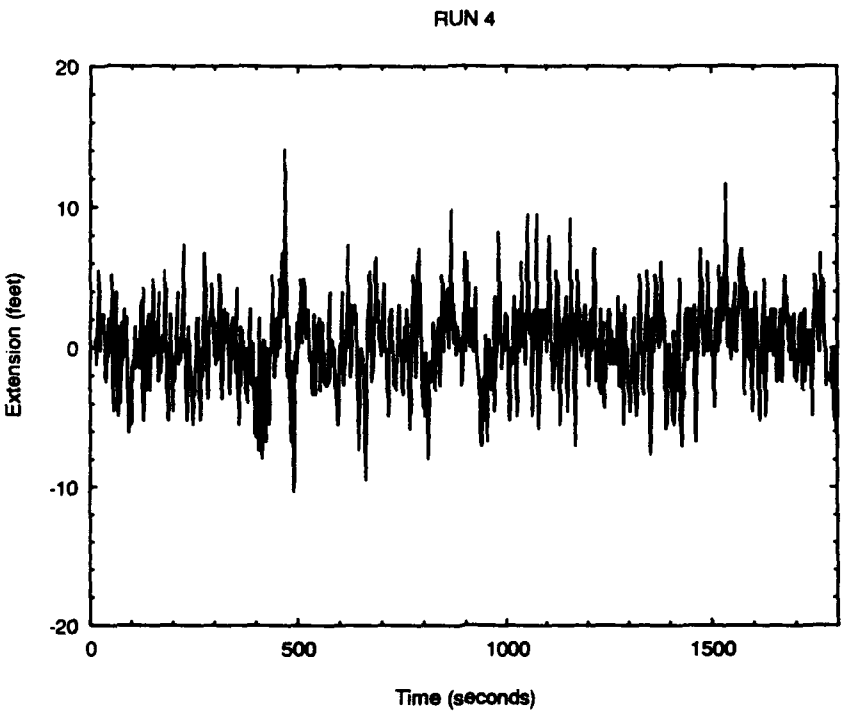

Figure 4.8

Wave Measurement

The wave measurement buoys provide an acceleration versus time history of the waves in close proximity to the tow. The wave buoys were deployed 100-200 yards off the track of the tow and transmitted wave data for approximately 40 minutes. The length of the wave data record is sufficient for estimating the relevant statistics of the waves (Milgram, 1990).

The wave time histories were converted to wave acceleration spectra by calculating the Fourier transforms of the waves' autocorrelation functions. The wave elevation spectra were computed from the acceleration spectra using the relationship:

$$S_{elev}(\omega) = \frac{S_{acc}(\omega)}{\omega^4} \qquad (1)$$

where

$S_{elev}(\omega)$ = Wave elevation spectrum

$S_{acc}(\omega)$ = Wave amplitude spectrum

ω = circular frequency

The wave measurement buoys were not properly calibrated during data collection run 1. No wave information, other than a visual estimate of the significant

wave height was successfully recorded.

Figures 4.10 through 4.12 are the measured wave spectra for runs 2 through 4.

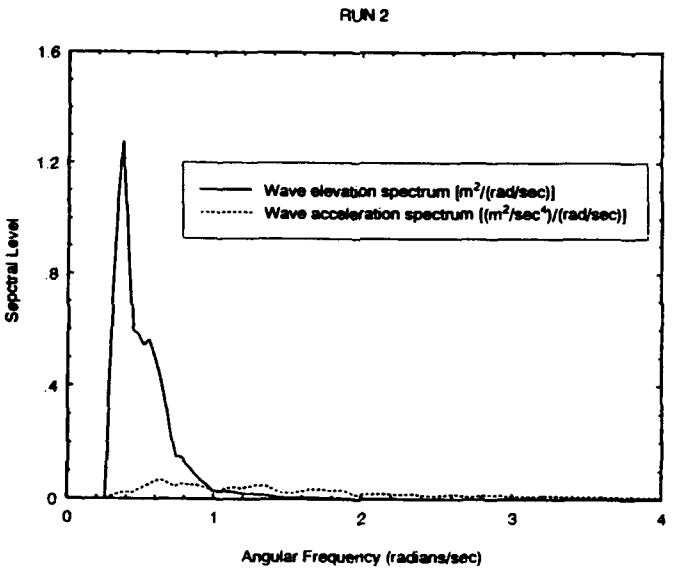

Figure 4.10

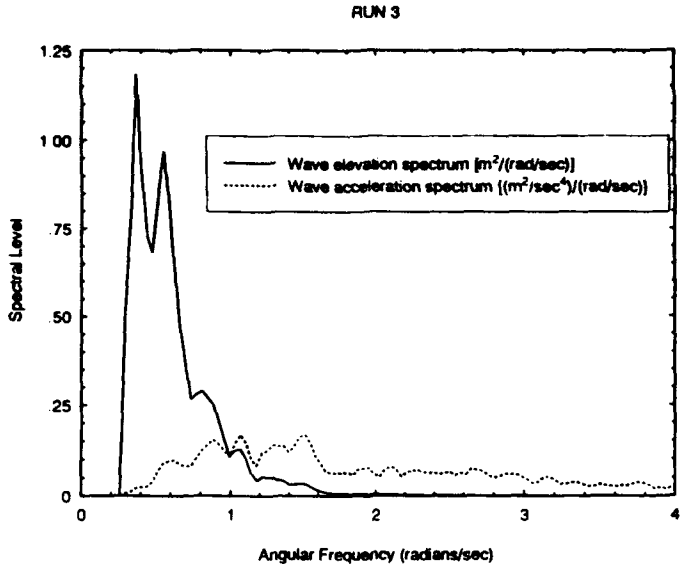

Figure 4.11

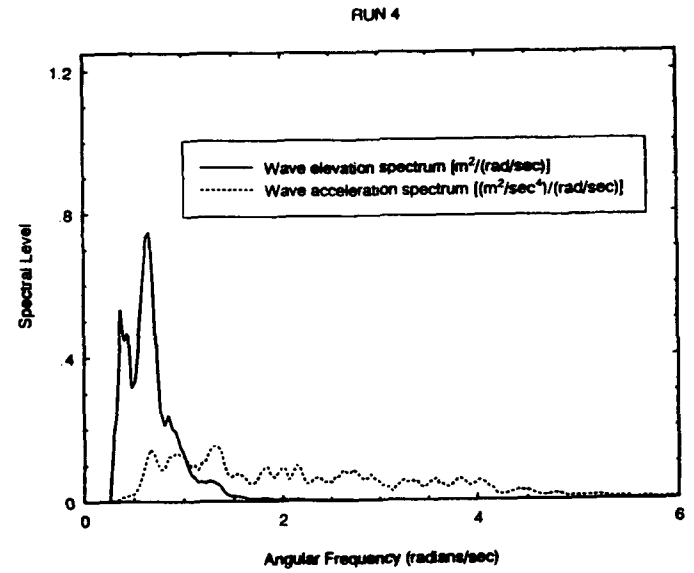

Figure 4.12

Measured (tug) ship motion spectra were compared with generated ship motion spectra using the measured wave spectra and the theoretical ship frequency responses for ship heave acceleration, pitch angle, and surge acceleration.. This method provided a measure of the accuracy of the ship motion measuring equipment, wave measurement buoys, and the motion transfer functions. A problem with this method of comparison is that if the predicted ship motion spectra and measured ship motion spectra are not in agreement, determining which attribute- measured wave spectra, measured ship motions, or motion transfer functions, is inaccurate can be difficult.

The ship motion spectra were generated using:

$$S_{ai}(\omega) = [H(\omega)]^2 S_{wave}(\omega) \qquad (2)$$

where

$S_{ai}(\omega)$ = Ship motion acceleration spectrum in i^{th} direction

$H(\omega)$ = Motion transfer function

$S_{wave}(\omega)$ = Wave acceleration spectrum

The frequency of the measured ship motions is the encounter frequency, ω_e. The encounter frequency is defined as (Newman, 1977):

$$\omega_e = \omega - \frac{\omega^2 U}{g}\cos\theta \qquad (3)$$

where

ω = Wave frequency

U = Ship speed

g = Gravitational constant

θ = Angle between ship's heading and the direction of wave propagation; $\theta = \pi$ for head waves

To compare the motion spectra generated from measured accelerations with the motion spectra generated from measured wave accelerations, the spectra must be expressed in the same frequency "space". Equation (3) relates encounter frequency and wave frequency. The frequency shift does not affect the average power of the measured spectra. Assuming linear independence of the spectral components, the fixed point power in a band $\Delta\omega$ must equal the power in the corresponding encounter band $\Delta\omega_e$ (Milgram, 1990). The relationship between the spectral levels is given by (Milgram, 1990):

$$S(\omega)\,\Delta\omega = S_e(\omega)\,\Delta\omega_e \qquad (4)$$

Equation (4) can be rearranged (Milgram. 1990):

$$S_e(\omega) = \frac{S(\omega)}{\frac{d\omega_e}{d\omega}} \qquad (5)$$

Equation (3) can be used in equation (5) to yield the following (Milgram, 1990):

$$S_e(\omega_e) = \frac{S(\omega)}{1 - \frac{2\omega U}{g}\cos\theta} \qquad (6)$$

The transformation from wave frequency "space" to encounter frequency "space" is equivalent to multiplying the wave frequency spectral ordinates by the Jacobian of the frequency transformation, (3) (Principles of Naval Architecture, 1967).

Figures 4.13 through 4.15 show the comparison between the measured and generated ship motion spectra.

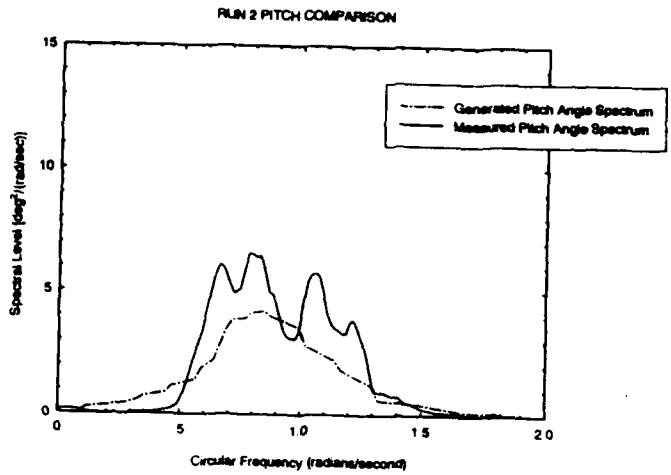
RUN 2 PITCH COMPARISON
Generated Pitch Angle Spectrum
Measured Pitch Angle Spectrum
Spectral Level [deg²/(rad/sec)]
Circular Frequency (radians/second)
0
5
10
15
20

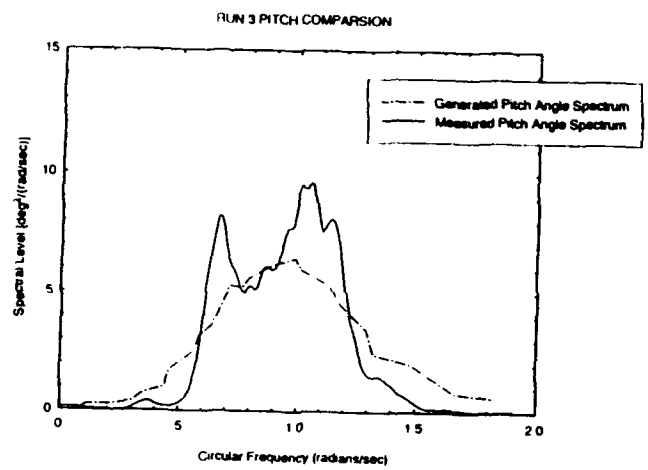
RUN 3 PITCH COMPARISION
Generated Pitch Angle Spectrum
Measured Pitch Angle Spectrum
Spectral Level [deg²/(rad/sec)]
Circular Frequency (radians/sec)
0
5
10
15
20

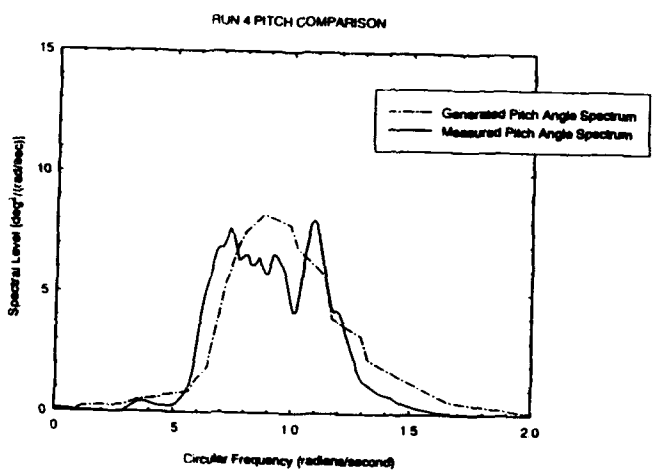
RUN 4 PITCH COMPARISON
Generated Pitch Angle Spectrum
Measured Pitch Angle Spectrum
Spectral Level [deg²/(rad/sec)]
Circular Frequency (radians/second)
0
5
10
15
20

Figure 4.13

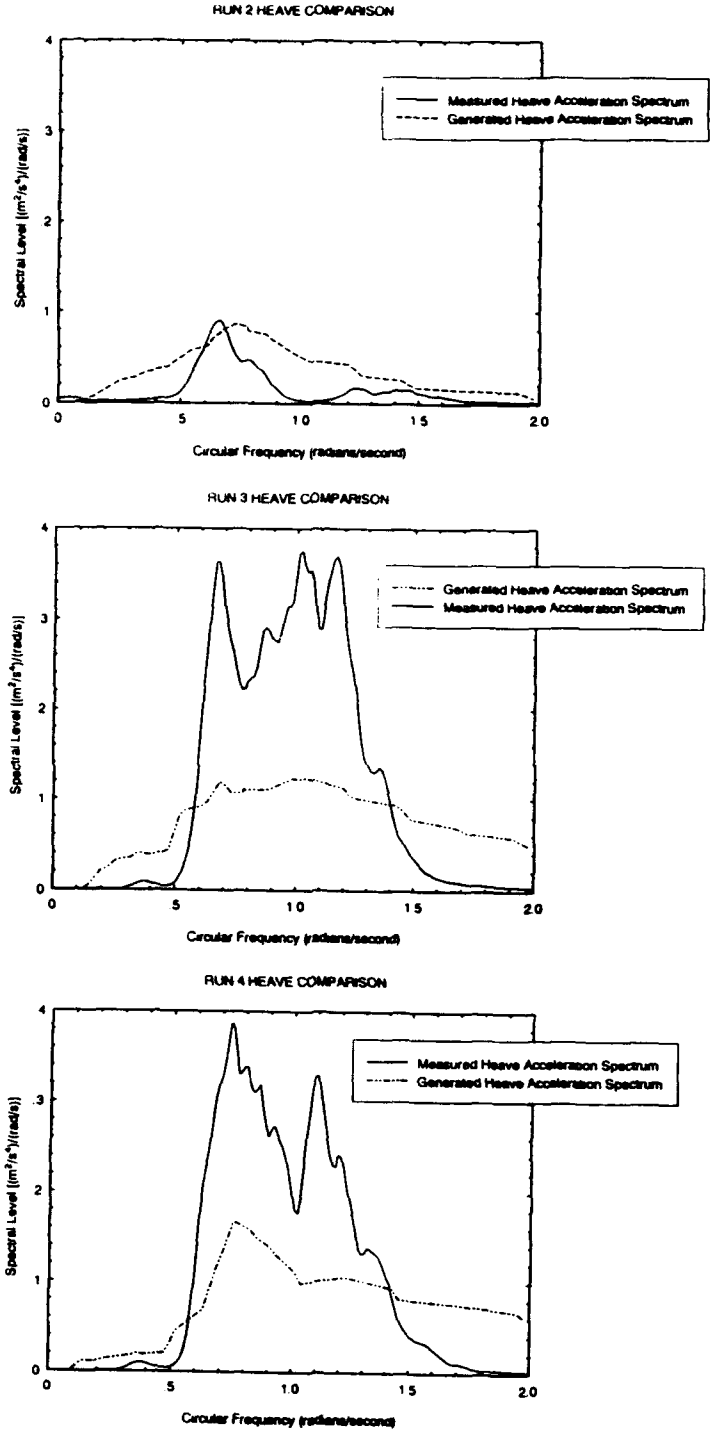
RUN 2 HEAVE COMPARISON
Measured Heave Acceleration Spectrum
Generated Heave Acceleration Spectrum
Spectral Level [(m²/s⁴)/(rad/s)]
Circular Frequency (radians/second)
RUN 3 HEAVE COMPARISON
Generated Heave Acceleration Spectrum
Measured Heave Acceleration Spectrum
Spectral Level [(m²/s⁴)/(rad/s)]
Circular Frequency (radians/second)
RUN 4 HEAVE COMPARISON
Measured Heave Acceleration Spectrum
Generated Heave Acceleration Spectrum
Spectral Level [(m²/s⁴)/(rad/s)]
Circular Frequency (radians/second)

Figure 4.14

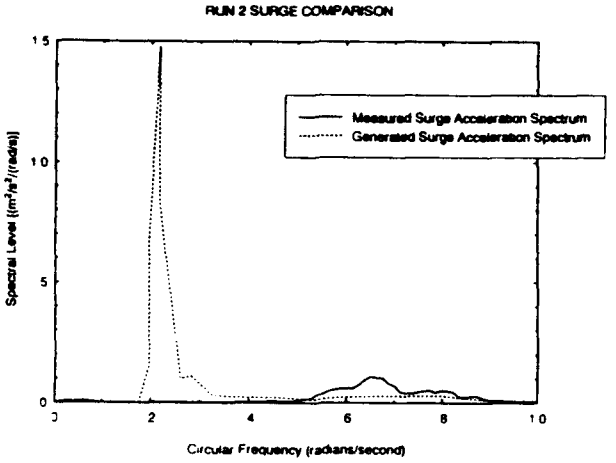
RUN 2 SURGE COMPARISON
Measured Surge Acceleration Spectrum
Generated Surge Acceleration Spectrum
Spectral Level ((m²/s³)/(rad/s))
Circular Frequency (radians/second)

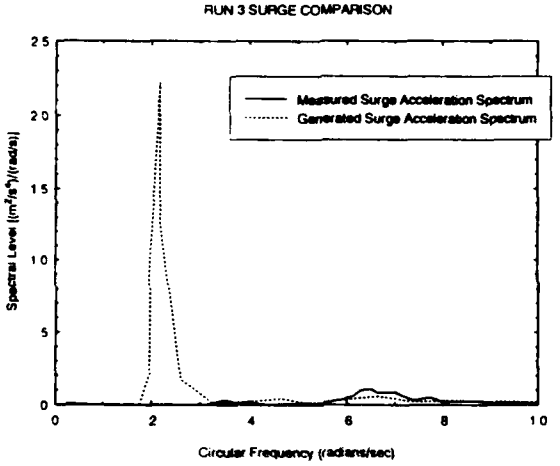
RUN 3 SURGE COMPARISON
Measured Surge Acceleration Spectrum
Generated Surge Acceleration Spectrum
Spectral Level ((m²/s³)/(rad/s))
Circular Frequency (radians/sec)

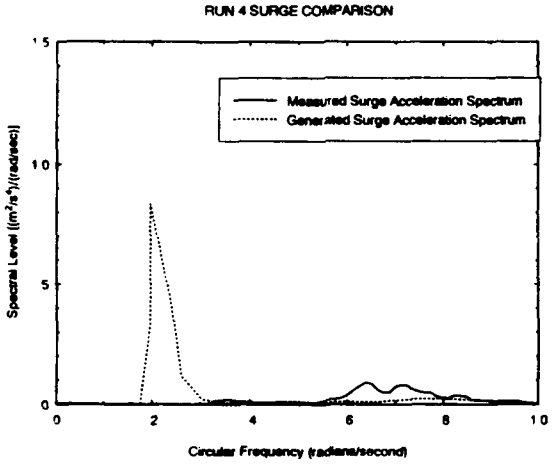
RUN 4 SURGE COMPARISON
Measured Surge Acceleration Spectrum
Generated Surge Acceleration Spectrum
Spectral Level ((m²/s³)/(rad/sec))
Circular Frequency (radians/second)

Figure 4.15

The generated and measured pitch angle spectra compare reasonably well for the three data runs. The heave spectra compare well for run 2. The heave spectra do not compare as well for run 3 and run 4. The difference in the heave spectra for runs 3 and 4 correspond to a difference in RMS heave accelerations of approximately 30% for each run. The possible causes for the disparity between the measured and predicted heave motions are:

a. Inaccuracies in wave motion measurements;

b. Overprediction of the transfer functions in heave; or,

c. Inaccurate heave acceleration measurements.

The good correlation between the measured and generated pitch spectra indicate that the wave spectra measurements are reasonable. The heave transfer functions used are typical of monohulls. The most probable cause of the difference between the measured and generated heave spectra is the combination of slightly underpredicted sea spectra and moderate inaccuracies in the measured heave acceleration.

For all motions, the generated spectra are less than the measured spectra. The most probable cause for the underprediction is an underprediction of the wave spectra. The significant wave heights during the data runs were estimated visually by

experienced seamen. Table 4-2 contains estimates of the significant wave height from "seaman's eye" and significant wave heights calculated from the measured sea spectra. The significant wave heights generated from the measured wave spectra were calculated using the relationship:

$$H_{1/3} = 4 m_o^{1/2} \quad (7)$$

where

$H_{1/3}$ = Significant wave height[1].

m_o = Total energy of the wave spectrum, determined by calculating the area under the spectrum versus frequency curve.

Table 4-2. Significant Wave Height Comparison

Run Number	Estimated Significant Wave Height (feet)	Measured Significant Wave Height (feet)
2	8	6.9
3	12	9.2
4	12	7.2

[1]Significant wave height is defined as the average of the one-third highest waves.

The measured and generated surge acceleration spectra do not compare well over the full range of frequencies measured. A ship's surge spectrum should exhibit a resonance peak at the systems' natural frequency. The generated surge spectra show this peak at frequencies close to the system natural frequency. The equipment used to measure the surge acceleration lacked the frequency range to accurately measure low frequency surge motions, however. the presence of low frequency motions is shown in the spectra generated from the measured extension time histories. Figure 4.16 shows a comparison between the extension spectra generated from the extension time history and a surge amplitude spectrum generated from the measured surge acceleration spectrum using the relation:

$$S_{amp} = \frac{S_{acc}}{\omega^4} \qquad (8)$$

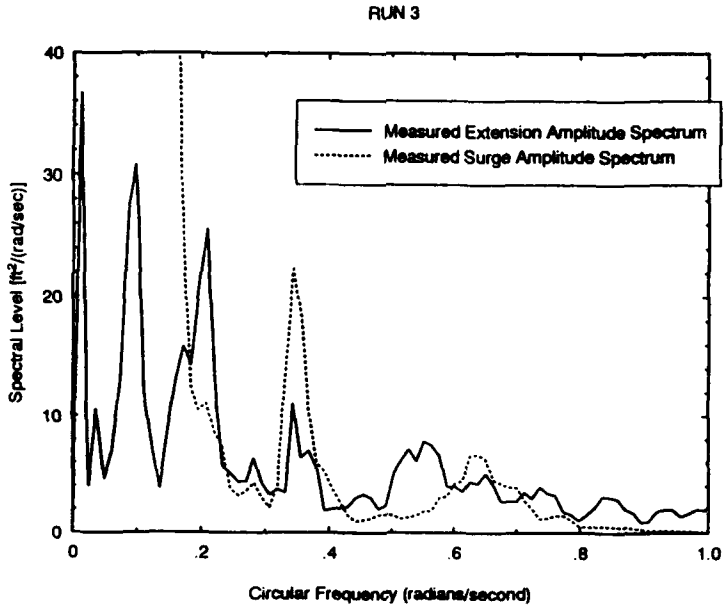

Figure 4.16

At very low frequencies, the calculated accleration increases without bound. However, its application to the measured surge spectrum, as shown above, demonstrates that the lower limit to the accuracy of the surge measurement equipment is approximately 0.3 radians per second.

4.2 Evaluation of Cable Numerical Model

The accuracy of the composite cable numerical model was evaluated using the measured extension time-history for each run as end point motion input to the finite difference program written to solve the cable dynamic equations. The resultant dynamic tension time-histories were compared with the measured dynamic tension for the corresponding runs. Figure 4.17 shows the comparisons of measured and calculated tension time-histories.

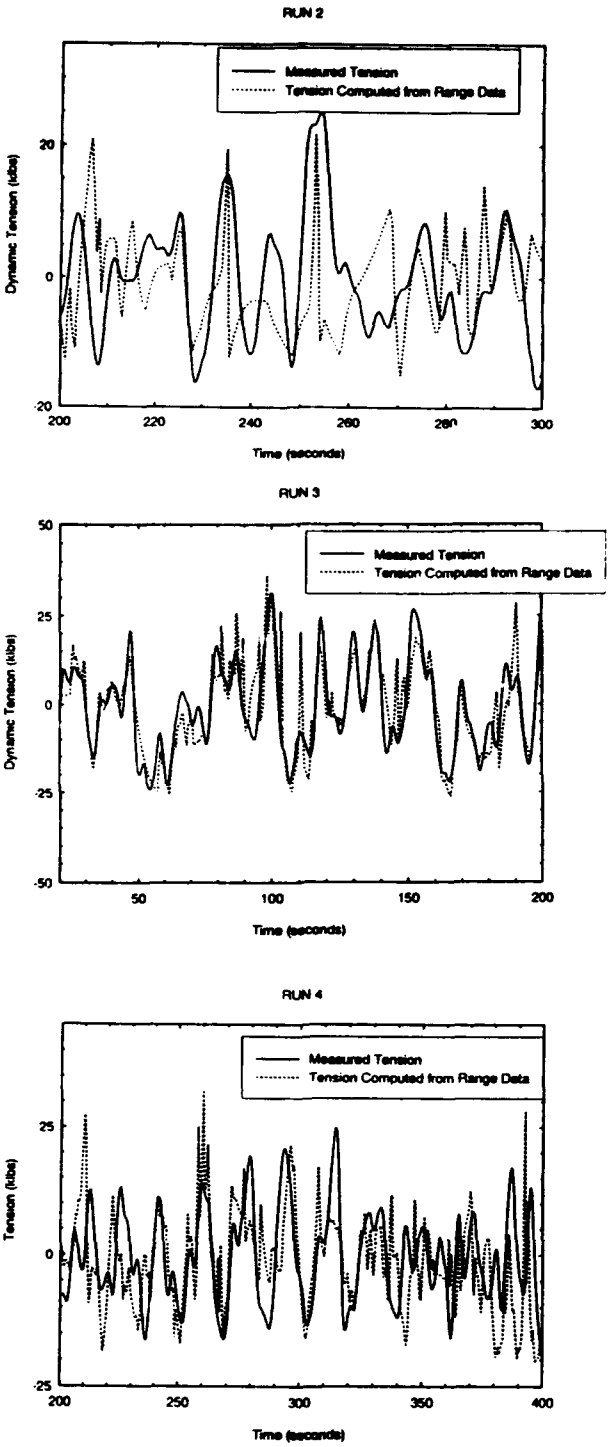
RUN 2
Measured Tension
Tension Computed from Range Data
Dynamic Tension (kips)
Time (seconds)
RUN 3
Measured Tension
Tension Computed from Range Data
Dynamic Tension (kips)
Time (seconds)
RUN 4
Measured Tension
Tension Computed from Range Data
Tension (kips)
Time (seconds)

Figure 4.17

The measured and calculated tension time-histories compare well for run 3 and run 4. The results do not compare as well for run 2. The difference between the measured and calculated tensions for run 2 is attributed to the laser range finder operator difficulties previously discussed. On subsequent runs the laser range finder operator performed much better, and more complete and continuous extension time-histories were generated.

Based on the comparisons shown in figure 4.17 it appears that the dynamic equations for a composite cable have been accurately solved.

4.3 Comparison of Measured Tensions with Tensions Predicted by the Nonlinear Extreme Tension Prediction Program[2]

Frimm and Milgram (1991) developed a semi-empirical correction for the low frequency tension not accounted for in the original Nonlinear Extreme Tension Prediction Program (Milgram et al, 1988). They proposed the addition of twice the low frequency RMS tension to the extreme tension predicted by the Nonlinear Extreme Tension Prediction Program. The RMS low frequency tensions were

[2]Portions of this analysis are documented in "The Influence of Stretchers on Extreme Towline Tensions", Milgram, Frimm, and Thomas, October 31, 1993. "The Influence of Stretchers on Extreme Towline Tensions" is a status report submitted to the project's sponsors.

obtained from previous towing experiments. Figure 4.18 is a graph of the RMS low frequency tension to be used as a semi-empirical correction to the predicted extreme tension.. In their discussion of the semi-empirical correction, Frimm and Milgram (1991) postulate that the correction is conservative, in part because "the low frequency and high frequency tensions do not occur at the same time".

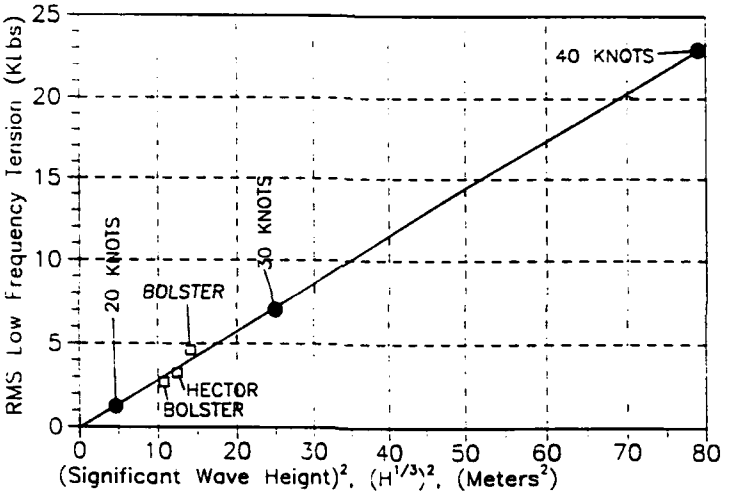

Figure 4.18

A part of this project was the analysis of low frequency tension. The analysis was intended to:

1. Contribute data to the low frequency tension database;
2. Improve the semi-empirical correction to the Nonlinear Extreme Tension Prediction Program; and,
3. Use the measured low frequency tension and extension data to aid the development of an accurate analytical tool for including low frequency effects in the full time simulation.

The measured tension time-histories were transformed into the frequency domain and separated in to high and low frequency parts. The high and low frequency parts were transformed back into the time domain and the data records were compared. Figures 4.19 (a) and 4.19 (b) show comparisons of the low and high frequency tension time histories for portions of the data runs.

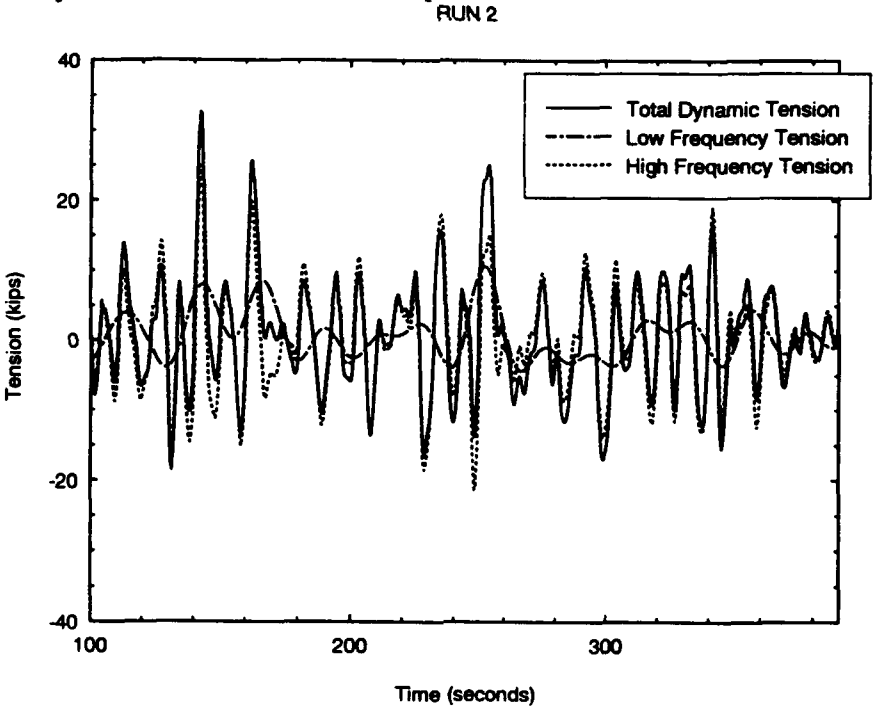

Figure 4.19 (a)

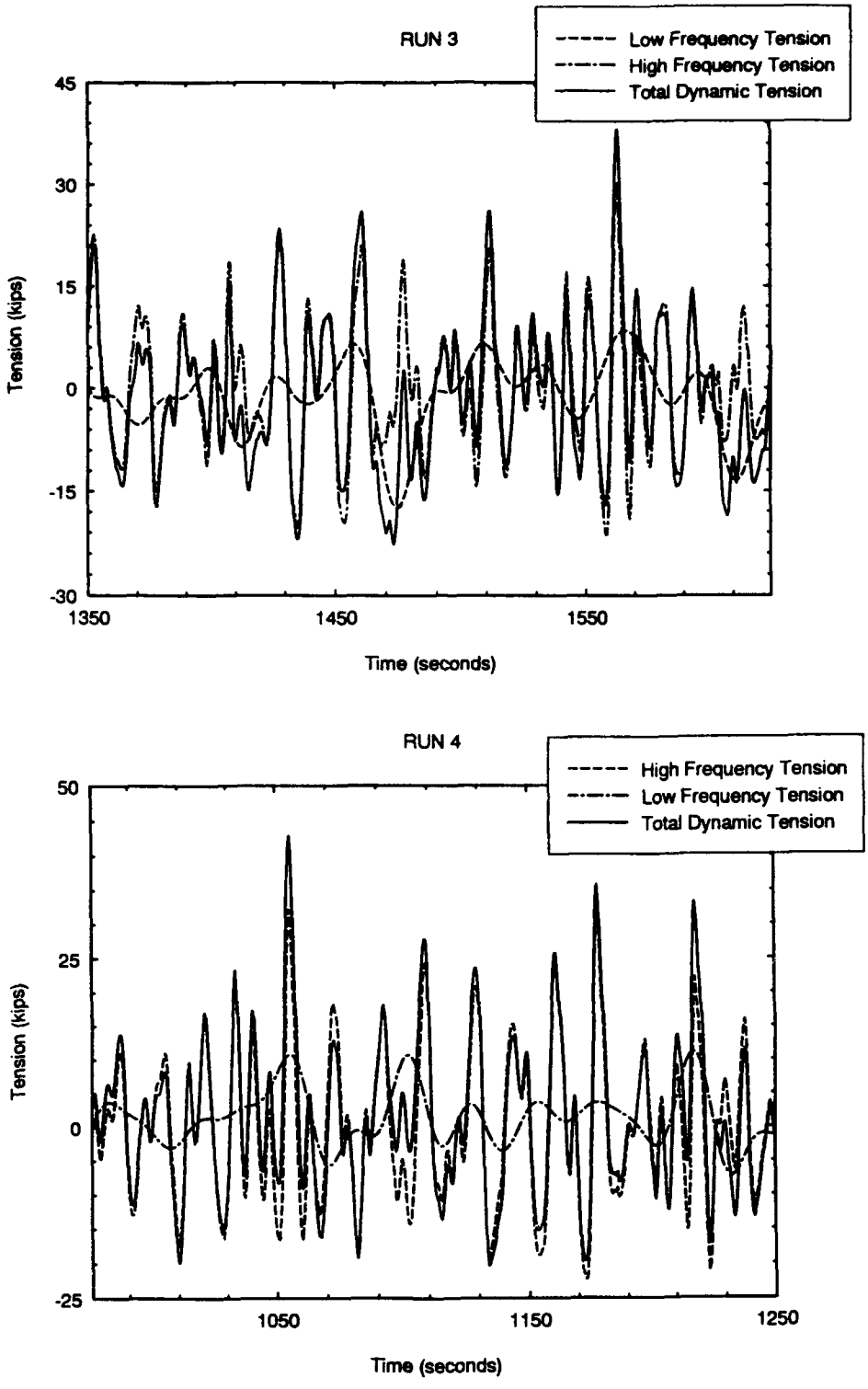
RUN 3
Low Frequency Tension
High Frequency Tension
Total Dynamic Tension
45
30
15
0
-15
-30
1350
1450
1550
Tension (kips)
Time (seconds)
RUN 4
High Frequency Tension
Low Frequency Tension
Total Dynamic Tension
50
25
0
-25
1050
1150
1250
Tension (kips)
Time (seconds)

Figure 4.19 (b)

Figures 4.19 (a) and 4.19 (b) show that the large low frequency and high frequency tensions for a given data run occur at the same time. This analysis indicates that the semi-empirical correction is not overly conservative as originally believed.

The measured sea spectrum and measured steady towline tension were used as input to the Nonlinear Extreme Tension Prediction Program for the purpose of comparing predicted tensions with measured tensions. The Nonlinear Extreme Tension Prediction Program and a correction for the RMS low frequency tension were used to estimate the tension level that would be exceeded in 50% of data records of 30 minutes duration ($T_{\alpha,t}$) . This estimate was compared with the measured tension records. Figures 4.20 (a) and 4.20 (b) graphically show the results of this comparison.

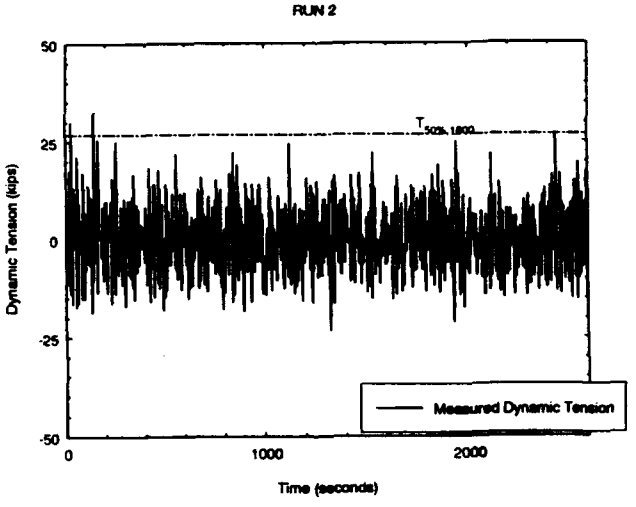

Figure 4.20 (a)

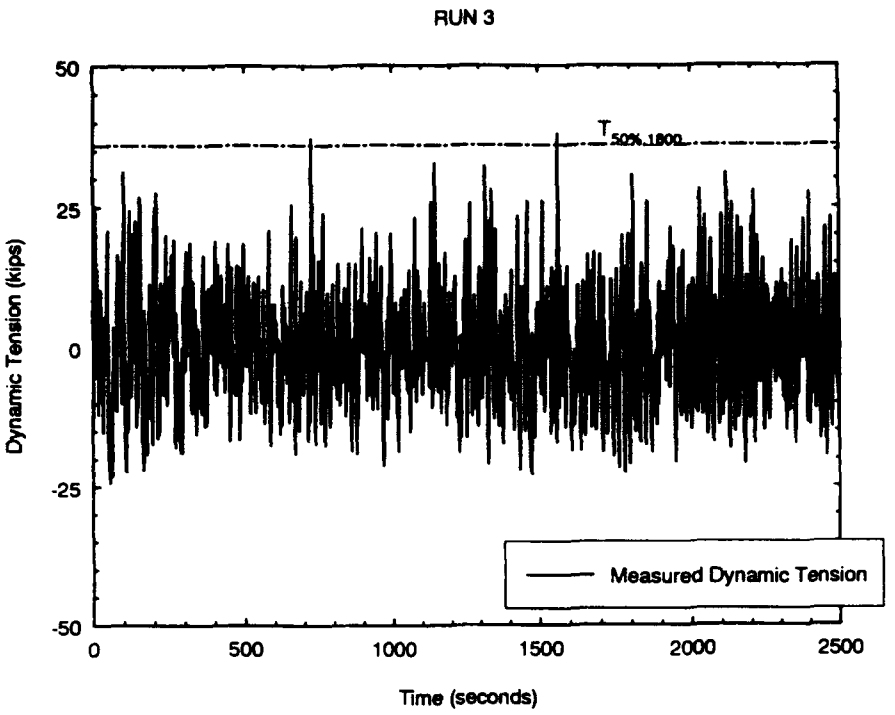
RUN 3
50
25
0
-25
-50
Dynamic Tension (kips)
$T_{50\%,1800}$
Measured Dynamic Tension
0
500
1000
1500
2000
2500
Time (seconds)

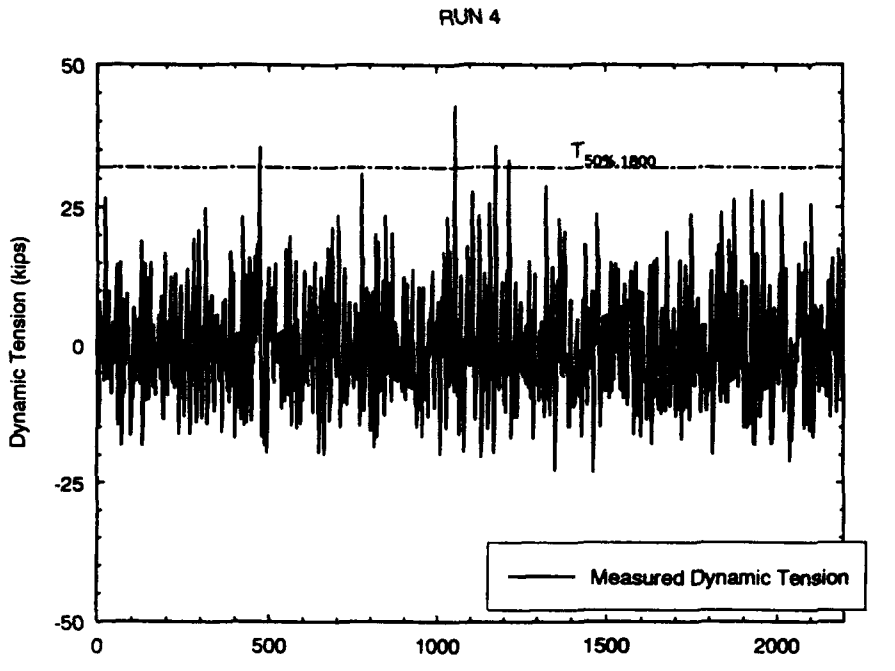
RUN 4
50
25
0
-25
-50
Dynamic Tension (kips)
$T_{50\%,1800}$
Measured Dynamic Tension
0
500
1000
1500
2000

Figure 4.20 (b)

The low frequency corrections were generated by low-pass filtering the measured dynamic tension time-histories. The RMS value of the low frequency tensions were multiplied by 2.0 and added to their respective tensions predicted by the Nonlinear Extreme Tension Prediction Program to obtain the 50% exceedence levels shown in Figure 4.20. The predicted and measured tensions are in good agreement. The 50% exceedence level is exceeded twice for Run 2 and Run 3 and three times in Run 4. A summary of the extreme tensions ($T_{0.1\%,\,24\,hrs}$) predicted for Run 2, Run 3, and Run 4 are provided in Table 4-3.

Table 4-3. Extreme Tension Summary

Run Number	Predicted Extreme Dynamic Tension (klbs)	Maximum Measured Dynamic Tension (klbs)
2	47.6	33.1
3	56.4	37.8
4	42.7	42.8

The difference between the measured and extreme tensions are reasonable for

Run 2 and Run 3. The maximum measured tension for Run 4 slightly exceeds the predicted extreme tension. The reason for the underprediction of the extreme tension for Run 4 is the measured spectra. In Table 4-2 it was shown that the measured sea spectra for Run 4 was significantly below what was visually observed. The measured significant wave height is 25% below the visually observed wave height. The measured sea spectra was used as input for generating the extreme tensions shown in Table 4-3. The apparent inaccuracy in the input excitation has caused the low extreme tension prediction.

Based on the increased understanding of the relationship between the low frequency and high frequency tension peaks a better "conservative" empirical correction is addition of 3.5 times the low frequency RMS tension to the extremes predicted by the Nonlinear Extreme Tension Prediction Program.

Given the errors identified in the wave spectrum and ship motion transfer functions identified earlier, the similarity between predictions and measurements should be viewed with caution. The potential for inaccuracies in the motion transfer functions and the wave spectra used for comparison must be considered when evaluating the validity of the Nonlinear Extreme Tension Prediction Program.

4.4 Comparison of Measured Tensions with Tensions Predicted by Time Simulation

The towline tension time simulation was run using a generated wave spectrum as input excitation. The wave spectrum chosen for input was a 30 knot Pierson Moscowitz Spectrum. This spectrum reflects an upper limit to the sea spectrum for which a tow would continue without laying to.

The time simulation is based on a method developed by Professor Jerome Milgram. The time simulation determines the two vessels' linear pitch and heave motions in the time domain using the fourier transform of their frequency responses. The frequency responses are based on a time realization of the random process whose spectrum matches the desired sea spectrum. The two vessels' linear and nonlinear surge motions are computed in the time domain. The heave, pitch, and surge motions determine the towline endpoint motions which in turn determine the tension time-history.

Three time simulations were performed. The simulations were performed for the following towline configurations:

a. 1435' of wire + 90' of chain;

b. 1435' of wire + 300' of stretcher + 90' of chain; and,

c. 1435' of wire + 600' of stretcher + 90' of chain.

The time simulations were run for 2500 days. The output of the time simulation is a continuous tension time-history for the 2500 days. This output was used for:

a. Predicting the extreme tension;

b. Producing a histogram of tension level exceedences; and,

c. Generated a tension spectrum for comparison with the tension spectra generated from measured tension time histories.

Table 4-4 provides a summary of the extreme tensions predicted by the time simulation and by the Extreme Tension Prediction Program for a 30 knot Pierson - Moscowitz Sea Spectrum.

Table 4-4. Summary of Predicted Extreme Tensions

Towline Configuration	Nonlinear Extreme Tension Prediction Program	Time Simulation
1435' wire + 90' chain	205	480 klbs
1435' wire + 300' stretcher + 90' chain	119 klbs	139 klbs
1435' wire + 600' stretcher + 90' chain	103	109 klbs

A histogram of tension level versus probability of exceedence for each of the time simulations is provided as Figure 4.21. The probability that tension in one day exceeded a specified tension level, T(i) is determined by:

$$P(i) = \frac{i}{2500} \qquad (9)$$

where i is the number of days that the tension exceed T(i).

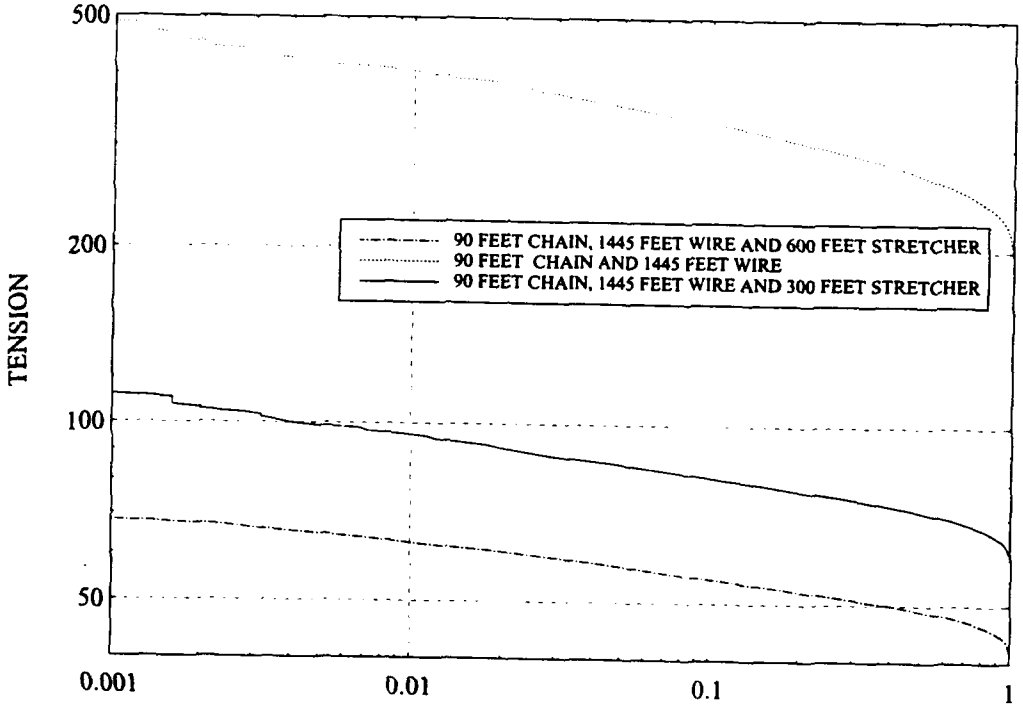

Figure 4.21

The shape of the tension histogram matches a similar plot produced from the measured tension data. The probability that a tension peak, T_{peak} , will exceed a specified tension level, T_o , is given by (Ochi, 1973):

$$P(T_{peak} \geq T_o) = 1 - [1 - \frac{N(T_o)}{N(0)}]^{(N(0))} \qquad (10)$$

where

$N(T_o)$ is the number of tension peaks in a data record above T_o

N (o) is the total number of positive tension peaks

Figure 4.22 shows the results of applying equation (8) to the measured tension data.

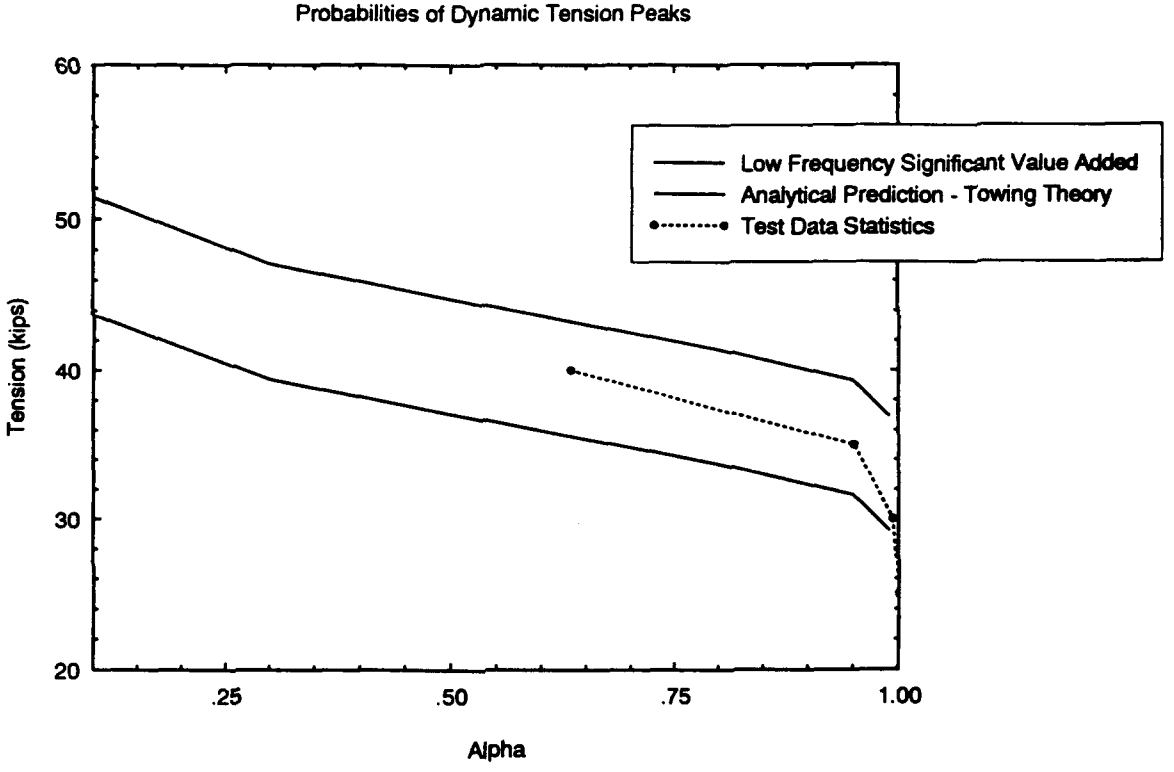

Figure 4.22

Figure 4.23 shows spectra generated from the measured tension data for Run 4 and from the tension time-history generated by the time-simulations.

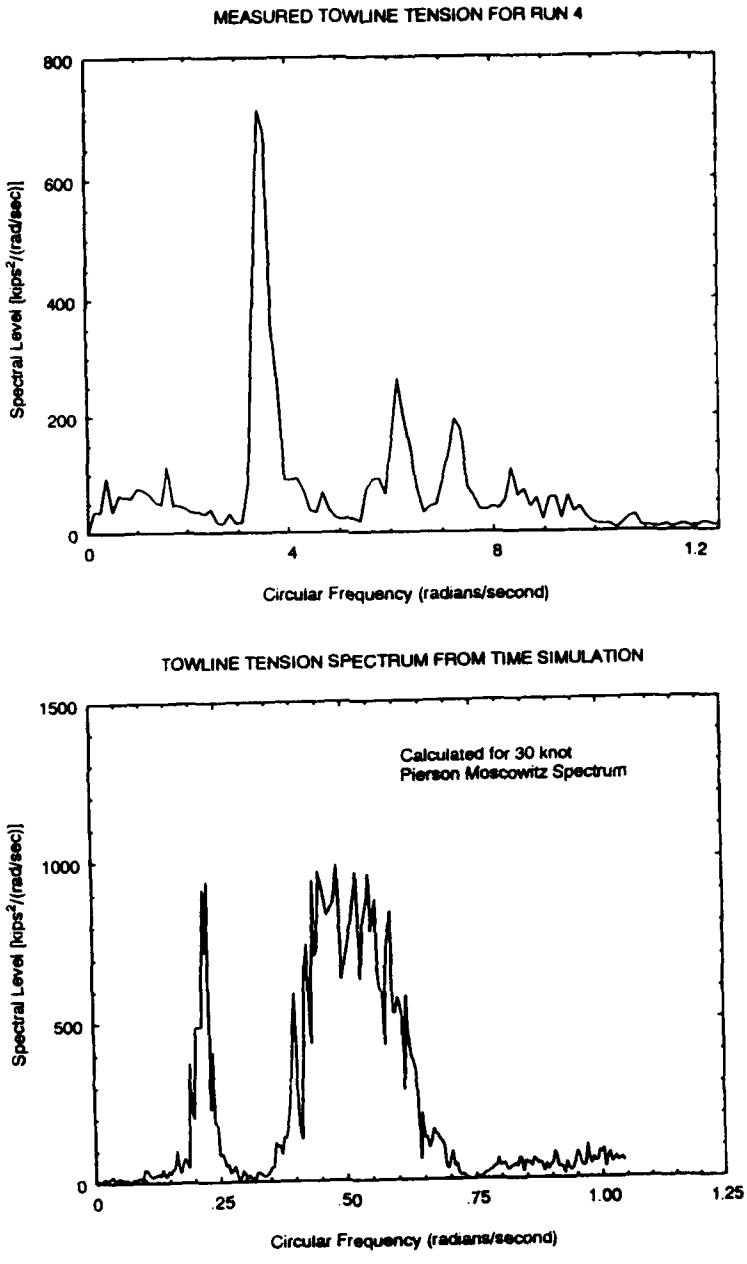

Figure 4.23

The tension spectra comparisons show that the tensions generated by time simulation capture the low and high frequency behavior of the dynamic towline tension. The time simulations predict an extreme tension higher than that predicted by the Nonlinear Extreme Tension Prediction Program. The reasons for this is that the time simulation does not use the equivalently linearized spring for determining anything other than the effect of the towline in pitch and heave motions of the tow vessels. Unlike the Nonlinear Extreme Prediction Program, which uses the equivalent linear spring for determining the effect of the towline on ship motions, the time simulation uses the numerical towline model (the third order polynomial) to determine the effect of the towline on ship motions. The additional non-linearity introduced is sufficient to generate occasional ship motions large enough to significantly raise the extreme tension values.

The results from the time simulation for the all wire towline show that an all wire towline will not survive a tow in 30 knot seas. Either a stretcher or an ATM is required to control the dynamic tension.

Chapter Five

Conclusions

5.1 Summary

This thesis supported a long term U.S. Navy project for improving open ocean towing safety. The areas of emphasis of this thesis were:

a. An experiment in which time histories of ship motions, towline tension, tug-tow range extension, and sea waves were measured;

b. Validating existing methods for predicting extreme towline tensions by comparing the measured and predicted towline tensions;

c. Comparing measured and predicted ship motions. Accurate ship motion prediction is an important aspect of accurate towline tension prediction;

d. Analyzing the low frequency component of towline dynamic tension;

e. Supporting the development of a numerical full time simulation of the coupled 12 degree of freedom towing problem; and,

f. Evaluating the ability of in-line synthetic stretchers to limit the magnitude of dynamic tension variations.

The difficulties associated with acquiring data on a "Tow of Opportunity" were reaffirmed during the test program conducted in support of this project. Though useful data and insight were gained during the test program, the incurred costs were quite high.

This thesis and the associated test program demonstrated the following:

a. The linear ship motion transfer functions obtained from standard seakeeping programs are reasonably accurate and suitable for use in estimating extreme towline tension. This was demonstrated by the comparison of measured and predicted tension and experimentally confirmed for the tug, but the accuracy of the linear ship motion operators with respect to the submarine motions was unable to be verified directly due to equipment failure;

b. The dominant ship motion in generating towline dynamic tension is surge. The accuracy of the predicted second order surge response is determined by the accuracy of the added resistance operators. The accuracy of the added resistance operators could not be directly verified by measured surge data due to the inability of the surge acceleration measurement equipment to measure low frequency surge accelerations. However, the calculated second order ship surge motions compared favorably with the measured range separation data;

c. The extreme towline tension predicted by a Nonlinear Extreme Tension Prediction Program that does not account for the second order wave-ship

interactions requires a low frequency tension correction equal to 3.5 times the estimated RMS value of low frequency tension for the given sea state. The fact that the largest low frequency and high frequency tensions occur at the same time for a given measured tension time history justifies the addition of the low frequency correction to the calculated extreme tension;

d. A full time simulation of the towing problem can provide a long enough tension time-history to calculate extreme towline tension from the generated data record. A data record of sufficient length to calculate extreme tension statistics can be generated in under 24 hours on a personal computer with moderate computing power (16 Mb of Random Access Memory, 66 Mhz). The computer program developed as part of this project includes directly the second order wave-ship interactions and the resultant effect on dynamic tension. The extreme tensions predicted by the time simulations are comparable to those generated by the combination of the Nonlinear Extreme Tension Prediction Program and the low frequency correction identified above;

e. Synthetic stretchers are effective at limiting the magnitude of dynamic tension variations. This fact has been demonstrated by analysis performed using both the Nonlinear Extreme Tension Prediction Program and the time simulation. Additional data at higher sea states is desirable for confirmation of the predicted behavior under increased towline endpoint motion amplitudes;

f. Two of the three critical parameters for analysis of the towline dynamic tension, the towline tension and the towline extension, were measured with

excellent accuracy. The importance to the success of accurately measuring these two parameters cannot be overstated. The laser range finder (used for measuring towline extension) data sampling rate was 2Hz and the range resolution was +/- 6 inches. This degree of precision is required to obtain data necessary to validate the towline dynamics numerical models. The accuracy of the measured wave data appears satisfactory for the purpose of analyzing ship motion transfer functions and producing sea spectra measurements. An independent means of calibrating and verifying the performance of the wave measurement buoys is desirable; and,

The ability of an ATM to control dynamic tension variations is limited. The response of the ATM is slow enough to allow large dynamic tension fluctuations.

5.2 Recommendations for Future Work

The following are required to improve the prediction of extreme towline tension in offshore towing:

a. An additional means for validating the measured wave information is required to confirm the accuracy of the transfer functions used for predicting ship response. NOAA wave buoys provide wave information at various fixed points in the ocean. For future tests the information from these buoys should

be obtained and compared with the measured data;

b. The accuracy of the added resistance operators used in the time simulation is important to predicting low frequency dynamic tension. Second order wave-ship interactions are the focus of current ocean engineering research and as new methods for predicting second order forces and damping are developed they must be evaluated for inclusion in the full time simulation;

c. The performance of ATM's under conditions of rapidly varying dynamic towline tensions should be evaluated in detail. The towline dynamic tension time-history should be measured and analyzed while the ATM is in operation. If ATM's are found to be incapable of controlling rapidly varying towline tensions and confidence in the performance of synthetic stretchers as the means of controlling dynamic tension has not been established, a towing configuration that should be considered is a composite towline (wire plus synthetic stretcher) and an ATM; and,

d. Consideration should be given to conducting dedicated tows for the purpose of gathering information regarding the performance of composite towlines and ATM's under a range of headings, speeds, and sea states.

References

Christensen, E.N. (1989), "Plans and Specifications for A Full-Scale Towing Model Validation Experiment", Engineers and Masters Thesis, MIT, Cambridge, Massachusetts.

David W. Taylor Naval Ship Research and Development Center (1981), "The Standard Ship Motion Program", Bethesda, Maryland.

David W. Taylor Model Basin Towing Tank Data (1991), "Hydrodynamic Towing Evaluation of SSN-637 Class Short-Hull and Long-Hull Submarines with Modified Bows", DTRC-SHD 0540-25, Requests for this document shall be referred to David Taylor Research Center, Code 15, Bethesda, Maryland 20084-500.

DeBord, F, Purl, J., Mlady, J., and Wisch, D., and Zahn, P. (1987), "Measurement of Full-Scale Barge Motions and Comparison with Model Test and Mathematical Predictions", *SNAME Transactions*, Vol. 95, SNAME, New York, N.Y.

Faltinsen, O.M. (1990), Sea Loads on Ships and Offshore Structures, Cambridge University Press, Cambridge, England.

Frimm, F.C. (1987), "Non-linear Extreme Tension Statistics of Towing Hawsers", Ph.D. Thesis, MIT, Cambridge, Massachusetts.

Frimm. F.C. and Milgram, J.H. (1991), "Towline Measurements at Sea", Document submitted to the Naval Sea Systems Command (NAVSEA OOC).

Gerritsma J. and Beukelman, W. (1972), "Analysis of the Resistance Increase in Waves of a Fast Cargo Ship", *Intern. Shipbuilding Prog.*, Vol. 19.

Hara, S. and Yamakawa, K. (1994), "On the Dynamic Towline Tension During Towing", Document produced by the authors as members of the Ship Research Institute, Ministry of Transport, Tokyo, Japan.

Jackson, H.E. (1992), "Submarine Design Notes", document prepared for the Professional Summer Program at the Massachuesetts Institute of Technology, requests for copies of the document should be referred to MIT Department of Ocean Engineering.

Longett-Higgins, M.S. (1963), "The Effect of Non-Linearities on Statistical Distributions in the Theory of Sea Waves", *Journal of Fluid Mechanics*,

Vol. 17.

Milgram, J.H., Triantafyllou, M.S., Frimm, F.C., and Anagnostou, G, (1988), "Seakeeping and Extreme Tensions in Offshore Towing", Paper presented at the *Annual Meeting of the Society of Naval Architects and Marine Engineers*, New York, N.Y., November 1993.

Milgram, J.H. (1990), "Introduction of Random Processes in Ocean Engineering", document prepared for instruction in the Ocean Engineering Department at the Massachusetts Institute of Technology.

Milgram, J.H. (1993), 1993 Annual Letter on: Dynamics and Extreme Tensions in Open-Ocean Towing of Submarines, Document submitted to the Naval Sea Systems Command (NAVSEA OOC).

Milgram, J.H., Frimm. F.C., and Thomas, G.R., "The Influence of Stretchers on Extreme Towline Tensions", document prepared for the Naval Sea Systems Command (NAVSEA OOC).

MIT Five Degree of Freedom Seakeeping Program (1975).

Naval Sea Systems Command (1988), U.S. Navy Towing Manual (Revision 1) (SL740-AA-MAN-010), Washington, D.C.

Newland, D.E. (1984), An Introduction to Random Vibrations and Spectral Analysis, Longman, Inc., New York, N.Y.

Newman, J.N. (1977), Marine Hydrodynamics, The MIT Press, Cambridge, Massachusetts and London, England.

Ochi, M.K. (1973), "On the Prediction of Extreme Values", *Journal of Ship Research*, Vol. 17, SNAME, New York, N.Y.

Parzen, E (1960), Modern Probability Theory and Its Applications, John Wiley and Sons, Inc., New York, N.Y.

Principles of Naval Architecture (1967), SNAME, New York, N.Y.

Salvesen, N., Tuck, E.O., and Faltinsen (1970), "Ship Motions and Sea Loads", *The Society of Naval Architects and Marine Engineers Transactions*, Vol. 78, The Society of Naval Architects and Marine Engineers (SNAME), New York, N.Y.

Sclavounous, P.D. (1991), "User's Manual for Strip Theory Program **NIREUS**", Unpublished document available through the author at the Massachusetts Institute of Technology.

Sellars, F.H. (1967), "The Dynamic Calibration of Shipborne Wave Gages", (Report No. 67-11), MIT, Cambridge, Massachusetts.

Triantafyllou, M.S. and Chryssostomidis, C. (1980), "Environment Description, Force Prediction, and Statistics for Design Applications in Ocean Engineering", document prepared for instruction in the Ocean Engineering Department at the Massachusetts Institute of Technology.

Triantafyllou, M.S. (1987), "Dynamics of Cables and Chains", *The Shock and Vibration Digest*, Vol. 19, No. 12.

Triantafyllou, M.S. (1990), "Cable Mechanics with Marine Applications", document prepared for instruction in the Ocean Engineering Department at the Massachusetts Institute of Technology.

Appendix A

Equipment Description

This appendix provides:

(1) A detailed description of the equipment required to measure the critical experimental parameters; and,

(2) A listing of the equipment used to obtain and record other experimental data.

A.1 Equipment for Measuring Critical Parameters

Tension Measuring Equipment

Tension Load Links

Manufacturer-	Metrox, Inc., San Diego, California.
Manufacturer's Part #-	TL101-200K.
Capacity-	200,000 lbs.
Overload-	150% of capacity without damage.
	300% of capacity without failure.
Sensing Element-	Dual bridge 350 ohm strain gages.

	Dual bridge chosen for temperature compensation.
Output-	~2mV/volt at rated capacity.
Excitation-	10 volts D.C. or A.C. nominal; 15 volts maximum.
Calibration Error-	Less than 0.25% of full capacity.
Temperature Range-	30°F to 130°F operating; -40°F to 180°F storage.
Temperature Effects-	< 0.01% of capacity sensitivity shift per °F and < 0.01% of capacity zero shift per °F over operating temperature range.
Construction-	Stainless steel, seal welded.
Electrical Connector-	Brantner MSJ-4-BCR (mating connector not supplied).
Electrical Connections-	Pin 1 = +ex; pin 2 = +out; Pin 3 = -out; pin 4 = -ex.
Weight-	200 lbs.

Electrical Cable from Load Cells to Data Acquisition System

Electrical Connection to Load Links:

Manufacturer-	Brantner & Associates.
	El Cajon, California.
Manufacturer's Part #-	XSJ-4-CCP.
Description-	Glass reinforced epoxy
	connector.
	Delrin locking sleeve.

Cable:

Manufacturer-	Vector Cable Company.
	Sugarland, Texas.
Manufacturer's Part #-	7-46 NT
Description-	7 conductor armored cable.
Nominal Diameter-	0.464".

Electrical Connection to Data Acquisition System Cable:

Manufacturer-	Marsh & Marine™ Connectors

Manufacturer's Part #-	RM-4-MP
Description-	Molded in-line female connector with stainless steel locking sleeve.

Data Acquisition Cable:

Manufacturer-	Vector Cable Company.
Manufacturer's Part #-	18/4 SO.
Connector-	RM-4-FS (male) with stainless steel locking sleeve.

Remarks

The tension load link load test certification paperwork and calibration data must be provided to the Navy.

The tension load link was installed by U.S. Navy divers one week prior to the tow start date. Adequate time was available for post-installation electrical checks.

As provided, the electrical connection to the load link is not adequately protected for use in an open-ocean towing environment. Additional protection is desirable to prevent damage to the connection by the towline. U.S. Navy divers

provided adequate protection upon installation. Additional support to the electrical connection is recommended in the future.

Equipment for Measuring Tug-Tow Separation

Laser Range-Finder

Manufacturer-	Laser Atlanta Optics, Inc. Norcross, Georgia.
Manufacturer's Part #-	ProSurvey™ 1000 Advanced Lidar System.
Physical Characteristics:	
Dimensions-	10" x 3.3" x 11".
Weight-	4.25 lbs.
Power-	12 VDC.
Operational Specifications:	
Target Range-	5 ft. - 10000 ft.
Range Accuracy-	+/- 6"
Laser Specifications:	
Wavelength-	Near infrared.
Eye Safety-	CDRH Class One Eye Safe.

Communications Protocol:

Baud Rate-	4800
Data Bits-	8
Parity-	None
Interface-	Two-wire RS-232 serial port.
Format-	NMEA 0183C.

Real Time Range Measurement:

Firing frequency-	500 hz.

Two bytes per range.

Target-	Reflective cloth mounted on front of the submarine's sail.

Remarks

The laser range-finder information is vitally important to a successful experiment. A minimum of one backup range-finder is recommended.

The laser range-finder is hand-held. At least two operators are required. After 10 minutes of obtaining range data the operator requires a relief.

Equipment for Measuring Ship Motions

Motions in 6 Degrees of Freedom

Nomenclature- Humphreys Stable Platform

Manufacturer- Humphreys

Manufacturer's Part #- CF77-0101-1

System Description:

Vertical Gyro- Pitch and roll angular displacement and stabilizing element for a three axis accelerometer.

Three Axis Accelerometer- Measure fore-aft, lateral, and vertical accelerations independent of vehicle pitch and roll angular position.

Directional Gyro- Yaw angular displacement.

Three Axis Rate Gyro- Measure pitch, roll, and yaw angular velocity.

Inverters- Power conversion, 28 VDC to 115 VDC and 26 VAC, 400 hertz.

System Specifications:

System Input Characteristics-

Input Voltage- 28 VDC +/- 3 VDC

Input Current- 5 amps (Start Up)

Input Current- 2.5 amps (Running)

Erection System-

Time to Erect- 5 min. to within 0.5 degrees of true vertical from a 25 degree offset.

Erection Accuracy- +/- 0.5 degrees of true vertical.

Output Specifications-

Vertical Gyro:

Output Voltage- +/- 5 VDC

Accuracy- +/- 1% of full scale

Time to Full Operation-

3 minutes

Output Impedance- 1000 ohms

Performance Specifications:

	Range (degrees)	Accuracy (degrees)
Pitch Angle-	+/- 45	+/- 2
Roll Angle-	+/- 178	+/- 2

Directional Gyro:

Output Voltage- +/- 5 VDC

Time to Full Operation-

3 minutes

Performance Specification:

	Range (degrees)	Accuracy (degrees)
Yaw Angle-	+/- 178	+/- 2
Pitch Angle-	+/- 45	+/- 2
Drift-	0.5 degrees/minute maximum average drift under dynamic conditions. Test conditions to be +/- 7.5 degrees simultaneous pitch, roll, and yaw motion. Drift calculation to exclude earth rate.	

Accelerometers:

Output Impedance- 1000 ohms

Wave Measurement Buoys

The wave measurement buoys consisted of an accelerometer, a frequency modulator circuit board, a VHF transmitter, and an antenna mounted to a float. The accelerometer, modulator, and transmitter were housed in a waterproof plastic container.

Equipment was installed on the escort ship to receive and record the wave buoy transmissions. For some data runs, the wave data was recorded on a cassette recorder stored in the plastic container.

Accelerometer

Nomenclature-	Accelerometer Potentiometer Model 602A
Manufacturer-	Bourn
Manufacturer's Part #-	602A-900-890
Range-	+0.5 g to +3.5 g

Transmitter

Nomenclature-	2 Channel VHF Business Band Transceiver
Manufacturer-	Realistic
Manufacturer's Part #-	19-1201

Transmitter Frequency- 151.625 MHz

151.145 MHz

Modulator

Figure A.1 is the circuit diagram for the modulator.

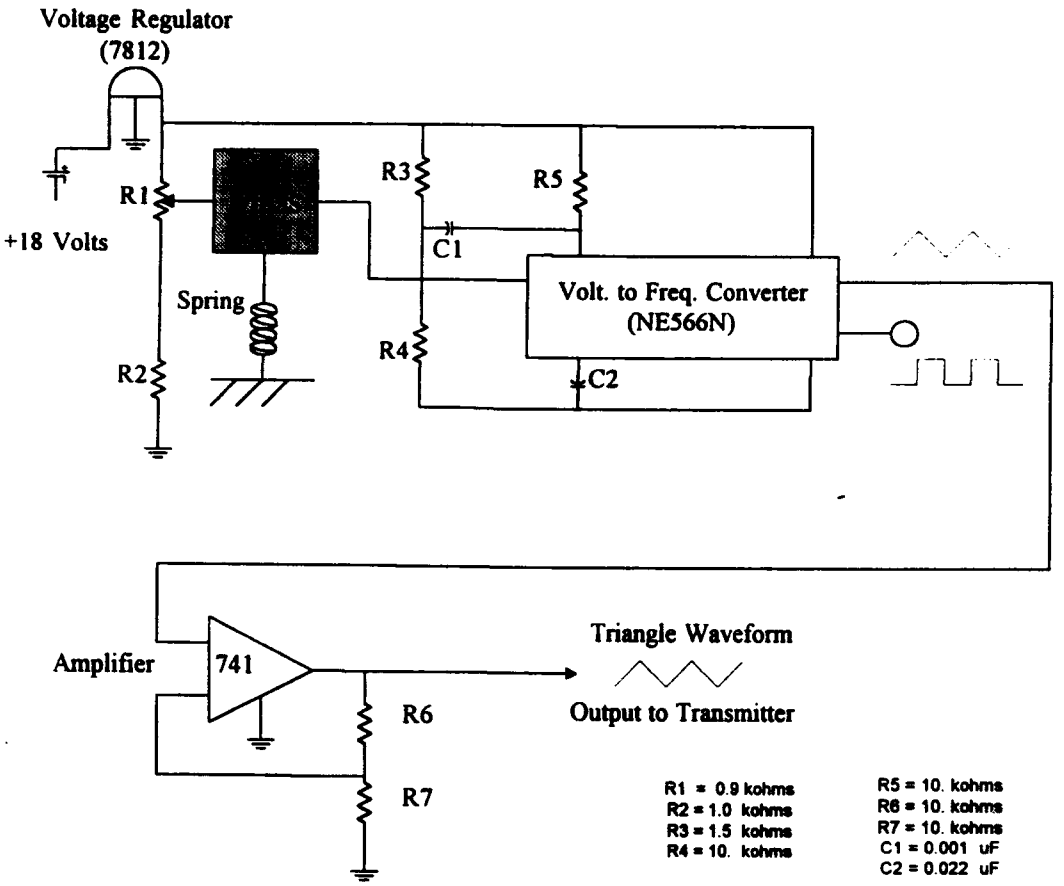

Figure A.1

Floats

The wave floats were constructed of two 3.5 ft. by 3.5 ft. by 1/4 inch painted plywood sheets with a 3 inch thick layer of low density closed cell foam between them. The plastic container containing the accelerometer and transmitter package was form fitted into a hole in the center of the float.

Receivers and Recording Device

ICOM R-100 Receiver

Business Band Transceiver

Radio Shack Cassette Tapedeck

Remarks

The wave measurement buoys were deployed by lowering them over the side of a ship escorting the tug and tow. The buoys were lowered over the side using grappling hooks and ropes. At the end of a data run the buoys were retrieved using grappling hooks. A total of 9 buoys were constructed anticipating an inability to retrieve the buoys in high sea states.

The construction of the wave buoys was initially unsuited for their intended

environment. The electrical connections were poorly soldered, the containers poorly waterproofed, and the antennae were not mounted high enough on the float to eliminate interference with the modulator circuit. These problems were corrected at sea.

The accelerometers used were electro-mechanical devices. A spring-mounted weight sliding on a lubricated shaft provided an output voltage signal proportional to the total acceleration of the float. The accelerometers occasionally exhibited stick-slip behavior. Gross stick-slip behavior could be readily detected and eliminated from the data. However, more subtle stick-slip behavior can exist in such devices.

Solid state accelerometers were also purchased and their suitability in wave measuring devices explored. These devices consisted of a small thin beam ($\sim$ 3/4 inch long) with a weight mounted at the center of the beam. The beam was instrumented with strain gages. As the axis of the beam tilted the measured strain changed producing an output form the strain gages proportional to the change in acceleration experienced by the device.

Little thought was originally given to the calibration of the wave buoys. Once at sea, the buoys were calibrated by tipping the buoys at known angles from the horizontal and correlating the angle with the change in measured acceleration. The buoys should have their calibration checked prior and subsequent to their

deployment.

A.2 Other Data Acquisition Equipment

On Submarine

Data Acquisition System- Toshiba T5200/100 Portable Computer
Dash-16 A-D Converter, Interface Box, and Input Filters

Magellan Global Positioning System Receiver and Antenna

Repco 9600 Baud Transmit Modem

KVH Fluxgate Compass

Omni-directional Antenna for Modem Transmissions

Yagi Antenna for Spread-Spectrum Modem Transmissions

On Tug

Data Acquisition System- Toshiba T5200/100 Portable Computer
Dash-16 A-D Converter, Interface Box, and Input Filters

Texas Instruments Notebook

Computer

Magellan Global Positioning System Receiver and Antenna

Repco 9600 Baud Receive Modem

Omni-directional Antenna for Modem Transmissions

Yagi Antenna for Spread-Spectrum Modem Transmissions

KVH Fluxgate Compass

A.3. Submarine Mounted Data Acquisition Equipment Enclosure and Power Supplies

A box was manufactured by Global Phillips Cartner (GPC) for housing the data acquisition equipment inboard the submarine. The box was sized to house or provide a mounting surface for the following:

Data Acquisition System (Computer and Dash-16)

Magellan GPS Receiver

IMD/Humphreys Stable Platform

Repco 9600 Baud Transmit Modem

Load Cell Signal Conditioner Box

24 VDC Inverter

IMD/Humphreys Stable Platform Serial Listener Box

KVH Fluxgate Compass

6 Cel-Cell 12VDC Batteries

2 SunSelector Solar Panel Charging Controllers

2 Solar Panels

2 Wind Generators

2 Inline Ventilation Fans

GPS Antenna

The material of construction was 6361-TB Aluminum. The dimensions of the box were 72" x 48" x 40". The box was mounted on top of the towing support equipment deckhouse constructed by Charleston Naval Shipyard (NAVSEA Drawing Number 845-6149852A).

Appendix B

Data Acquisition

This appendix contains a copy of the data acquisition procedure for the towing project.

Data Acquisition Procedure

I. Safety.

A. The only departure from the normal submarine towing procedures and configuration required during this tow is the temporary bypassing of the automatic towing machine (ATM) during data acquisition. This involves the installation of a carpenter stopper as detailed in section III.

B. The carpenter stopper should be removed and ATM operation resumed for the following:

1. Data acquisition complete, as identified by the MIT Data Acquisition Coordinator.
2. In seas on or abaft the beam during Sea State 4 or higher.
3. In seas forward the beam during Sea State 7 or higher.
4. If the towline tension exceeds 105,00 lbs at any time.

(This represents a factor of safety of 2 for the weak link).

5. At the direction of the OTC or Commanding Officer, USS GRAPPLE.

II. Prior to Departure From Charleston:

A. All equipment used to support data acquisition will be pre-tested at MIT.

B. All equipment installed by MIT on the submarine will be verified to be in proper working order after installation.

C. Upon USS GRAPPLE's arrival in Charleston, the data acquisition communication system (FM telemetry between towing vessel and tow) will be verified to be in proper working order.

III. Data Acquisition and Collection.

A. Professor Jerome Milgram is the Data Acquisition Coordinator. He will be embarked on board USS Grapple from Charleston to the Panama Canal.

B. During Periods where data is not being taken, the equipment on board the tow will be shut down, to conserve energy and to minimize equipment operating time.

This will be accomplished remotely via FM telemetry.

C. Once the tow is in the open ocean and sea conditions are favorable for data acquisition, with the concurrence of the OTC/OIC and Commanding Officer, USS GRAPPLE, the following data acquisition procedure will be performed in sequence:

1. Establish VHF communications between MIT personnel on board USS GRAPPLE and the escort ship, USS JESSE L. BROWN, prior to powering up data acquisition equipment. NOTE: MIT will have at least one person on board USS JESSE L. BROWN during the transit to the Panama Canal. This person is responsible, with assistance from ship's force, for the deployment and retrieval of the wave data acquisition buoys.

2. Power up data acquisition equipment on board the salvage ship and the escort ship. Verify proper operation. NOTE: This is to performed by MIT personnel. All data acquisition equipment is connected to the computer and, with the exception of the LASER range finder, requires no operator interface other than power on/power off.

3. When directed by the MIT test coordinator via VHF communications, and with the permission of Commanding

Officer, USS JESSE L. BROWN, deploy wave buoy. Verify proper operation. NOTE: MIT personnel embarked on board USS JESSE L. BROWN will deploy the wave buoy with assistance from ship's force.

4. Attach carpenter stopper to tow hawser. NOTE: Procedure for performing this step is the only departure from normal towing procedure it will only occur after the MIT Data Acquisition Coordinator has verified proper operation of all data acquisition equipment.

5. Begin data acquisition run. The data from the acquisition equipment will be recorded on disk on the computers located on the towing vessel and the tow. USS GRAPPLE is requested to provide the following data which will be manually recorded by MIT personnel every 5 minutes:

Parameter	Instrument
Wind Speed	Installed sensor
Wind Direction	Installed sensor
Ship's Position	LORAN, NAVSAT, visual
Speed Over Ground	LORAN, NAVSAT, visual
Speed	Installed sensor
Wave Height	Seaman's eye

Hawser Length	Tow machine*
Shaft RPM	Installed sensor*
Propeller Pitch	Installed sensor*
Ordered Course	*
Ordered Speed	*
Wave Direction	Seaman's eye*

*- To be recorded for any change

Data record sheets will be provided by MIT personnel.

6. During each test run, data will be recorded for a total of 60-90 minutes. The first 30-45 minutes of data will be recorded while the carpenter stopper is attached. This will be terminated when the Data Acquisition Coordinator is satisfied that a valid round of data has been acquired, or at the direction of the OTC/OIC or Commanding Officer, USS GRAPPLE. Immediately following the removal of the stopper, an additional 30-45 minutes of data will be taken while operating on the ATM. The overall procedure is as follows:

a. Notify escort ship of intentions.

b. Attach carpenter stopper.

c. Record data.

d. Notify escort ship of intentions.

e. Remove carpenter stopper from tow hawser and resume towing on ATM. (Ship's force).

f. Record similar data while operating on ATM.

NOTE: This will provide additional data on tow reactions while on ATM. Data may also be taken in this configuration in the case of exceptional sea states.

g. Secure power to data acquisition equipment.

h. Make reasonable effort to retrieve wave buoy.

i. Record time on manual data recording log.

D. The performance of this testing is secondary to the safe and timely completion of the tow. It is not the intent of this procedure to involve excessive special maneuvers (e.g. course and speed changes) solely for the purpose of collecting test data under various specific conditions or to spend excessive time/effort resolving test problems (e.g. equipment failures). Any such proposed actions shall be approved by both the OTC and the Commanding Officer, USS GRAPPLE.